SYNTHESIS AND CHARACTERIZATION OF COPOLYMERS OF DIISOCYANATES AND DIALCOHOL

A THESIS SUBMITTED TO
THE GRADUATE SCHOOL OF NATURAL AND APPLIED SCIENCES
OF
MIDDLE EAST TECHNICAL UNIVERSITY

BY

SELDA KESKİN

IN PARTIAL FULFILLMENT OF THE REQUIREMENTS
FOR
THE DEGREE OF DOCTOR OF PHILOSOPHY
IN
POLYMER SCIENCE AND TECHNOLOGY

SEPTEMBER 2008

Approval of the thesis:

SYNTHESIS AND CHARACTERIZATION OF COPOLYMERS OF DIISOCYANATES AND DIALCOHOL

submitted by **SELDA KESKİN** in partial fulfillment of the requirements for the degree of **Doctor of Philosophy in Polymer Science and Technology Department, Middle East Technical University** by,

Prof. Dr. Canan Özgen
Dean, Graduate School of **Natural and Applied Sciences** _____

Prof. Dr. Cevdet Kaynak
Head of Department, **Polymer Science and TechnologyDept., METU** _____

Prof. Dr. Ali Usanmaz
Supervisor, **Chemistry Dept., METU** _____

Examining Committee Members :

Prof. Dr. Kemal Alyürük
Chemistry Dept., METU _____

Prof. Dr. Ali Usanmaz
Chemistry Dept., METU _____

Prof. Dr. Arife Doğan
Prosthodontics Dept., Gazi University _____

Prof. Dr Duygu Kısakürek
Chemistry Dept., METU _____

Assoc. Prof. Dr. Hasan Nur Testereci
Chemistry Dept., Kırıkkale University _____

Date : _____

I hereby declare that all information in this document has been obtained and presented in accordance with academic rules and ethical conduct. I also declare that, as required by these rules and conduct, I have fully cited and referenced all material and results that are not original to this work.

Name, Last Name : Selda Keskin
Signature :

ABSTRACT

SYNTHESIS AND CHARACTERIZATION OF COPOLYMERS OF DIISOCYANATES AND DIALCOHOL

Keskin, Selda

Ph.D., Department of Polymer Science and Technology

Supervisor: Prof. Dr. Ali Usanmaz

September 2008, 184 pages

This study was aimed to synthesize low molecular weight hydroxyl terminated polyurethane acrylate polymers that can be used in biomedical applications. Acrylate end capping via inter-esterification reaction was successfully achieved with the methacryloyl chloride addition to the hydroxyl ends of the polyurethane at low temperatures. Isocyanate terminated polyurethane acrylates were also synthesized for the sake of comparison. TDI, HDI and MDI were used as diisocyanates for urethane synthesis and they were end capped with MMA and HEMA. Nature of the monomers used had an effect on thermal, morphological, and rheological properties that were interpreted in terms of the level of hydrogen bonding and degree of phase separation.

Synthesized polymers were characterized by NMR, FTIR-ATR, DSC, TGA, GPC, Mass Spectroscopy, SEM and rheometry.

In the literature, polyurethane acrylate polymers have been synthesized from the isocyanate terminated polyurethanes in which the urethane chains were ended with isocyanate groups. However, the toxicity of the isocyanate groups limited their biomedical applications especially in prosthetic dentistry as a soft lining material. Therefore, it is inevitable to explore the cytotoxicity of polyurethane acrylate polymers. For this purpose, silver nanoparticles that have an average particle size of 40 nm, were incorporated to the synthesized polymers. This addition, which intends to improve the degree of cytotoxicity, was successful to a certain extent.

Keywords: Polyurethane, acrylate end capping, biocompatibility, silver nanoparticle.

ÖZ

DİİZOSİYANAT VE DİALKOL KOPOLİMER SENTEZİ VE KARAKTERİZASYONU

Keskin, Selda
Doktora, Polimer Bilimi ve Teknolojisi Bölümü
Tez Yöneticisi: Prof. Dr. Ali Usanmaz

Eylül 2008, 184 sayfa

Bu çalışma, biyomedikal uygulamalarda kullanılabilecek düşük molekül ağırlıklı hidroksil sonlu poliüretan akrilat polimerlerini sentezlemeyi amaçlamıştır. İnter-esterleşme reaksiyonu ile düşük sıcaklıkta metakriloil klorürün hidroksil sonlu poliüretana eklemesiyle akrilat sonlanması başarılı bir şekilde gerçekleştirilmiştir. İzosiyanat sonlu poliüretan akrilatlar da karşılaştırma amacıyla sentezlenmiştir. TDI, HDI ve MDI, üretan sentezinde kullanılan diizosiyanatlardır ve akrilat sonlandırması MMA ve HEMA kullanılarak yapılmıştır. Kullanılan monomerlerin ısıl, morfolojik ve reolojik özelliklere etkisi hidrojen bağının seviyesine ve faz ayrım derecesine göre değerlendirilmiştir. Elde edilen polimerler NMR, FTIR-ATR, DSC, TGA,

GPC, Kütle Spektrometresi, SEM ve reometre analizleriyle karakterize edilmiştir.

Literatürde poliüretan akrilat polimerleri, zincir sonları izosiyanat gruplarıyla sonlanmış poliüretanlardan sentezlenmektedir. İzosiyanat gruplarının toksisitesi, bu poliüretanların özellikle protetik diş hekimliğinde yumuşak astar malzemesi olarak kullanılmalarını sınırlandırmıştır. Bu nedenle poliüretan akrilat polimerlerinin sitotoksisite özelliklerinin araştırılması kaçınılmaz olmuştur. Bu amaçla, ortalama parçacık boyutu 40 nm olan gümüş nano parçacıkları sentezlenen polimerlere eklenmiştir. Sitotoksisiteyi iyileştirmeyi amaçlayan bu ekleme belirli oranda etkili olmuştur.

Anahtar Kelimeler : Poliüretan, akrilat eklemesi, biyouyumluluk, gümüş nanopartikül.

To my mother

and

To the memory of my father

ACKNOWLEDGEMENTS

I would like to express my deepest gratitude to my supervisor Prof. Dr. Ali Usanmaz for his support, encouragement, and guidance throughout the study. I am grateful to Prof. Dr. Arife Doğan for her encouragement, and advice throughout the research. She provided not only the necessary guidance, but also expanded my knowledge in many areas especially in dentistry.

I would like to thank to my friend and colleague Dr. Kemal Behlülgil for his suggestions, comments and valuable contributions throughout the study and I am thankful to my friend Binnur Özkan for her moral support and help during this research. Special appreciation is due to my dear friend Serhan Demirci for his moral support, continuous encouragement, personal advices and his support on the graphics.

I would like to express my appreciation to Prof. Dr. Çiğdem Erçelebi and Prof. Dr. Hayrettin Yücel for their understanding and support throughout the study and during the period of writing of my thesis. I am also grateful to METU Central Laboratory research associates and staff. Especially worth mentioning are the contributions from the following individuals: Elif Kemeröz, Dr. Elif Tarhan Bor, Assoc. Prof. Necati Özkan, Leyla Molu, Seda Bilgi, Sedat Canlı, Dr. Burcu Akata Kurç, Dr. İbrahim Çam.

Help of my lab mates, Elif Vargün, Bengi Aran, Selin Kozanoğlu, and Şule Altınsoy are gratefully acknowledged.

I would also like to thank Şükran Yılmaz from ŞAP Institute for the cytotoxicity analysis. I also want to thank to my friends Yusuf Nur for the mass spectroscopy analysis, Dr. Ertuğrul Sahmetlioğlu for the GPC analysis and Dr. Seha Tirkeş for his help and valuable discussions during this work.

I am truly in debt to my mother for her endless support, understanding, and belief in me.

This study was supported by the Scientific and Research Council of Turkey (TÜBİTAK) Grant No: 104T424.

TABLE OF CONTENTS

LIST OF TABLES

TABLES

LIST OF FIGURES

FIGURES

CHAPTER 1

INTRODUCTION

Polyurethanes are a unique class of polymers that have a wide range of applications [1,2]. Since their properties can be readily tailored by the variation of their components, they have been used extensively as biomaterials. The attributes of polyurethane as an attractive material for a number of biomedical devices are its good biocompatibility, processing ability and excellent physical mechanical properties. The applications include vascular prostheses, catheters, heart valves, and dental materials [3-14].

Block copolymers that provide a combination of different properties are the most suitable materials for various uses. Acrylate functional group containing block copolymers have found many applications due to their optical and biocompatible properties. However, the low impact strength, lower thermal stability, and low abrasion resistance limits their application.

This thesis has focused on the synthesis of various polyurethanes end capped with different types of acrylates. Isocyanate and hydroxyl terminated polyurethanes were synthesized and acrylate end capping reactions were achieved via two different chemical routes.

The second part of this research was aimed to investigate the biocompatibility of the synthesized polymers. In this respect, toxicity was investigated by introducing silver nanoparticles.

1.1 Urethane Polymers

1.1.1 Historical Background of Polyurethanes

Otto Bayer and co-workers discovered and patented the chemistry of polyurethanes in 1937 [15-19]. They produced linear polyurethanes from diisocyanates and diols via polyaddition principle. With development forced by World War II, polyisocyanates became commercially available by 1952. Commercial production of flexible polyurethane foam began in 1954, based on toluene diisocyanate and polyester polyols. In 1958, Schollenberger of BFGoodrich introduced a new "virtually crosslinked" thermoplastic polyurethane elastomers [20]. Spandex fiber called Lycra was announced by Du Pont at the same time. This product is a polyureaurethane based on polytetramethylene oxide, 4,4'-diphenylmethylene diisocyanate and ethylene diamine. By the early 1960s, new polyurethane based products like Estane, Texin, Desmopan and Elastollan were marketed by several companies. In addition, urethane based synthetic leather was introduced by Du Pont under the trade name Corfam in 1963. In 1969 Bayer pioneered an all-plastic car having RIM molded bumpers and fascia; in 1983 the first plastic body commercial automobile (Pontiac Fiero) was produced in the USA [21].

The extended use of polyurethanes in medical applications and orthopedics was started at 1970s. Polyurethanes are commonly used in a number of medical applications including catheter, general purpose tubing, hospital bedding, surgical drapes, and wound dressings [22-26].

1.1.2 Urethane Chemistry

Polyurethane name is derived from the urethane bond, which is illustrated in (1), forms the basis of the urethane chemistry [27-31]. Polyurethane has a significant number of these urethane groups that do not have to repeat in a regular order.

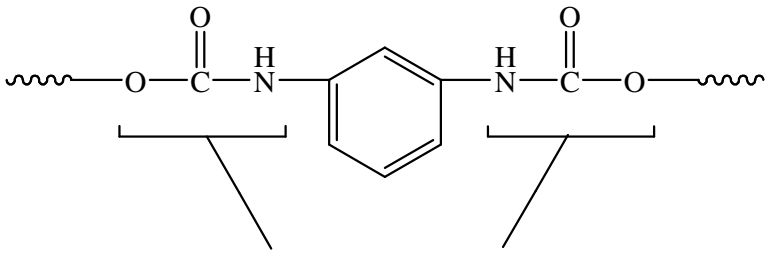

(1)

Polyurethanes can be formed by a variety of methods in which the reaction of di- or poly functional hydroxyl compounds with di- or polyfunctional isocyanates is the most widely used production method [32].

The chemistry involved in the synthesis of a polyurethane elastomer is centered on the isocyanate reactions. The observation of the isocyanate group electronic structure showed that the resonance structures in reaction (2) are possible.

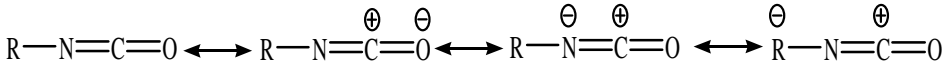

(2)

The electron density increases in the order of C< N< O. Isocyanate reactions mainly occur through addition to C=N double bond. The reactions of isocyanates with active hydrogen compounds proceed by the attack of a nucleophilic center upon the electrophilic carbon in the isocyanate group.

NCO bonded electron acceptor groups increase the reactivity and donor groups reduce it. Reactivity is reduced by steric hindrance in isocyanate groups, and in active hydrogen compounds [28].

The common reactions of isocyanates can be put into two main classes. One is the reaction of isocyanates with compounds containing reactive hydrogen to give addition products and the other is the self-polymerization reaction of isocyanates [27, 28, 32].

The addition of acidic hydrogen yield carbamic acid derivative in which the acidic H atom is inserted to C=N bond. This reaction shown in (3) is strongly influenced by the type of the catalyst used. Basic compounds and metal compounds tend to accelerate the reaction, whereas acidic compounds slow down [33-36].

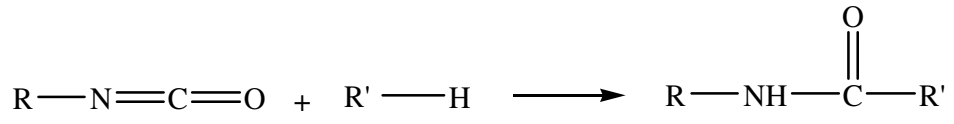

(3)

The hydroxyl containing compounds react with the isocyanate groups to produce urethane linkages, as shown in reaction (4). The reactivity of the OH group has a great importance in the extend of reaction. Primary hydroxyl compounds are the most reactive ones. Steric hindrance effects can also greatly

modify the reaction rate. The urethane formation is strongly catalyzed by mild and strong bases, metals, and weakly by acids.

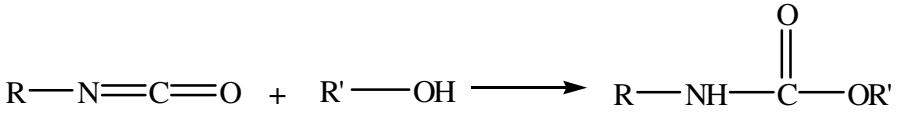

Urethane **(4)**

Other important reaction (5) of isocyanates is the formation of ureas through the addition of amines. The more basic the amine the faster is the reaction. Primary aliphatic amines are extremely reactive [33, 37].

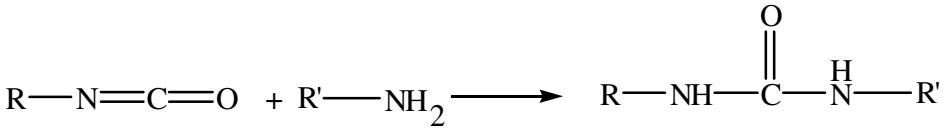

urea **(5)**

At elevated temperatures (up to 50 °C), isocyanates react with hydroxyl compounds to give urethanes. They produce ureas with amines and water as shown in reaction (6). Reaction of isocyanate with water is very important in the polyurethane foam production. The released CO_2 gas diffusion helps to blow the foam.

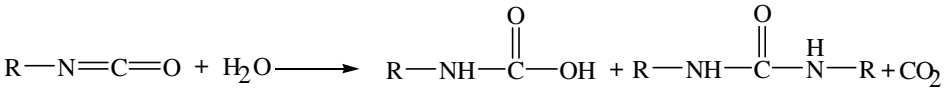

(6)

Polymer formation takes place when the reagents used in above reactions are di- or polyfunctional. While these reactions occur at different rates, urea formation being the most rapid among all. These basic addition reactions have the advantage that, they do not give rise to by products. Linear products are formed when bifunctional reactants are used. On the other hand higher functionality leads to the formation of branched or crosslinked products.

High temperature has a great effect in the isocyanate chemistry and secondary reactions take place to give allophanate, biuret crosslinking groups as in reaction (7) [21, 29, 38]. These secondary reactions occur at the presence of excess isocyanate that attacks the active hydrogen still present in the previously formed urethane and urea groups [30].

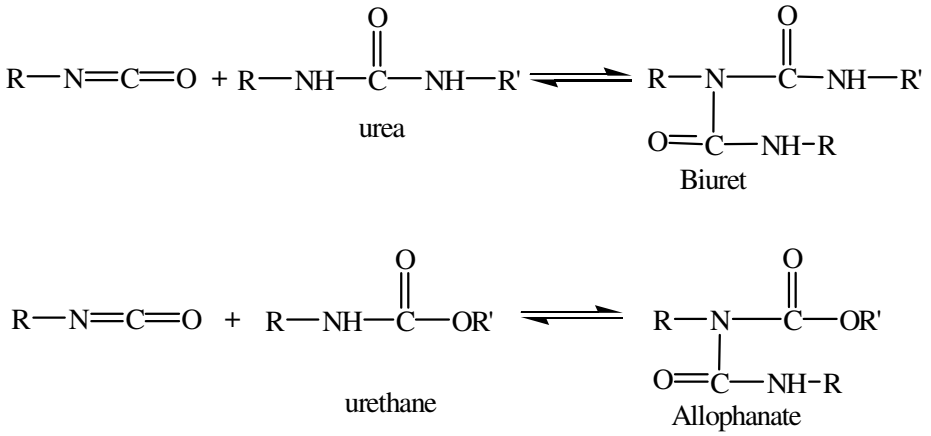

(7)

Isocyanates can also react with themselves to form dimers, trimers, carbodiimides and uretoneimines [39-41]. Dimerizaton of isocyanates resulted in the formation of uretidinediones at low temperatures, as given in reaction (8) and it is especially common in more reactive aromatic isocyanates.

Trimerization of isocyanates to give isocyanurate rings [42], unlike dimer rings, is exceptionally stable.

The self condensation reaction that takes place at high temperatures form carbodiimides [43-46] and further reaction with an excess isocyanate results in uretoneimine formation [47] as shown in reaction (9).

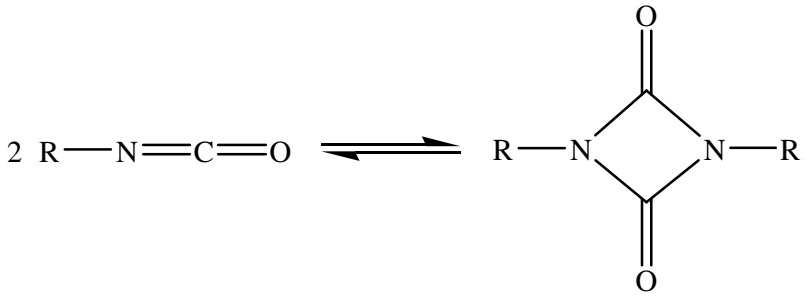

Uretidinedione **(8)**

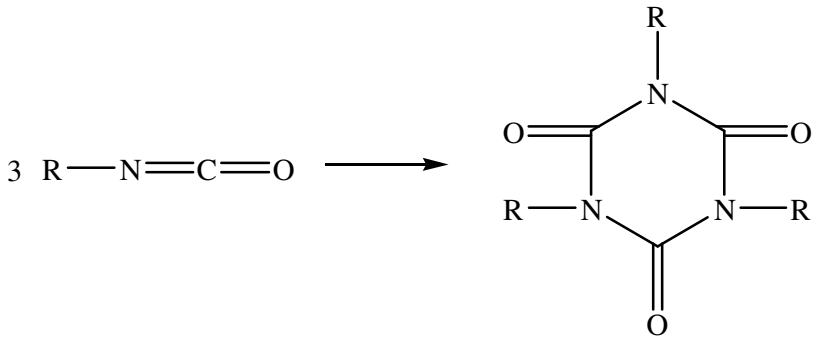

Isocyanurate

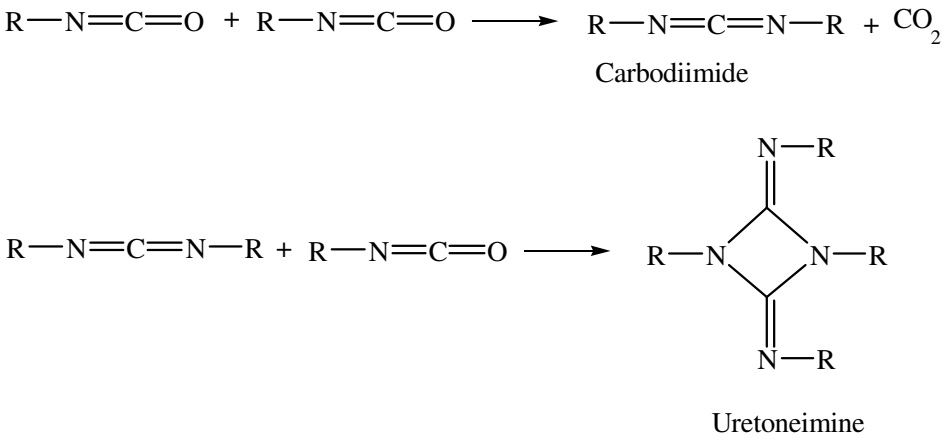

(9)

1.1.3 Raw materials

Isocyanates

There are several diisocyanates available in the market for the synthesis of urethane polymers, and some of them listed in Table 1. Isocyanates can be subdivided into two groups as aromatic or aliphatic.

TDI and MDI are well known aromatic isocyanates. TDI almost used as a mixture of 2,4 and 2,6 isomers, usually in a ratio of 80:20 or 65:35. Its functionality is two and the reactivity of the NCO group in the para position of the aromatic ring being more pronounced. Urethanes obtained from aromatic diisocyanates undergo slow oxidation in the presence of air and light, causing discoloration [48-50].

HMDI is the most important aliphatic diisocyanate used in polyurethane production [51]. Isophorone diisocyanate (IPDI) and 4,4`-dicyclohexylmethane

Table 1 Common diisocyanates available for polyurethane synthesis

Abbreviation	Chemical Name	Structure
TDI	Toluene-2,4-diisocyanate	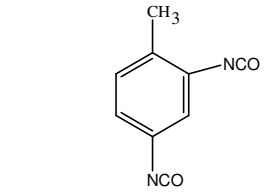
MDI	4,4`-Methylene bisphenylene diisocyanate	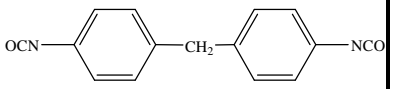
p-PDI	p-Phenylene, 1,4-diisocyanate	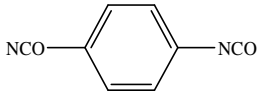
NDI	Naphthalene 1,5-diisocyanate	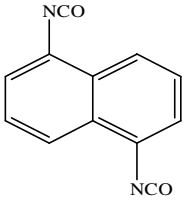
XDI	p-Xylene diisocyanate m-Xylene diisocyanate	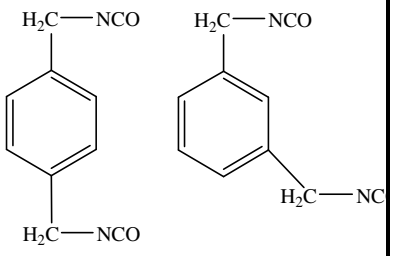
HDI	1,6-Hexamethylene diisocyanate	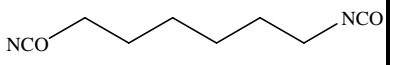
IPDI	3-Isocyanatomethyl-3,5,5-trimethylcyclohexyl isocyanate	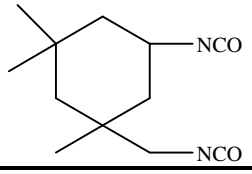

diisocyanate are the other aliphatic isocyanates that have a wide application area. Reactivity of diisocyanate is an important factor that mainly depends on the chemical structure. Electron withdrawing group attached to isocyanate group increases reactivity of the molecule by increasing the partial positive charge on carbon. This makes the charge transfer of the donor electron much easier. This fact explains the reason of higher reactivity of aromatic diisocyanates than that of aliphatic ones. Steric hindrance also decreases the reactivity of isocyanates. Therefore bulky groups near the reaction site reduce the reactivity.

Diols and Polyols

The initial studies on polyurethane synthesis were based on simple diols but the use of polymeric analogues gain more importance in increasing the molecular size. Polymers used for this purpose are usually polyether- or polyester- based compounds and they are available in various molecular weights [27]. In addition, polydiene or polyolefin based compounds are also used in the polyurethane production. Some of the polyether and polyester polyols are listed in Table 2.

Catalysts

The catalysts most widely used in polyurethane production are tertiary amines and metal catalysts. Tertiary amines are the catalysts for both the isocyanate-hydroxyl (4) and the isocyanate-water (6) reactions. The efficiency of tertiary amine catalyst increases as the basicity of the amine increases and the steric shielding of the amino nitrogen decreases. Triethylenediamine shown in (10), N, N, N`, N`-tetramethyl ethylene diamine, N-alkyl morpholines are the most commonly used tertiary amine catalysts [52]. Dibutyltin dilaurate (10) and tin octate are widely used as organotin catalysts. Organotin catalysts are most

effective for the isocyanate-hydroxyl reaction and do not promote isocyanurate formation (8).

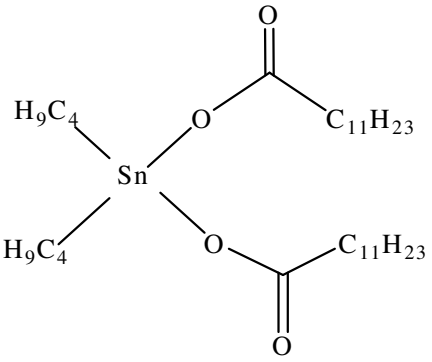

Dibutyl tin dilaurate

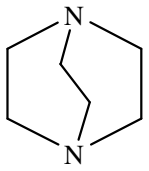

Triethylene diamine

(10)

Table 2 Polyether and polyester polyols

Abbreviation	Polyol	Chemical Structure
PEG	Poly(ethylene glycol)	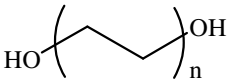
PPG	Poly(propylene glycol)	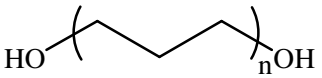
PTMO	Poly(tetramethylene oxide)	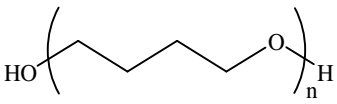
PEO	Poly(ethylene oxide)	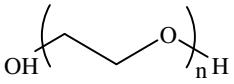

Britain and Gemeinhardt [53] first proposed the ternary complex formation between metal catalyst and an isocyanate. Complex formation could occur in two steps, with either the hydroxyl or the isocyanate compound reaction the first. The reaction (11) shows the mechanism for the case in which the isocyanate complexes first with the metal compound.

Smith [54] proposed an alternative mechanism, in which the metal complexes with the alcohol at some site other than the reactive hydroxyl group. Tin-alcohol complex forms a bridge complex with the tin-isocyanate complex. By this way, more than one tin-alcohol or tin-isocyanate complexes interact and urethane formation takes place by rearrangement of the hydroxyl proton to the nitrogen of the isocyanate group.

1.1.4 Polyurethane Synthesis

Polyurethane elastomers are synthesized by two basic techniques. These methods differentiated according to the medium of preparation and the addition sequence of the reactants. Polymerization can be carried out in a solvent free bulk or solution medium. Bulk polymerization gives an advantage of solvent-free synthesis and it has been used mainly in industrial synthesis for environmental reasons, while solution polymerization has largely been used for the laboratory or experimental synthesis of polyurethanes [27, 31].

Sequence of addition of reactants can either be in a one-step process or two step process (prepolymer process). Prepolymer route of urethane production is schematically illustrated in Figure 2 [27] in which the final polymer is formed in two separate steps.

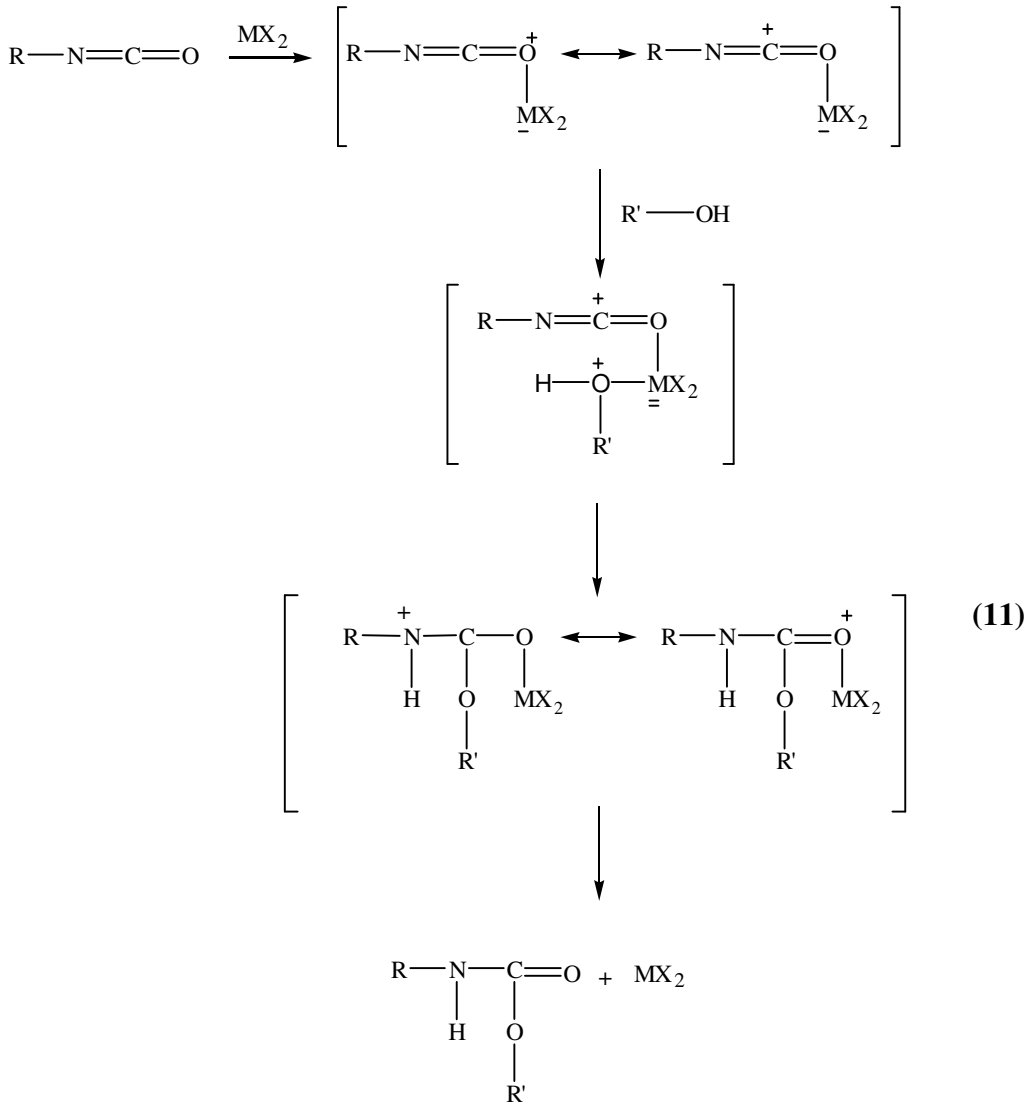

(11)

The first step is to produce a precursor to the final product by reacting a polyol component with an excess of an isocyanate component. This results in what is known as an isocyanate-terminated prepolymer. Second step is the chain extension step in which formed prepolymer is converted into the final high molecular weight polymer by further reaction with a diol or diamine chain extender.

Polyurethane formation with one shot process schematically represented in Figure 1 [27]. Polymerization carried out by simultaneously mixing together polyol, diisocyanate and chain extender either in bulk or in solution.

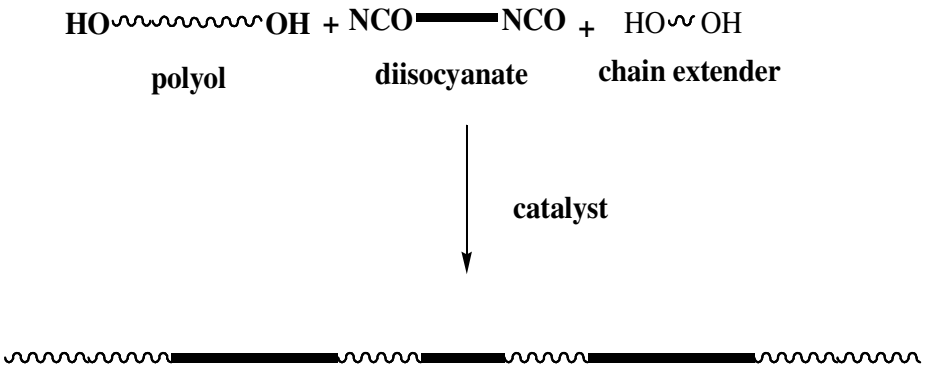

Figure 1 Scheme of one-shot process for polyurethane elastomer preparation

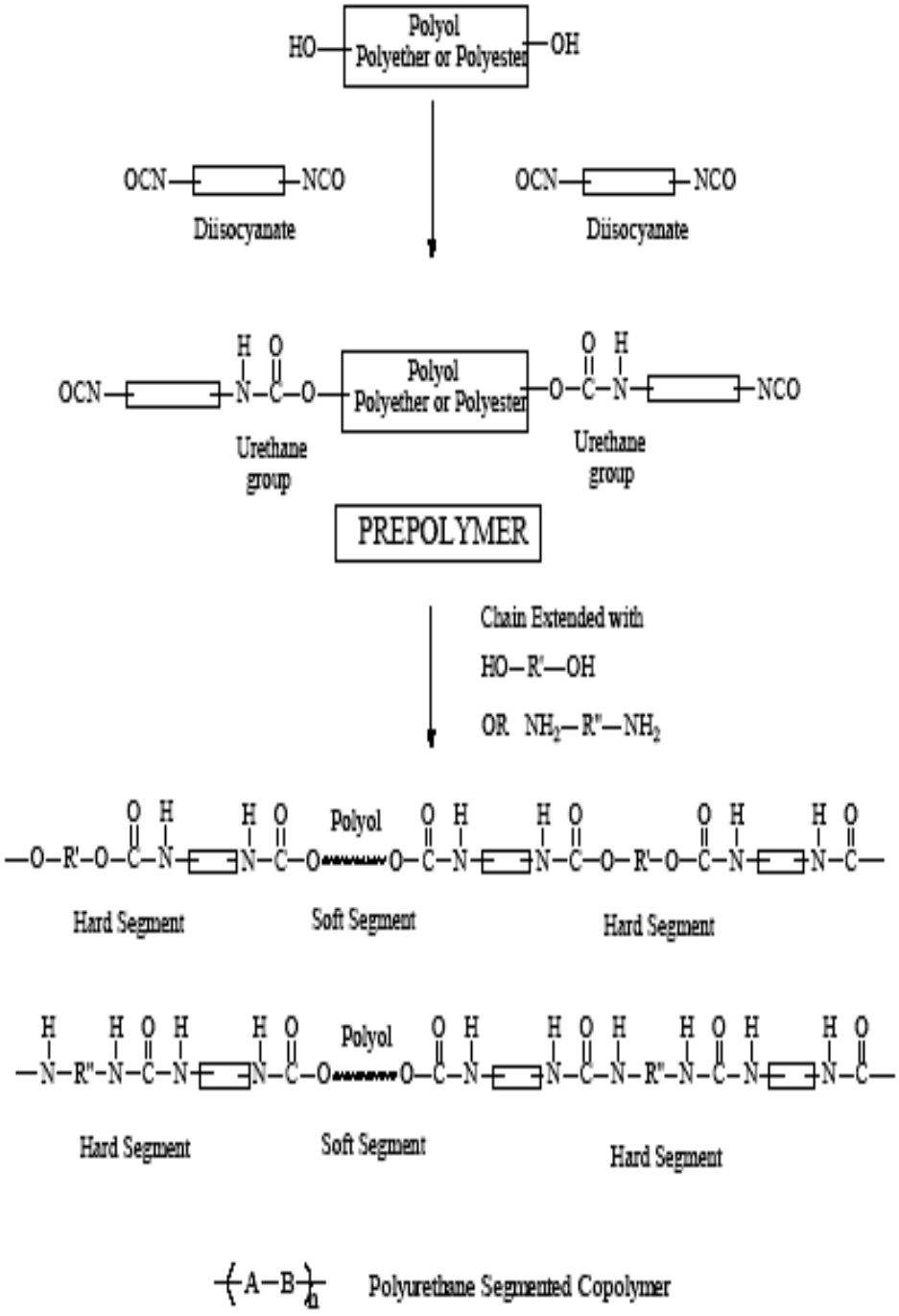

Figure 2 Scheme of prepolymer route for the formation of a polyurethane elastomer

1.1.5 Structure Property Relationship

Urethane elastomers can be regarded as a linear block copolymer of the type shown in Figure 3. These polymers can be considered in terms of long (1000 - 2000 nm) flexible segments and much shorter (150 nm) rigid units which are chemically and hydrogen bonded together. This segmented polymer structure has three basic building blocks: the polyol, diisocyanate and chain extender. The desired properties can be obtained by controlling the type and concentration of the segments present.

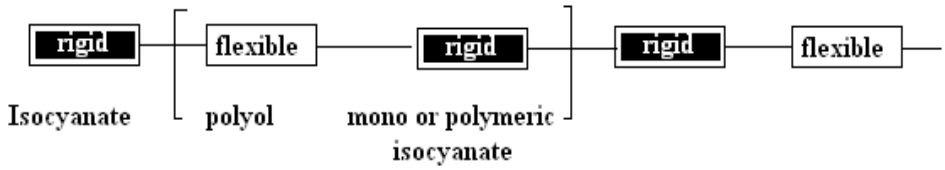

Figure 3 The basic units in polyurethane

Polyurethanes can contain a high concentration of polar groups (polar hard segment and less polar flexible segment), that results from isocyanate-hydroxyl reactions, as well as ester, urea and other groups. Hard and flexible (soft) segment incompatibility cause phase separation since heat of mixing is positive. The final properties of polyurethanes determined by the extent of interaction between these polar groups. The rigid segments in polyurethanes particularly affect the modulus, hardness and tear strength, and determine the upper-use temperature by their ability to remain at elevated temperatures.

The flexible blocks primarily influence the elastic nature of the product and its low-temperature performance, and they make important contributions towards

the hardness, tear strength and modulus. Such strong polar interactions in polyurethanes can lead to a supramolecular organization into aggregated structures, which may be in the form of glassy domains or crystallites.

Aliphatic polyethers or aliphatic polyesters are the usual materials used as flexible segments in polyurethane elastomer production. These have glass transition temperatures below room temperature and are low melting point solids or liquids. Polyethers have weaker interchain interface forces than polyesters, and generally give elastomers with inadequate physical properties.

Rigid segment properties determine the interchain interactions in the elastomers to a large extent and so determine the network structure in these materials. Preferred diisocyanates are those having large molecular structural bulk resulting in interchain steric hindrance and these have the highest levels of modulus, tear and tensile strengths. Elastomers based on the aliphatic isocyanate generally had superior mechanical properties. This pattern of behavior applies to both polyester and polyether based urethane elastomers [27].

The temperature of the reaction is important and up to 50 °C the linear chain forming reaction predominates but as higher temperatures (up to 150 °C) are reached then biuret and isocyanurate formation become effective and branching occurs. At above 150 °C some of the less stable links are affected and reversion or degradation can then take place. The isocyanate reactions are highly exothermic, and under conditions where heat transfer is slow appreciable temperature rises can be experienced and deterioration in properties results.

Hydrogen Bonding

Hydrogen bonding results from the attraction of hydrogen atoms in one molecule with an oxygen or nitrogen atom in another molecule [55]. The hydrogen bond is the strongest secondary chemical bond with a strength estimated to about 20-50 kj/mol [56]. Hydrogen bonding in polyurethanes plays an important role in determining the degree of phase separation. N-H group is the proton donor whereas the carbonyl and the etheric oxygen are the proton acceptors. Hydrogen bonding in urethane chains was illustrated in Figure 4 [57-60]. The FTIR analysis differentiate the hydrogen bonded N-H and free N-H, and also gave information about the presence of urethane carbonyl C=O and urea carbonyl C=O [61-70].

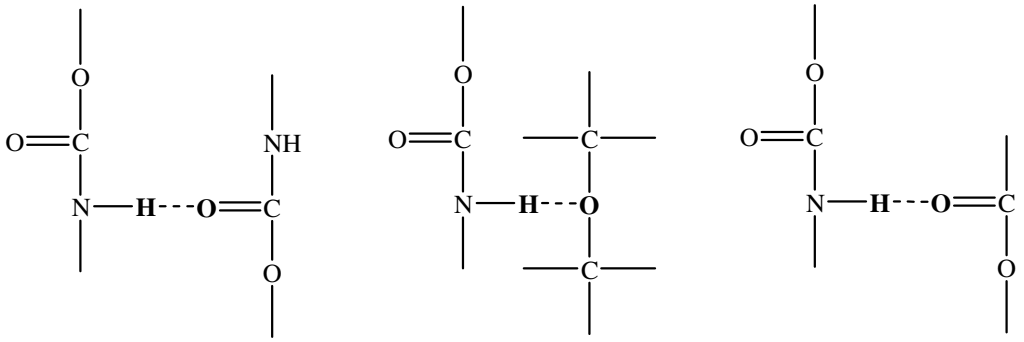

Figure 4 Hydrogen bonding interaction in polyurethanes

Degradation

Polymers can degrade by exposure to high temperature (thermal degradation), shear action (mechanodegradation), oxygen, electromagnetic, and ultrasonic radiation, moisture, and chemical agents. In general, polymers are susceptible to thermal degradation, which can occur either by chain scission, involving the breakage of the backbone bonds, or by non-chain scission, involving the elimination of a small molecule from substituent group and subsequent double bond formation.

Chain scission can occur by one of three mechanisms. These include (1) random degradation, where the chain is broken at random sites; (2) depolymerization, where monomer units are released at an active chain end; and (3) weak-link degradation, where the chain breaks at the lowest energy bonds [71].

Thermal degradation of polyurethanes can be explained by three ways. The predominant dissociation is occurred in the way of depolymerization in which the original products: polyol and diisocyanate are formed between temperatures 150-160 °C. On the other hand, they may form primary amines together with alkenes and carbon dioxide via reaction shown in (12).

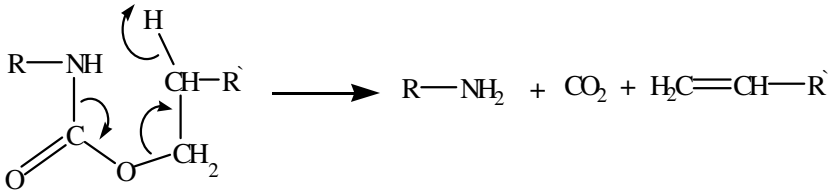

(12)

Formation of a secondary amine and carbon dioxide is also possible as shown in reaction (13) [72-76].

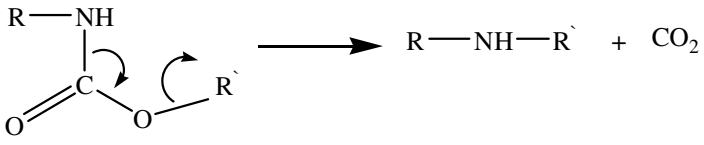

(13)

Photo degradation of the urethanes formed from aromatic diisocyanates was known by many researchers [77-80], and formation of yellow color caused many problems in storage and in actual application. This color formation was the result of ultraviolet-initiated auto-oxidation of the urethane linkage to quinone imide structures (14). There have been successful attempts in the use aromatic diisocyanates that are structurally incapable of forming such quinone species [78].

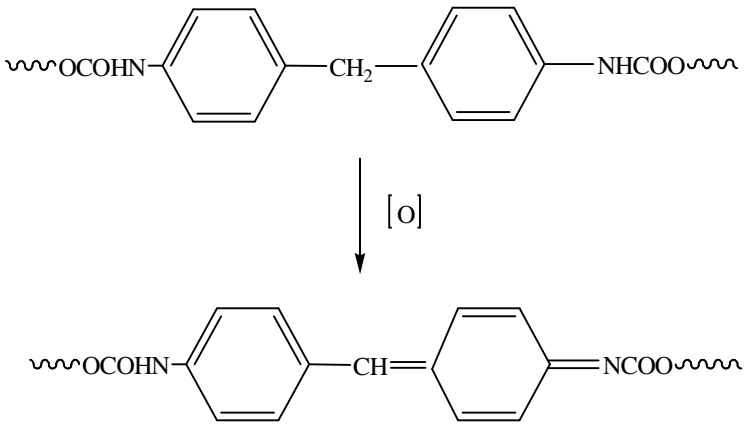

(14)

Quinoneimide

1.2 Urethane Acrylate Polymers

Urethane acrylate oligomers have been extensively investigated in the past as photo/radiation/laser curable coatings [81-86], photoresists for the fabrication of microelectronic devices [87], sealants and adhesives [88,89], biomaterials useful in contact lenses [90] and surgical implants, printing inks [91] and elastomeric and encapsulating coatings. The basic constituents are urethane oligomers tipped with acrylate functionality and vinyl monomers, which are added to make harder products and/or to reduce the viscosity to obtain better processability [92-93].

Classically, urethane acrylate synthesis shown in reaction (15) involves first the preparation of isocyanate-terminated macroglycol by the reaction of polyol with an excess of a diisocyanate and then obtaining acrylate end capped urethane oligomers with the addition of hydroxyl alkyl acrylate groups, thus bringing the reactive acrylic functions to the molecules.

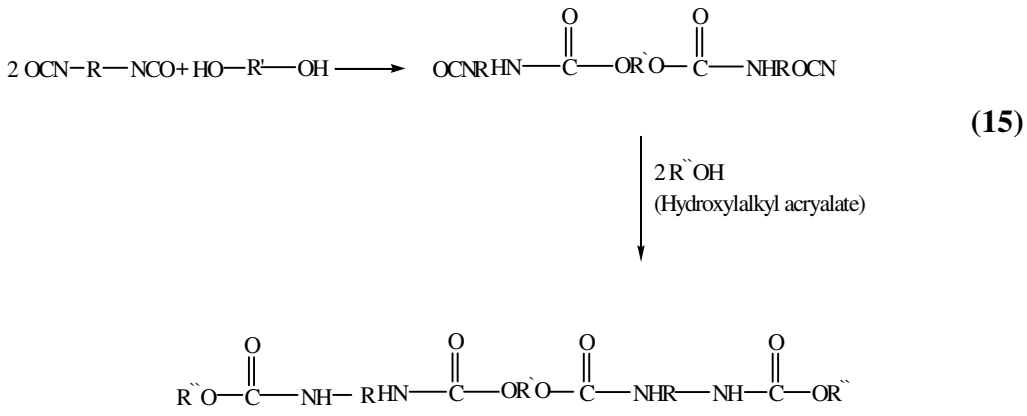

(15)

The hydroxyalkyl (meth) acrylates which are used widely in the preparation of urethane acrylate are 2-hydroxyethyl methacrylate (HEMA) [94-106], 2-hydroxyethyl acrylate (HEA) [107-112], and 2-hydroxypropyl methacrylate (HPMA) [107,113].

Poly (urethane-b-acrylate) block copolymers were synthesized by radical solution polymerization using macroazo initiators [114-117]. Cheikhalard et.al [117], have investigated the block copolymers based on polyurethane and polymethylmethacrylate or polystyrene sequences using macroazo initiators via radicalic mechanism.

Oprea et.al [118] have synthesized and characterized radiation and thermal sensitive polyurethane methacrylate. Polyurethane containing pendant methacrylic groups were obtained from the reaction of polyester diol, excess MDI, and methacrylic acid. These materials exhibit physical properties similar to those of linear segmented polyurethanes. This similarity was attributed to low amount of methacrylate groups present.

Barbeau et.al [119] have investigated the role of diisocyanate (IPDI, TDI, and 4,4 dicyclohexylmethane diisocyanate) on the properties of polyurethane acrylate (PUA) prepolymers based on polypropylene oxide. FTIR investigation of the hydrogen bonding in 2,4 TDI based PUAs showed that intermixing between soft polyether segments and hard urethane groups were enhanced and induced an increase of the Tg. The glass transition temperature of the synthesized PUAs varies in between - 58 to -55 °C. The rheological flow characteristic of 2,6 TDI based prepolymers showed that they have had the combination of shear thickening and thinning behavior, whereas all the other prepolymers behaved as Newtonian fluids.

UV curable urethane acrylates have been synthesized and characterized by several researchers and formulation usually contains reactive urethane

oligomers, reactive diluents, and photo-initiators [120-126]. Generally, UV curable telechelic (functionalized end group) urethane-(meth)/acrylate synthesis have been done via two synthetic strategies [120-122]. The first one is the reaction of diol with a diisocyanate to generate an oligomers of required molecular weight followed by end capping with a hydroxyl functional acrylate [121]. The second strategy is the reaction of a hydroxyl functional (meth)acrylate with the appropriate diisocyanate to give an isocyanate functional (meth)/acrylate followed by reaction with suitable diol [122]. Asha et.al [123], have synthesized via second strategy and characterized the UV cured prepolymers

UV-curable poly(ethylene glycol) based polyurethane acrylate hydrogels have been prepared and characterized by Kim and Paik [124]. Effects of diol molecular weight (PEG), the type of diisocyanate (HDI, HMDI, TDI), and the content of acrylamide and acrylic acid have been studied in terms of mechanical properties, water content, and X-ray diffraction profiles of the obtained films. Although it is expected to have poor mechanical properties with the increase in PEG molecular weight, PEG 4000 has showed the highest modulus, strength, and elongation due to the crystallization. In DSC thermograms, effect of hydrogen bonding is clearly observed for differing amounts of acrylamide and acrylic acid present in the final polymer.

Hsieh et.al [125] have prepared several urethane acrylates using N,N-azobisisobutyonitrile (AIBN) as the initiator. They have investigated the HEMA terminated polyurethanes for lithographic and coating applications. The curing analysis indicated the reaction rate equation correlates well with the film thickness, initiator concentration, double bond concentration and exposed energy.

Urethane di(meth)acrylates have been widely used in dental materials [127-132]. The matrix phases of dental composites, which are now widely used in

restorative dentistry, are mostly di(meth)acrylate monomers. Although some urethane di(meth)acrylates have been commercialized for dental applications [130], they still have much promise to overcome the shortcomings of the previously available resins. Atai et.al [132] have synthesized urethane dimethacrylate from HEMA end capped isocyanate terminated prepolymer, and characterized the prepolymer with the aim of reducing polymerization shrinkage. Rheological behavior has been studied and it was shown that complex viscosity decreased with increased temperature and remained constant with the increased frequency.

1.3 Soft Lining Materials

Denture lining materials act as shock absorbers and reduce and distribute the stresses on the denture bearing tissues [133,134]. These materials can be classified into three groups [135]:

1. Hard reline materials
2. Tissue conditioners
3. Soft lining materials

Soft lining materials serve to distribute the forces of mastication more evenly and absorb energy. They do not reduce the transmitted force but result in a smaller displacement of the oral mucosa. Since the stiffness of the soft lining material is less than that of the oral mucosa, it will absorb more of the energy and deform more. The energy is released as the lining returns to its pre-deformed shape.

The ideal properties of a soft lining material include the following:

1. Biocompatibility – non-toxic and non-irritant to the oral tissues.
2. Permanently compliant- soft enough for the comfort of the patient.

3. Permanently resilient- the actual level of resilience required is unknown as shown by the range available.
4. Adhere to the denture base and remain so in the mouth.
5. Low water uptake- a high uptake will cause distortion and may result in fouling of the lining due to ingress of bacteria etc.
6. Wetted by saliva- a thin film of saliva is necessary for the retention of the denture and it acts as a lubricant to prevent irritation of the mucosa.
7. Sufficient mechanical properties- enough to withstand normal handling, brushing etc.
8. Easy to clean -not adversely affect by denture cleansers, not stained easily etc.

Soft lining materials can be classified as follows depending on their chemical structure:

1. Natural rubber /PMMA Graft copolymer system
2. Vinyl resins
3. Polyurethanes
4. Soft acrylic materials
5. Silicone rubber materials
6. Elastomer/ methacrylate systems
7. Fluoroethylene copolymers

Polyurethanes have been used successfully in the fabrication of facial prostheses and they can be used as a soft lining material. However, there is a concern over the toxicity of the isocyanates used in the production of these materials [136]. In addition to their toxicity, these materials have high water uptake into their cellular inner structure. This resulted in early stagnation and fouling. Their fabrication and application were technically difficult therefore; the material did not gain any real measure of general application [165].

1.4 Dynamic Mechanical Properties

The behavior of materials of low molecular mass is described in terms of two ideal cases: the elastic solid and the viscous liquid. Polymers can display properties between these two cases depending on the temperature and chosen time scale. The elastic solid has a definite shape and is deformed by external forces into a new shape. The removal of these forces reverts the material to its original form by the help of stored energy obtained from external forces. On the contrary, a viscous liquid has no definite shape and flows irreversibly under the action of external forces [137]. In viscous systems all the work done on the system is dissipated as heat, whereas in elastic systems all the work is stored as potential energy. It is this dual nature of polymers that makes their behavior so complex and therefore they are viscoelastic materials.

In linear viscoelastic behavior, the stress and the strain will both vary sinusodially, but there is a lag in between as shown in Figure 5. Thus, they are expressed as:

$$\text{Strain} \quad e = e_0 \sin \omega t \tag{16}$$

$$\text{Stress} \quad \sigma = \sigma_0 \sin (\omega t + \delta) \tag{17}$$

Where ω is the angular frequency and δ is the phase lag. The expanded form of the stress equation (17) is:

$$\sigma = \sigma_0 \sin \omega t \cos \delta + \sigma_0 \cos \omega t \sin \delta \tag{18}$$

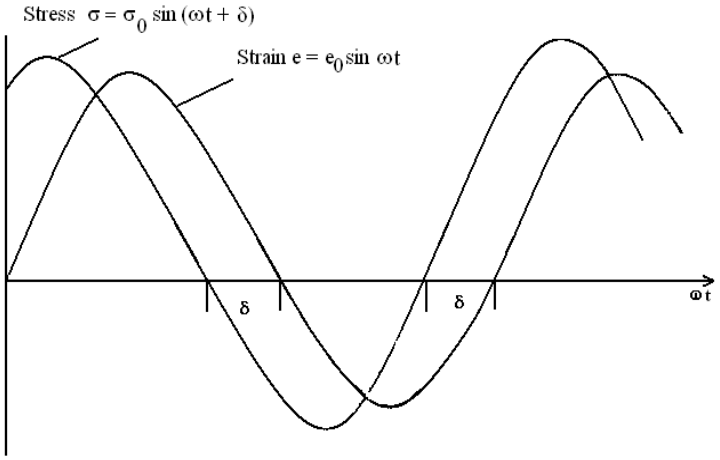

Figure 5 The strain lags behind the stress

Stress has two components: one is in phase with the strain (an elastic stress), the other is 90° out of phase with the strain (or in phase with the strain rate, viscous stress). The viscous and elastic stresses can be related to material properties through the ratio of stress to strain, or modulus. Thus, the ratio of the elastic stress to strain is referred to as the elastic (or storage) modulus (G'), which represents the ability of a material to store energy elastically. The ratio of viscous stress to strain is referred to as the viscous (or loss) modulus (G''), and is the measure of materials ability to dissipate energy. Therefore the stress-strain relationship can be expressed in terms of G' and G'' terms as:

$$\sigma = e_0 G' \sin \omega t + e_0 G'' \cos \omega t \qquad \textbf{(19)}$$

G' and G'' define a complex shear modulus G^*, which indicates the total energy required to deform the material, so that:

$$G^{*} = G^{'} + iG^{''} \quad \textbf{(20)}$$

The ratio of the viscous modulus to the elastic modulus is the tangent of the phase angle shift between stress and strain. The tangent of the phase angle is:

$$\tan \delta = \frac{G''}{G'} \quad \textbf{(21)}$$

Tan δ is a measure of the damping property of the material. For solids, which are purely elastic tan δ equals zero. On the other hand, polymers have several degrees of δ values.

The variation of $G^{'}$, $G^{''}$ and tan δ with frequency is given in Figure 6 [137]. Viscoelastic solid is rubber like and has a low modulus at low frequencies. At high frequencies, the rubber is glassy. These two stages are independent of frequency. On the other hand in the viscoelastic region, modulus increases with frequency. Similarly, loss modulus $G^{''}$ rises to a maximum value. The loss factor tan δ also has a maximum in the viscoelastic region.

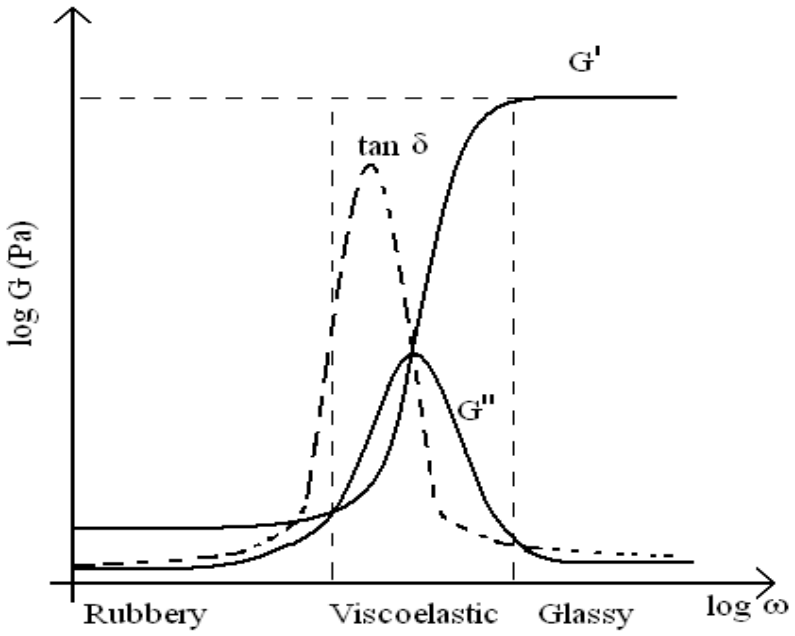

Figure 6 Complex modulus as a function of frequency

Newton's law describes the mechanical behavior of an ideal viscous fluid. When a fluid moves by virtue of being pushed through a pipe, or dragged through a screw in an extruder, etc., the movement is termed shear. Newton's law relates the shear stress (τ) to the rate of strain (or shear rate) $d\gamma/dt$:

$$\tau = \eta \frac{d\gamma}{dt} \qquad \textbf{(22)}$$

Newtonian fluid viscosity is independent of the rate of shear. In polymers, viscosity decreases with increasing frequency or rate of shear. This decrease is a result of the storage of energy in the melt at high rates of deformation [138].

In dynamic measurements on polymer melts, the angular frequency ω becomes analogous to the rate of shear in the usual rheological measurements [139,140]. The complex viscosity can be expressed as:

$$\eta^* = \eta' - i\,\eta'' \qquad \textbf{(23)}$$

The real part of the complex viscosity is an energy dissipation term, just as is the imaginary part of the complex modulus.

$$G' = \omega\eta'' \quad \text{and} \quad G'' = \omega\eta' \qquad \textbf{(24)}$$

Melts of high molecular weight polymers and their concentrated solutions display three characteristic regions, as illustrated in Figure 7. At low shear rates, η is nearly independent of shear rate (i.e. Newtonian behavior) and approaches a limiting zero shear rate value of η_0. At higher shear rates, η decreases with increasing γ. Fluids that display this behavior are termed shear thinning. Finally, η once again approaches a limiting Newtonian plateau, η_∞ at very high shear rate.

The molecular basis for shear thinning behavior is the effect of shear on entanglements, as illustrated in Figure 8. At low shear rates, the entanglements impede shear flow and, therefore, viscosity is high. As the shear rate increases, chains begin to orient in the flow direction and disentangle from one another- the viscosity begins to drop.

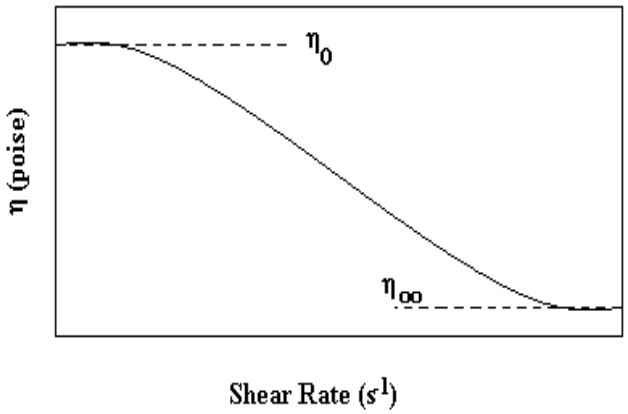

Figure 7 Typical dependence of viscosity of a polymeric melt on shear rate.

Finally, the molecules become fully oriented in the flow direction at very high shear rates. At this point, stable entanglements are no longer possible and the viscosity reaches a low level that is again independent of shear strain rate. This second Newtonian plateau region is observed in the case of polymer solutions, but is rarely observed for polymer melts, because the shear rates required for

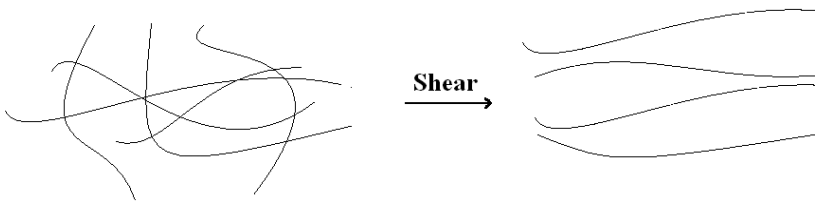

Figure 8 Idealized view of the effect of shear on the entanglements of melts and concentrated polymer solutions.

chain orientation in the melt are so high that the chains actually be broken. In rare cases, viscosity may increase with increasing shear rate. Fluids that exhibit this behavior are called shear thickening (or dilatant).

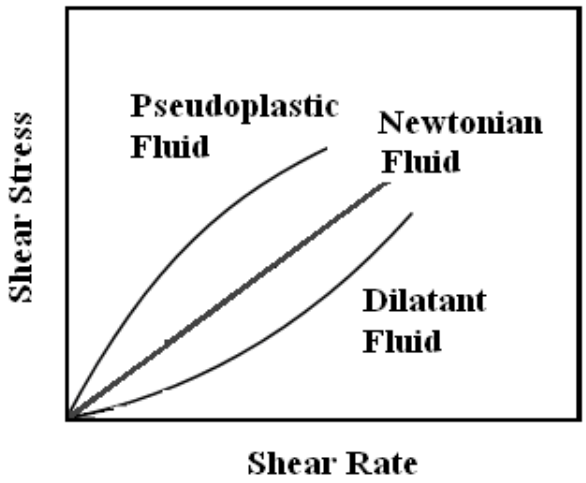

Figure 9 Shear stress versus shear rate of pseudoplastic, dilatant and Newtonian fluids

The significance of entanglements to shear thinning flow suggests that molecular weight should significantly influence the rheological properties of polymers. It has been shown that the zero shear viscosity is directly related to the weight average molecular weight [141].

The viscosity of most polymers changes greatly with temperature. For Newtonian liquids or for polymer fluids at temperatures far above the glass temperature or the melting point, the viscosity follows the Arrhenius equation:

$$\eta = K \exp(Ea / RT) \quad \textbf{(25)}$$

In equation (25), K at a given shear stress is a constant characteristic of the polymer and its molecular weight, Ea is the activation energy of the flow process, R is the gas constant, and T is the temperature in degrees Kelvin. The energy of activation for flow increases as the size of the side groups increases and as the chain becomes more rigid [142]. If activation energy is evaluated at a constant shear stress, Ea is constant independent of the value of shear stress. However, if Ea is evaluated at a constant shear rate, the energy of activation generally decreases with increasing rate of shear [143]. For amorphous polymers at temperatures less than 100 °C above their Tg, equation (25) does not fit the data well. Therefore the Williams-Landel-Ferry equation describes viscosity temperature relation much better [139,144]:

$$\text{Log} \frac{\eta}{\eta_g} = - \left[\frac{17.44(T - Tg)}{51.6 + T - Tg} \right] \quad \textbf{(26)}$$

The viscosity at Tg at low rates of shear is η_g, T is the temperature in degrees Kelvin. Figure 10 illustrates how the viscosity changes with temperature according to both equations (25) and (26).

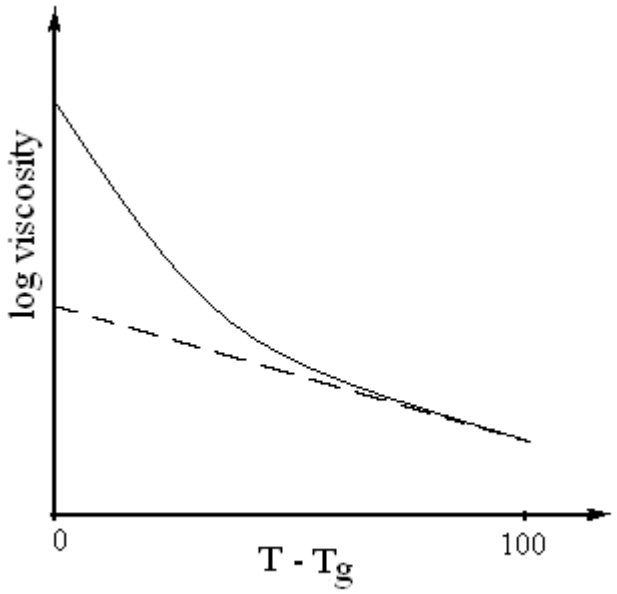

Figure 10 Viscosity as a function of temperature according to W-L-F equation (solid line) and to Arrhenius equation (dashed line)

Rheometers characterize the viscous properties of fluids, as well as the reading their elastic responses. Their name is derived from rheology, which is the study of the behavior of fluids. Samples are subjected to either a dynamic (sinusoidal) or steady shear strain deformation, and then the resultant torque expended by the sample in response to this shear strain is measured. Commercial instrumentation to determine the stress response of polymeric solutions and melts to static or dynamic shear strains is based on simple shear geometries such as cone and plate, Couette cylınder, and rotating paralel plates (Figure 11) [71].

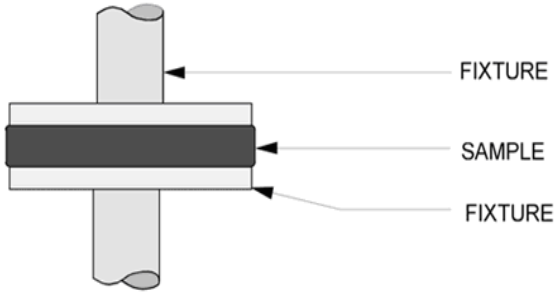

Figure 11 Parallel plate geometry

The apparent viscosity is obtained from steady shear measurements. Values of complex viscosity are obtained by applying an oscillatory rather than steady shear to the cone in a cone-and-plate rheometer or to the cylinder in the case of a Couette rheometer. Alternately, the dynamic properties of polymer solutions and melts can be obtained directly by using steady shear flow in a rheometer with parallel plate geometry [71].

1.5 Nanoparticles

Nanoparticles are defined as particulate dispersions with a size in the range of 10-100 nm. Figure 12 illustrates the main stages of how an individual atom transforms into a bulk metal through a cluster, nanosize and colloidal particles (active metals) [145].

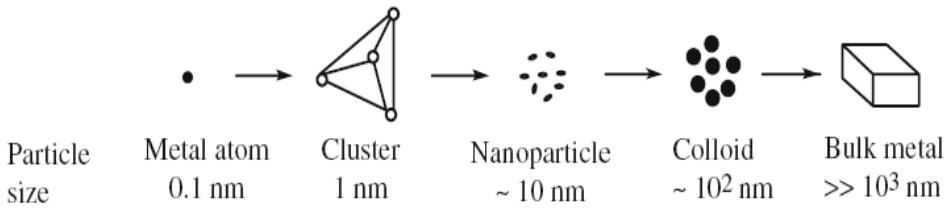

Figure 12 The main stages of the transformation metal atoms into a bulk metal

There exist many methods for the preparation of nanoparticles. Most widely used method is based on chemical reactions on solution. Nano sized metals with sizes in the range of 1-50 nm are obtained as a dispersion of a solid in liquid. Reduction of metal salts produces small metal particles of varying size distributions. Reducing agents used include alcohols [146], glycols [147], and metal borohydrides [148]. Fined particles that are produced tend to aggregate in order to reduce their high surface energy. Additives that reduce the surface energy can restrain aggregation. Stabilizing agents are added to overcome the aggregation of particles. These agents employed include surfactants such as long chain thiols, amines, and polymers [149]. The use of polymers as steric stabilizers is effective because of their intensive short range steric repulsions that they are able to produce. In addition, the advantage of using polymeric stabilizer allows isolating and storing clusters in a stable polymer embedded form.

Particle size and the size distribution are the most important characteristics of nanoparticle systems. Depending on the size of particle present, nanoparticle

containing solutions posses different colors. The biological properties, toxicity, antibacterial performance are determined by the obtained size of the particles.

1.6 Aim of the study

The purpose of this work was to synthesize and to study the properties of polyurethane acrylate polymers based on PEG, two types of acrylate: MMA and HEMA, and three types of diisocyanates: TDI, HDI and MDI. The effects of the diisocyanate nature, termination type of urethane, the thermal and the rheological properties of the resulting polymers were investigated. The results were discussed in the light of specific interactions such as hydrogen bonding. In addition to structural characterization, the cytotoxicity of the polymers was investigated with the addition of silver nanoparticles.

CHAPTER 2

EXPERIMENTAL

2.1 Chemicals and Purification Procedures

2, 4 – Tolylenediisocyanate (TDI)

Supplier: Aldrich

Molecular Formula: $C_9H_6N_2O_2$

Molecular Weight: 174.16 g/mole, 95%.

Chemical Structure:

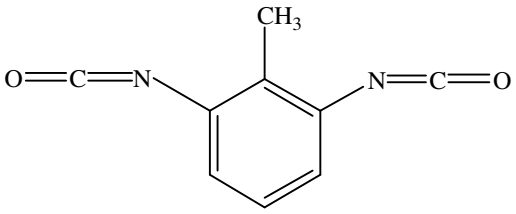

2,6 isomer

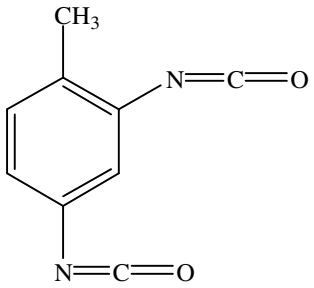

2,4 isomer

Purification Procedure:

TDI was distilled under vacuum and stored at 4 ºC under nitrogen atmosphere. Purity of the reagent was checked before every set of reaction with NMR spectroscopy.

Methylene diphenyl diisocyanate (MDI)

Supplier: Aldrich

Molecular Formula: $C_{15}H_{14}N_2O_2$

Molecular Weight: 250.26 g/mole

Chemical Structure:

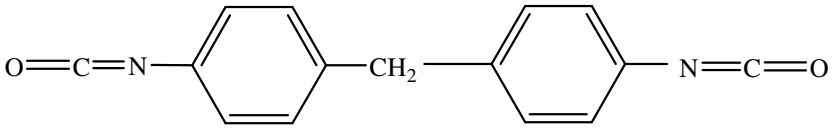

Purification Procedure:

MDI was distilled at 150ºC under vacuum. It was stored at 4 ºC under nitrogen atmosphere. Its purity was checked before each reaction with NMR spectroscopy.

1, 6 Hexane diisocyanate (HDI)

Supplier: Acros Organics

Molecular Formula: $C_8H_{12}N_2O_2$

Molecular Weight: 168.19 g/mole, 99.5%.

Chemical Structure:

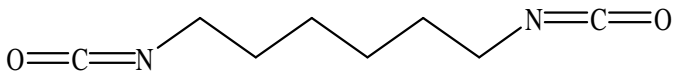

Purification Procedure:

HDI was used as received without any further purification. It was stored at 4 ºC under nitrogen atmosphere and purity was checked before every reaction with NMR spectroscopy.

Polyethylene glycol (PEG)

Supplier: Sigma Aldrich

Molecular Formula: $(C_2H_4O_2)_n$

Molecular Weight: 200,600, 1000, 6000 g/mole

Chemical Structure:

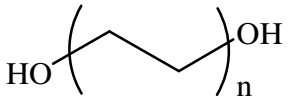

Purification Procedure:

PEG was dehydrated at 80ºC under vacuum for 2 hours and fresh PEG was used for each set of reaction to remove any absorbed moisture.

1, 4 Butanediol (BD)

Supplier: Aldrich

Molecular Formula: $C_4H_{10}O_2$

Molecular Weight: 90.12 g/mole

Chemical Structure:

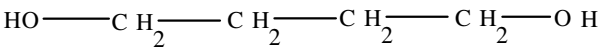

Purification Procedure:

Butanediol was distilled under vacuum and fresh BD was used for each reaction.

Methyl methacrylate (MMA)

Supplier: Acros Organics

Molecular Formula: $C_5H_8O_2$

Molecular Weight: 100.12 g/mole, 99%.

Chemical Structure:

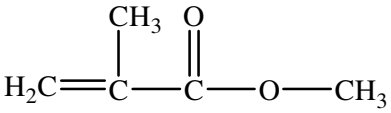

Purification Procedure:

MMA was washed twice with aqueous 5% NaOH to remove hydroquinone and twice with water. It was dried with $CaCl_2$, then with CaH_2 under nitrogen at reduced pressure. The distillate was stored at low temperature and redistilled before use.

2-Hydroxy ethyl methacrylate (HEMA)

Supplier: Acros Organics

Molecular Formula: $C_6H_{10}O_3$

Molecular Weight: 130.14 g/mole

Chemical Structure:

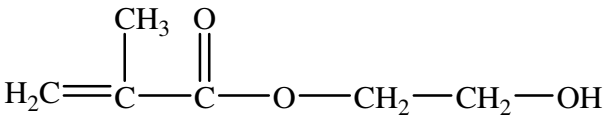

Purification Procedure:

The purity of the reagent was checked with NMR and used as received. HEMA was distilled under reduced pressure when necessary.

Methyl ethyl ketone (MEK)

Supplier: Acros Organics

Molecular Formula: C_4H_8O

Molecular Weight: 72.11 g/mole, 99+ %.

Chemical Structure:

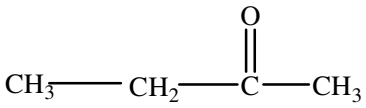

Purification Procedure:

MEK was used without further purification since its purity is better than 99%.

Dibutyl tin dilaurate (DBTDL)

Supplier: Aldrich

Molecular Formula: $(C_4H_9)_2Sn\ (O(O)C\ (CH_2)_{10}CH_3)_2$

Molecular Weight: 631.56 g/mole, 95%.

Chemical Structure:

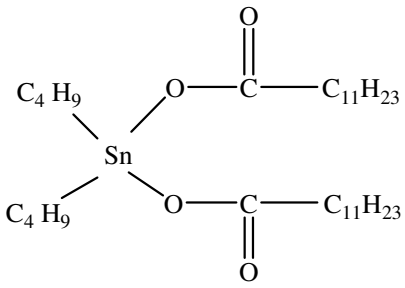

Purification Procedure:

DBTDL was used as catalyst without further purification. The concentration of the catalyst is usually around 100 ppm in the polyurethane synthesis reactions.

Methacryloyl chloride (MAC)

Supplier: Fluka

Molecular Formula: C_4H_5OCl

Molecular Weight: 104.54 g/mole, 97%.

Chemical Structure:

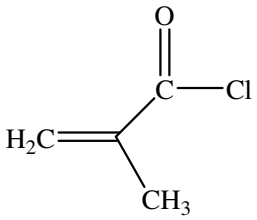

Purification Procedure:

Methacryloyl chloride was used as received. It was stored at -10ºC and after each addition nitrogen was flushed into the bottle.

Azobisisobutyronitrile (AIBN)

Supplier: Aldrich

Molecular Formula: $C_8H_{12}N_4$

Molecular Weight: 164.21 g/mole

Chemical Structure:

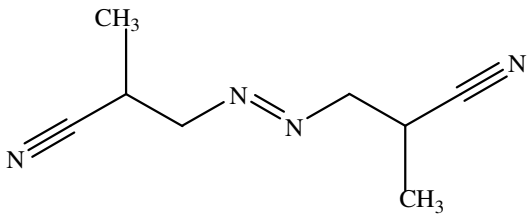

Purification Procedure:

It was used without further purification.

Silver nitrate ($AgNO_3$)

Supplier: Aldrich

Molecular Formula: $AgNO_3$

Molecular Weight: 169.88 g/mole

Chemical Structure:

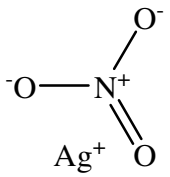

Purification Procedure:

No purification was applied and it was used as received.

Sodium borohydrate ($NaBH_4$)

Supplier: Aldrich

Molecular Formula: $NaBH_4$

Molecular Weight: 37.83 g/mole

Chemical Structure:

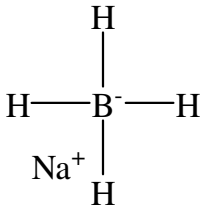

Purification Procedure:

No purification was applied and it was used as received.

Toluene

Supplier: Aldrich

Molecular Formula: $C_6H_5CH_3$

Molecular Weight: 92.14 g/mole, 99%.

Chemical Structure:

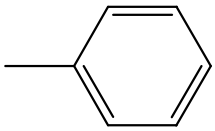

Purification Procedure:

No purification was applied and it was used as received.

Methanol (MeOH)

Supplier: Aldrich

Molecular Formula: CH_3OH

Molecular Weight: 32.04 g/mole, 95%.

Chemical Structure:

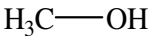

Purification Procedure

No purification was applied and it was used as received.

Hydroquinone

Supplier: Aldrich

Molecular Formula: $C_6H_4 (OH)_2$

Molecular Weight: 101 g/mole

Chemical Structure:

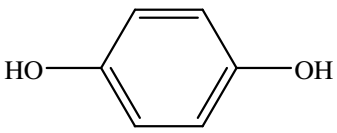

Purification Procedure

No purification was applied and it was used as received.

2.2 Synthesis Methods

2.2.1 Polyurethane synthesis via one step solution polymerization under vacuum

Polyurethane was synthesized via a one step solution polymerization of 1,4 butanediol (BD) and toluene 2,4 diisocyanate (TDI) under vacuum conditions with the addition of a catalyst dibutyltindilaurate (DBTDL) in toluene. An example of a divalent tin compound acting as a catalyst is illustrated in Figure 13 [150].

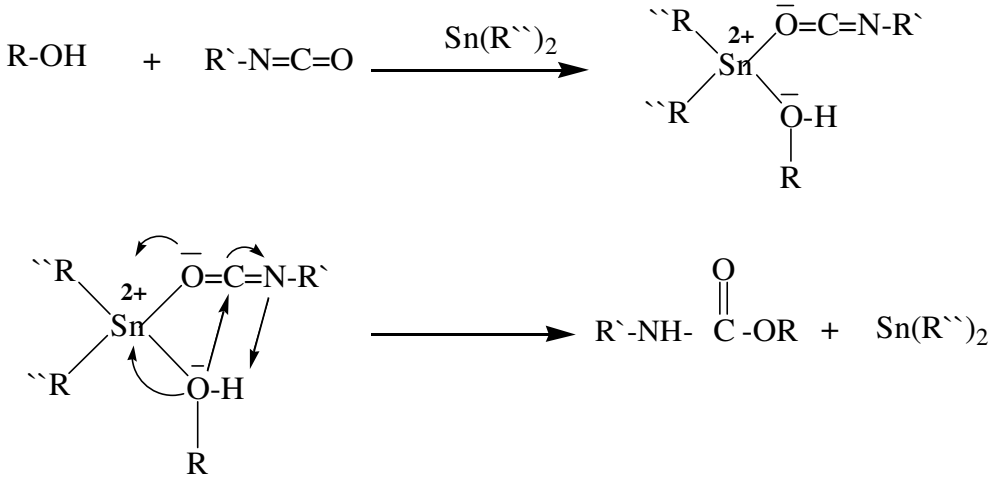

Figure 13 Proposed mechanism for the alkyl tin catalyst in polyurethane synthesis.

Polymerizations were conducted at 60, 70, 90ºC temperature in a circulating water bath for 1 day, 1 week and 1 month periods for varying BD / TDI ratios

of 1:1.0, 1:1.5, 1:2.0 . The reaction procedure is given below, using equal molar amounts from each reactant.

0.01 mole from each reagent (BD, 0.901 gr; TDI, 1.74 gr) was put into toluene (10 ml) separately and cooled down to 5ºC. These two solutions were combined as a stock solution and DBTDL (100 ppm) was added at 5ºC. From this stock solution 4 ml was taken and transferred to a Pyrex test tube. In this way 5 test tubes that contain same amount of stock solution were prepared and each tube was then cooled down to liquid nitrogen temperature. These tubes were connected to vacuum line in order to attain inert atmospheric conditions and tubes were degassed three times under the vacuum with the removal of N_2 dewars. After 6 hours, vacuum line was disconnected and tubes were taken without interrupting the vacuum.

When proposed polymerization periods were completed, Pyrex tube heads were broken and the synthesized polymers, in the form of a white solid, were filtered and precipitated from toluene and then dried in a vacuum oven. Characterization of the obtained polymers was carried out by several spectroscopic and thermal analysis methods.

2.2.2 Polyurethane synthesis via prepolymer route

Polyurethane was synthesized via a two step prepolymer route by the reaction between a difunctional polyether polyols; PEG (Mn=200, 600, 1000 and 6000 g/mol) and an equal molar amount of diisocyanate; TDI. Polymers were prepared in three-neck, round bottom, 250 ml Pyrex reaction flasks equipped with an addition funnel carrying a nitrogen inlet, reflux condenser, an immersion thermometer and a Teflon clad magnetic stirring bar as illustrated in Figure 14. The nitrogen purge was maintained throughout the synthesis to ensure a dry atmosphere and to minimize the side reactions between NCO and

residual moisture. Synthesis of polymer from PEG (Mn=200 g/mol) and TDI is used here as a representative procedure.

Dried PEG (0.01 mole, 2 g) was charged into a round bottom Pyrex flask. TDI (0.01 mole, 1.74 g) was mixed with MEK (50 ml) and stirred under the purge of nitrogen gas. This solution was added to dried PEG drop wise through the dropping funnel under the nitrogen stream at room temperature. High molecular weight diols were solid at room temperature, therefore before the TDI addition, they were heated to their melting temperatures. When diisocyanate addition was completed, DBTDL (100 ppm) catalyst was added to the system and the solution was stirred for 2 hours at 60ºC. Polymerization reaction continued until all the NCO was consumed. NCO concentration was determined by titration method using di-n-butyl amine back titration as described in ASTM D-2572 [151]. The final product was a viscous, yellow fluid. It was washed with the 1:1 mixture water-methanol several times and dried in a vacuum oven at 80ºC for 1 day.

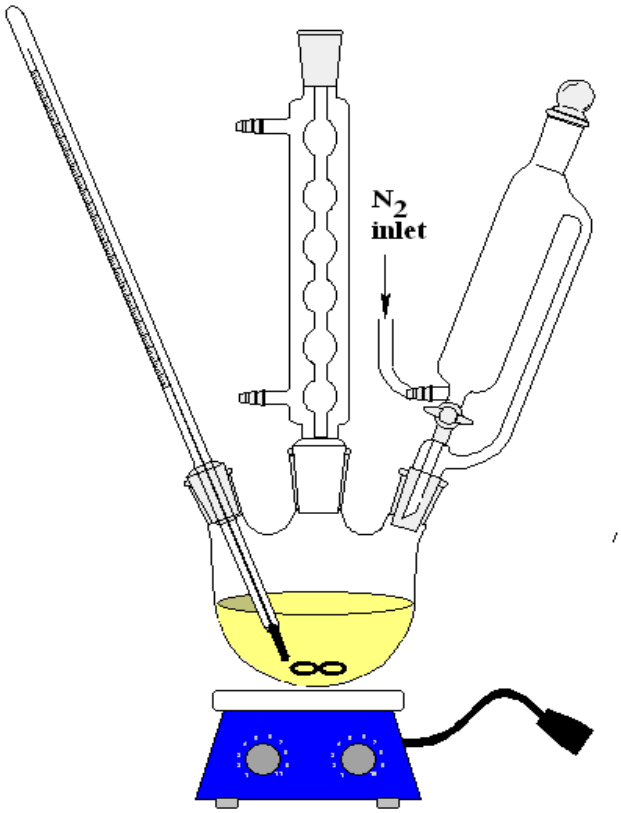

Figure 14 Apparatus for the urethane synthesis

2.2.3 Isocyanate Terminated Prepolymer synthesis

Isocyanate terminated urethane prepolymers were synthesized by the reaction between a difunctional polyether polyol; PEG (Mn=200 g/mol) and a diisocyanate; TDI, MDI and HDI. Prepolymers were prepared in three-neck, round bottom, 250 ml Pyrex reaction flask equipped with an addition funnel carrying a nitrogen inlet, reflux condenser, an immersion thermometer and a Teflon clad magnetic stirring bar. The nitrogen purge was maintained throughout the synthesis to ensure a dry atmosphere and to minimize the side reactions between NCO and residual moisture. Synthesis of prepolymer from

PEG (Mn=200 g/mol) and TDI is used here as a representative procedure (Figure 15).

A certain amount of dried PEG (0.01 mole, 2 g) was charged into a round bottom Pyrex flask. TDI (0.02 mole, 3,48 g) was mixed with MEK (50 ml) and stirred under the purge of nitrogen gas. This solution was added drop wise via dropping funnel with continuous stirring under the nitrogen stream to the diol containing flask at room temperature. When diisocyanate addition was completed, DBTDL (100 ppm) catalyst was added to the system. For the synthesis involving TDI, the reaction between NCO and OH groups was much faster compared to other diisocyanates, and did not require any catalyst. After stirring the solution for 4 hours, temperature was increased gradually to 60ºC. During the polymerization, MEK (50 ml) was added to reduce the viscosity. Polymerization reaction continued until the theoretical NCO concentration was obtained. NCO concentration was determined by titration method using di-n-butyl amine back titration as described in ASTM D-2572 [151]. The final product was a viscous fluid having a color that changes from yellow to brown depending on the diisocyanate used.

2.2.4 Hydroxyl Terminated Prepolymer synthesis

Hydroxyl terminated urethane prepolymers were synthesized by the reaction between a diisocyanate; TDI, MDI and HDI, and an excess of difunctional polyester polyol; PEG (Mn=200 g/mol) (Figure 16). Prepolymers were prepared in a three-neck, round bottom, 250ml Pyrex reaction flask equipped with an addition funnel, a reflux condenser, a thermometer and a magnetic stirrer. Synthesis of prepolymer from PEG (Mn=200 g/mol) and TDI is given in the below procedure as an example.

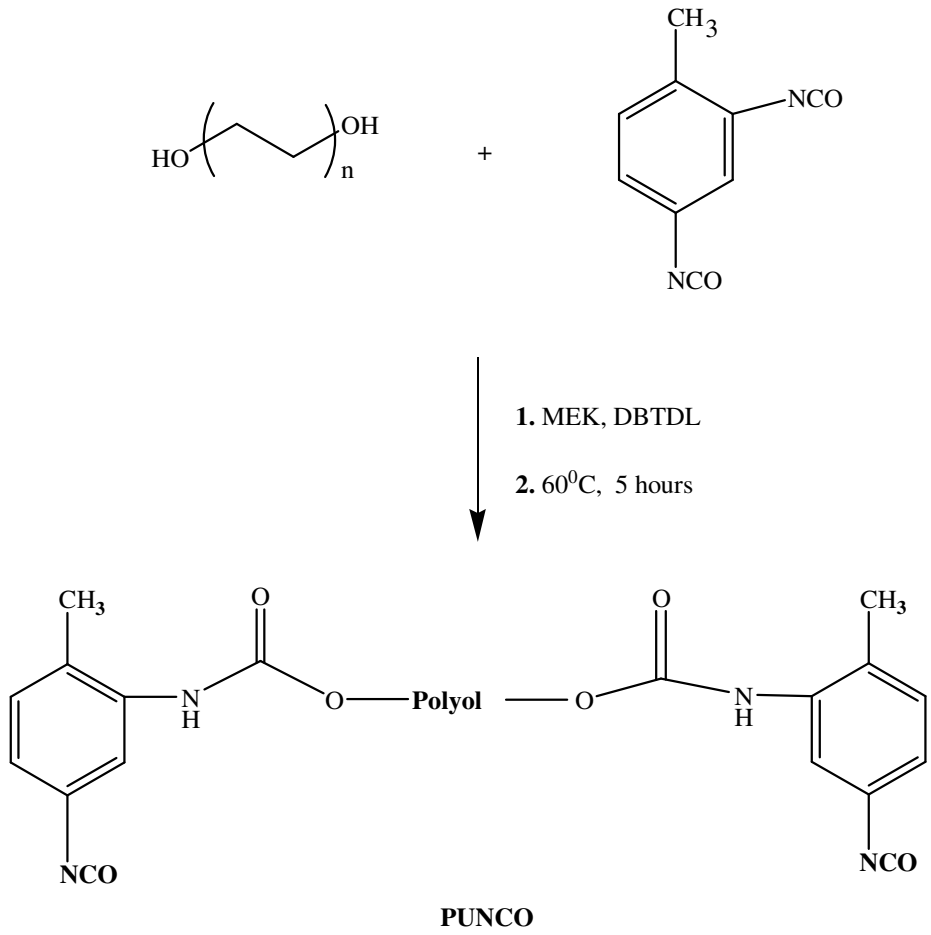

Figure 15 Isocyanate terminated prepolymer synthesis

Dried PEG (0.02 mole, 4 g) was poured into a flask containing MEK (50 ml). TDI (0.01 mole, 1.74 g) mixed with MEK (50 ml) was added through the dropping funnel under the nitrogen atmosphere. Solution was stirred with magnetic stirrer continuously. When addition of TDI was completed, DBTDL (100 ppm) catalyst was added and reaction was continued for 4 hours at 40ºC. In addition to di-n-butyl amine back titration method, NCO concentration was monitored by examining the disappearance of the vibration band at 2270 cm^{-1} in the ATR-FTIR spectrum.

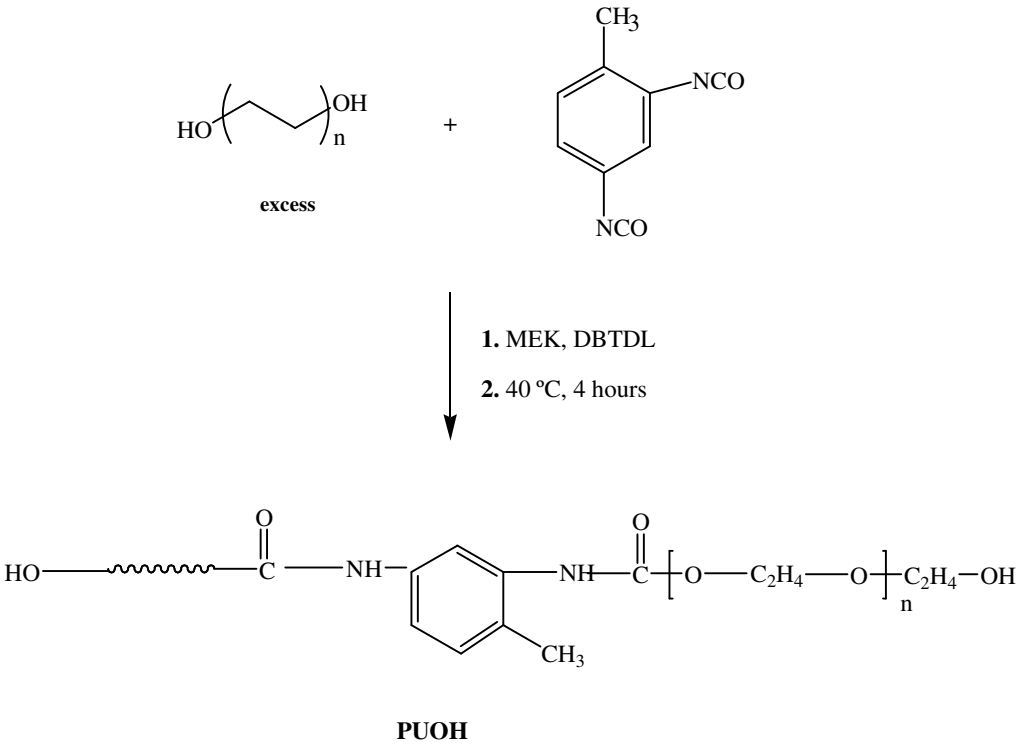

Figure 16 Hydroxyl terminated prepolymer synthesis

2.2.5 Acrylate End Capping of Isocyanate Terminated Polyurethane

Isocyanate terminated urethane prepolymers were end capped with acrylate monomers, MMA and HEMA. The end capping reaction procedure with MMA is as follows (Figure 17):

The reaction kettle containing diisocyanate terminated urethane prepolymer obtained in section 2.2.3, was charged with MMA (0.02 moles, 2.00 g) which was vacuum distilled and then stabilized with hydroquinone (100 ppm). DBTDL (100 ppm) catalyst was added and solution was mixed for 2 hours at 30ºC under the nitrogen gas flush. After the addition of AIBN (1 wt % based on acrylate, 0.02 g), reaction temperature was first raised to 50ºC for 2 hours

and then to 70ºC for 3 hours. Obtained polymer was filtered and washed with water and methanol several times and transferred to glass Petri dishes and dried in a vacuum oven at 80ºC for 1 day.

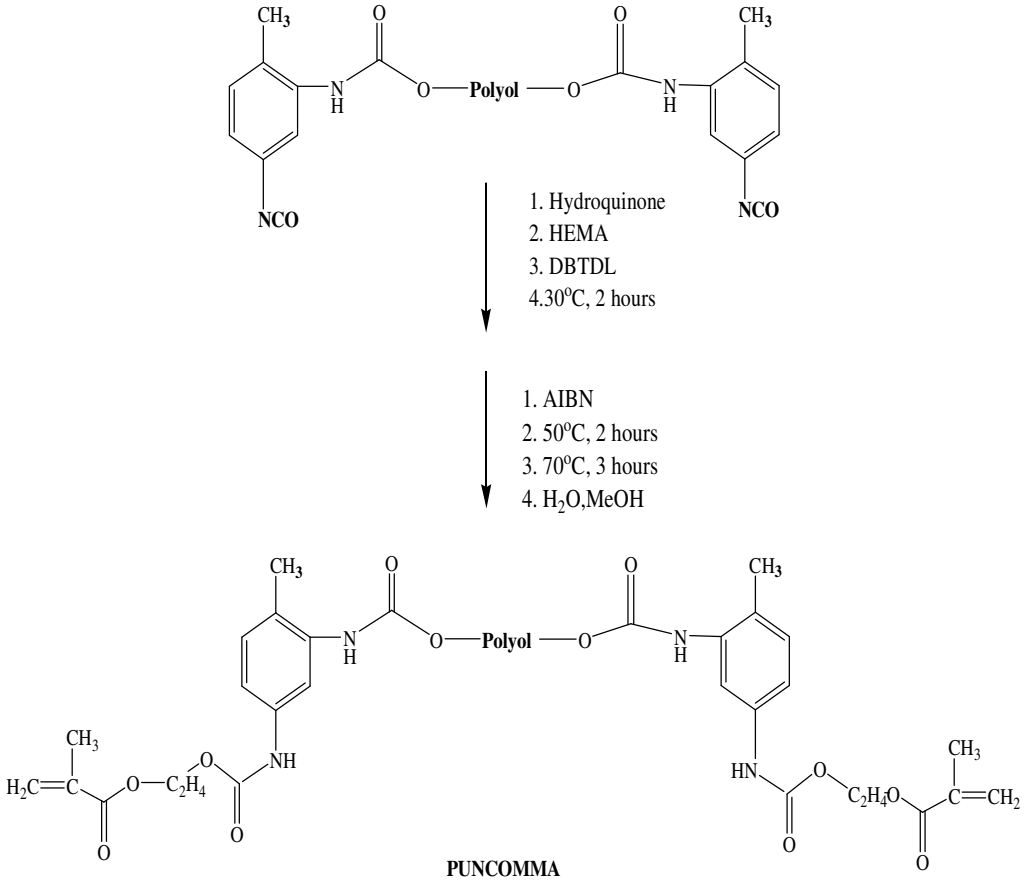

Figure 17 Acrylate end capping reaction procedure of isocyanate terminated polyurethane

2.2.6 Acrylate End Capping of Hydroxyl Terminated Polyurethane

Hydroxyl terminated urethane prepolymers were end capped with acrylate monomers, MMA and HEMA with the use of MAC catalyst for the first time. Possible reaction mechanism for the catalyst is given in Figure 18. The reaction procedure is schematically represented in Figure 19.

Hydroxyl terminated urethane prepolymer obtained at section 2.2.4 was diluted with MEK (100 ml) in order to decrease possible viscosity increase at low temperatures. Then mixture was cooled down to -5ºC with the dry ice bath.

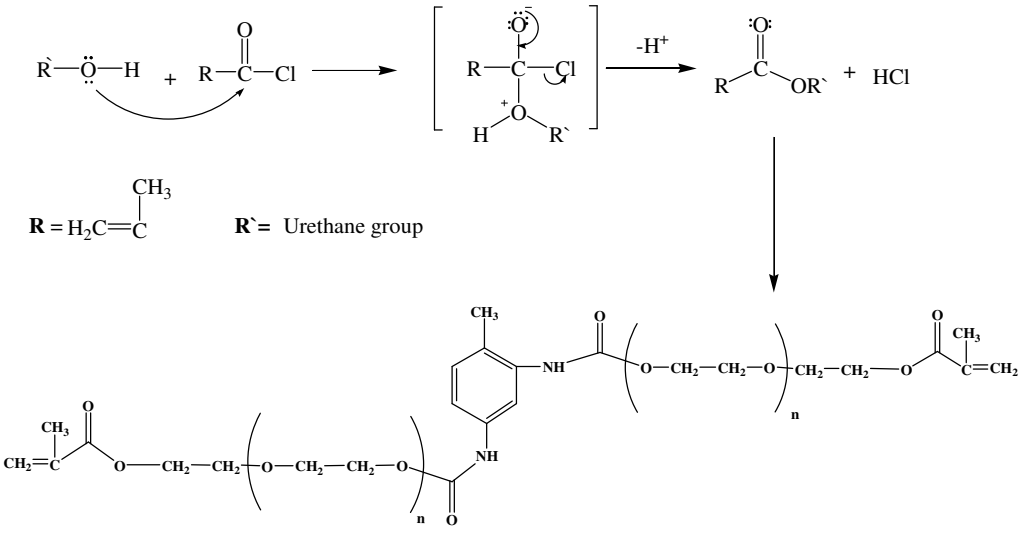

Figure 18 Reaction of methacryloyl chloride with hydroxyl ends

Temperature was maintained at this level for 30 minutes and with vigorous stirring MAC (1 ml) was added drop wise under the nitrogen atmosphere. It was allowed to react for 30 minutes. After then, hydroquinone and MMA (0.02

mole, 2.00 g) was added and mixture was stirred for an hour at -5ºC. Bath was removed and temperature increased to 30ºC gradually and reaction continued at this temperature for 1 hour. Following the addition of AIBN (1 wt % based on acrylate, 0.02 g), reaction temperature was first raised to 50ºC for 2 hours and then to 70ºC for 3 hours. Obtained polymer was filtered and washed with water and methanol several times and dried in a vacuum oven at 80ºC for 1 day.

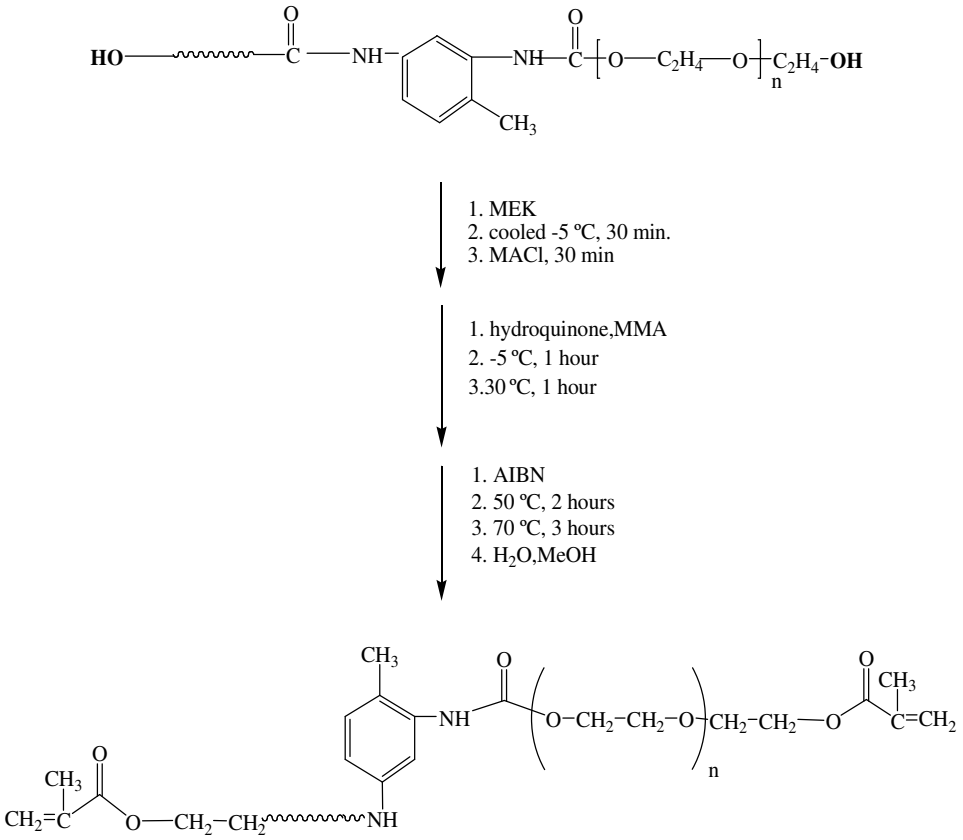

Figure 19 Acrylate end capping reaction procedure of hydroxyl terminated polyurethane

2.2.7 Ag nanoparticle preparation

Ag nanoparticles were prepared from the reduction of $AgNO_3$ with $NaBH_4$ (27). A 10-mL volume of 1.0 mM silver nitrate wasadded dropwise (about 1 drop /second) to 30 mL of 2.0 mM sodium borohydride solution that had been chilled in an icebath. The reaction mixture was stirred vigorously on a magnetic stir plate. The solution turned light yellow after the addition of 2 mL of silver nitrate and a brighter yellow when all of the silver nitrate had been added. The entire addition took about three minutes, after which the stirring was stopped and the stir bar removed. The clear yellow colloidal silver is stable at room temperature stored in a transparent vial.

$$AgNO_3 + NaBH_4 \longrightarrow Ag + 1/2H_2 + 1/2\, B_2H_6 + NaNO_3 \qquad \textbf{(27)}$$

2.3 Characterization Methods

2.3.1 Fourier Transform Infrared Spectroscopy (FTIR)

Fourier Transform Infrared (FTIR) spectra were recorded on a Bruker Vertex 70 FTIR spectrometer (Bruker Optics Inc., Ettlingen, Germany) using attenuated total reflectance (ATR) attachment (PIKE Technologies, USA) which has a MIRacle diamond crystal. All spectra were collected in between 4000- 600 cm^{-1} range using 16 scans with a resolution of 4 cm^{-1} in transmission mode. The spectra data were acquired by using OPUS 5.5 software.

2.3.2 Proton NMR Spectroscopy (^{1}H NMR)

^{1}H NMR spectra of polymers were obtained by Bruker 300 MHz NMR spectrometer (BioSpin, Ettlingen, Germany). DMSO-d_6 was used as a solvent. The sample concentration was approximately 8 mg/ml. The proton signals were referenced to tetramethylsilane (TMS) at 0 ppm as the internal standard. The data were evaluated by using XWINNMR software.

2.3.3 Carbon NMR Spectroscopy (^{13}C NMR)

^{13}C NMR spectra of polymers were obtained by Bruker 300 MHz NMR spectrometer (BioSpin, Ettlingen, Germany). Deuterated DMSO was used as a solvent. The data were evaluated by using XWINNMR software.

2.3.4 Gel Permeation Chromatography (GPC)

Polymer Laboratories, PL-GPC 220 GPC spectrometer (Varian Inc., England) was used in determining the number average molecular weight (Mn) and weight average molecular weight (Mw) of polymers using polystyrene standards. The samples were dissolved in (1% w/v solutions) dimethyl formamide, which was used also as a carrier solvent at a rate of 1ml/min.

2.3.5 Differential Scanning Calorimetry (DSC)

DSC thermograms were recorded to characterize the thermal properties of the obtained polymers. The measurements were performed on a Perkin Elmer (Massachusetts, USA) instrument provided with an intra-cooler device. Measurements in the temperature range –70 to 150ºC at heating rate of 10ºC /min under a nitrogen atmosphere were performed. Standard 40 µl alumina pans with perforated lids, were used. Some of the analysis was done with TA-

DSC910 S instrument with a heating rate of 10ºC/min under a nitrogen atmosphere from -50ºC to 300ºC.

2.3.6 Thermal Gravimetric Analysis (TGA)

TGA of obtained polymers were carried out on a Perkin Elmer Pyris TGA-FT-IR spectrometer (Massachusetts, USA).Thermograms were recorded in a temperature range of 25 – 500ºC with a heating rate of 10ºC/min under 20ml/min nitrogen atmosphere.

2.3.7 Mass Spectrophotometer (MS)

Waters, Quattro Micro GC, tandem quadrupole mass spectrometer (MA, USA) was used to obtain the mass spectra. Spectrometer is equipped with dedicated electron impact source and was utilized within the 18-1000 dalton m/z range. Heating rate was as follows: sample was heated up to 50ºC and remained there for 1 minute and after that, every minute temperature was increased 50ºC up to 500ºC. At this temperature spectrometer, waited 1 minute and analysis completed at a total time of 11 minutes.

2.3.8 Scanning Electron Microscopy (SEM)

SEM micrographs of sample surfaces that were coated with 2 nm AuPd were taken with, Quanta 400 microscope FEI Company (Netherlands) at a magnification of x150 and x 10000, respectively.

2.3.9 Particle Size Analyzer

The average particle size and particle size distribution of the dispersions were determined by Malvern Nano ZS90 (Worcestershire, UK). Measurements of the Ag nano particle sizes were carried out at room temperature.

2.3.10 Rheological Analysis

TA Instruments ARES Rheometer (NewYork, USA), working in a temperature range of 30-120°C with a ramp rate of 1°C/min and with a frequency range of 0.1-10 rad/s was used to investigate the rheological response of the polymers. Paralel plates with 25 mm plate diameter was used.

2.3.11 Cytotoxicity

Cytotoxicity tests were assessed as described in ISO 10993-5 Standard [152]. The test was performed on an extract of nano particle added polymers and extraction was performed in sterile, chemically inert closed containers.

Sample Preparation: 0.1 g from each sample was weighed for 1 ml of culture medium. Three replicates were used for each group. Samples were kept for 45 min under ultraviolet light to prevent bacterial contamination, and then they were aged with Dulbecco's modified Eagle medium/Ham's F12 nutrient mixture 1:1 (DMEM/F12) (Biochrom, Germany) medium in a humidified incubator at 37°C for 24 hours and 1 week. After each aging interval, the extracts were kept in -20°C. When the aging of all the samples completed, the extracts were used to assess cytotoxicity.

Cell Line: The cells used for the experiments were L929 mouse skin fibroblasts (L929, 95030802 HUKUK, Ankara, Turkey). The cells were grown as monolayer cultures in T25-flasks, subcultured three times a week at 37°C in an atmosphere of 5 % CO_2 in air and 100% relative humidity and maintained at third passage.

Culture Medium: The culture medium (pH= 7.3) was Dulbecco's modified Eagle medium/Ham's F12 nutrient mixture 1:1 (DMEM/F12) supplemented

with 10% (v/v) fetal bovine serum (FBS) (Biochrom, Germany) with 1 % gentamycine as antibiotics. Adherent cells at a logarithmic growth phase were detached with a mixture of 0.025 % trypsin and 0.02 % ethylenediamineteraacetic acid (EDTA) (Biochrom, Germany), incubated for 5-10 min at 37 °C and used for cell inoculation.

Cell viability assays (MTT assay)

The L-929 cell suspension was prepared at a concentration of $4x10^4$cell /ml and dispensed onto 96-well cluster cell culture plates (100 µL/well). The 96-well plates were incubated at 37ºC, 5 % CO_2 in air for 24 h. After 24 h, the culture medium was removed from the wells and equal volumes of the experimental material were added into each well. In control wells, 100 µL DMEM/F12 with 10 % FBS was added and incubated at 37ºC, 5 % CO_2 in air for 24 h. After 24 h the test extracts were removed and added 100 µL/well growth medium and 5 µL MTT was added to each well and kept in a dark environment for 4 h at 37 °C. Then, MTT was aspirated and 100 µL/well growth medium and 11 µL MTT were added to each well and kept in a dark environment for 4 h at 37ºC. Then, MTT was aspirated and 100 µL/well of 2-propanol was added to each well. Subsequently, the absorbance at 570 nm was measured using a UV-visible spectrophotometer (Molecular Devices, USA). MTT assay was repeated in three separate experiments.

CHAPTER 3

RESULTS AND DISCUSSION

3.1 Polyurethane synthesis

3.1.1 Polyurethane synthesis under vacuum

PU synthesized from 2,4-TDI and BD under vacuum as described in section 2.2.1, is depicted schematically below (28). The average values of the percent conversion results obtained after 1 day, 1 week, and 1 month periods at different temperatures are given in Appendix A. Since the obtained conversions are very low, they were not considered here. Compositions of these oligomers which were synthesized at 40ºC are given in Table 3. They are abbreviated with the letter 'v', which means that they were synthesized under vacuum. In order to understand the effect of soft segment on the properties of the synthesized PU, amount of BD was increased whereas the molar amount of TDI was kept constant.

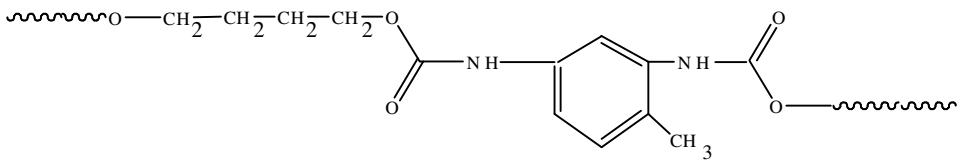

(28)

In addition to vacuum synthesis, polymers with the same composition were synthesized with solution polymerization at different temperatures as the way described in section 2.2.2. The initial composition of these polymers (PU1, PU2 and PU3) is also given in Table 3. Percent conversion of the polymer synthesized from the reaction of BD and TDI in 1:1 ratio via solution polymerization at 40, 60, 70, 90ºC and nature of the final product were given in Table 4. At higher temperatures, the control on the reaction is limited and therefore undesired gelation starts. However, the best thing is to reach the highest conversion without formation of gel. From the Table 4, it can be seen that gelation was not a problem at low temperature. In order to increase the conversion, some other methods have to be evaluated as using suitable catalysts or promoters. This was achieved with altering the other polymerization conditions.

Table 3 Chemical composition and equivalent ratios of synthesized polyurethanes

Sample	**Chemical Composition**	**Equivalent Ratio**	**Mn (g/mol)**	**Mw (g/mol)**	**Polydispersity (Pd)**
PU1v[a]	TDI/BD	1:1	469	906	1.82
PU2v[a]	TDI/BD	1:1.5	480	811	1.69
PU3v[a]	TDI/BD	1:2	466	805	1.73
PU1	TDI/BD	1:1	4426	8917	2.02
PU2	TDI/BD	1:1.5	2602	4869	1.87
PU3	TDI/BD	1:2	3709	4655	1.25

[a] vacuum synthesis

Table 4 Temperature versus percent conversion of PU1 (NCO/OH =1)

Temperature (ºC)	Percent Conversion	Nature of Product
40	73	Viscosity increased
60	84	gelation
70	82	gelation
90	89	Gelation and solidification

The molecular weights of the samples were determined by GPC method and the results are given in Table 3. Number average molecular weights of the polymers synthesized from varying the ratio of the isocyanate group to the hydroxyl group under vacuum conditions were compared and they are found to be almost the same and have a value between 400-500 g/mole. These low values can be attributed to the insufficient mixing of reactants and also the low temperature value (liquid nitrogen temperature) during the evacuation of the tubes. At this type of low temperature, isocyanates usually give self polymerization (homopolymer). Therefore, the molecular weights measured are much lower compared to the molecular weight obtained with the solution polymerization. Both the molecular weight and the poly dispersivity index (Pd) showed almost the same values which means that the vacuum polymerization might be prominent in some of the preparations. In this case the undesired affect of presence of oxygen is eliminated and also temperature control can be done much easily. The main purpose is to obtain low molecular weights with Pd close to 1 at this stage (before curing).

The molecular weight distribution of PU1 is given in Figure 20 as a representative distribution. The molecular weight distribution of PU1 gave a

mono model peak with a wide base. The molecular weight distributions of the other polymers are represented in Appendix B. The number average (Mn) and weight average (Mw) molecular weight of PU1 were 4426 and 8917 g/mol respectively (Table 3). Pd of 2.02 shows a narrow distribution in overall chain of products. Molecular weight is relatively increased when the BD amount is increased in the feed. There is a regular change in the weight average molecular weights which decreased with the BD ratio going from 1 to 2. However, the same trend is not observed for Mn. This can be due to the overall conversion in which low molecular weight fractions are higher at high conversions. Therefore, the fluctuation in Mn as observed will be more noticeable. Thus, the Pd decreased regularly in the given order.

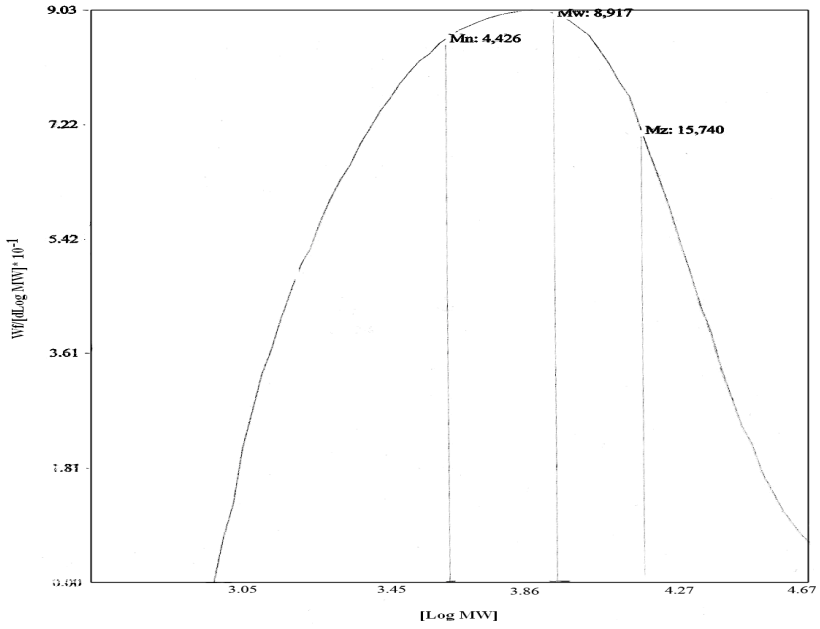

Figure 20 Molecular weight distribution of PU1

ATR-FTIR Analysis Results

FTIR is a well established analytical technique for functional group analysis and to study the hydrogen bonding and phase separation behavior of polyurethanes. The frequency shifts in hydrogen bonded N-H and carbonyl peaks relative to free N-H and C=O peaks determine the extent of hydrogen bonding and microphase separation between hard and soft segments [153-158]. If hydrogen bonding exists only within the hard segment domains (due to the hydrogen donor N-H group), phase separation occurs. On the other hand, if they can be formed between the hard and the soft segments, the interphase hydrogen bonding enhances the degree of phase mixing (Figure 4) [159]. Characteristic IR absorption frequencies of polyurethanes are listed in Table 5.

FTIR-ATR spectrum (4000-600 cm^{-1}) of PU1 is provided in Figure 21 together with the spectrum of TDI. The vibration band at 2240 cm^{-1} in the FTIR-ATR spectrum of TDI points out the presence of isocyanate groups which is not present in PU1 spectrum. Intensity of this band decreases as the polymerization proceeds and disappears at the end.

The spectrum of PU1 is mainly characterized by bands at 3150-3450 cm^{-1} (NH stretching vibrations), 2800-3000 cm^{-1} (CH stretching vibrations: symmetric and asymmetric), 1650-1750 cm^{-1} (amide I: C=O stretching vibrations), 1601 cm^{-1} (C-C stretching vibration, aromatic), 1532 cm^{-1} (amide II) [160], 1450 cm^{-1} (CH_2 scissoring vibration), 1224 cm^{-1} (amide III), 1057 cm^{-1} (C-O-C stretching vibration, ester group), 999 cm^{-1} (CH_2 rocking), 878 cm^{-1} (C-H bending vibration), 770 cm^{-1} (CH out of plane bending vibration, aromatic). N-H stretching vibration with a peak maximum at 3298 cm^{-1} indicates the presence of strong hydrogen bonding in this compound. This vibration is associated with the N-H…O hydrogen bond [161]. The hydrogen atom of the N-H group in urethane linkages is the donor proton, while the acceptor group can be oxygen atom of the ester group in BD.

Table 5 FTIR-ATR band assignments for polyurethanes

Frequency (cm^{-1})	Group	Assignment[a]
3400-3500	N-H	υ(N-H), free N-H
3310-3350	N-H	υ(N-H), bonded (N-H…O=C)
3260-3300	N-H	υ(N-H), bonded (N-H…O)
2890-3050	C-H	$\upsilon_a(CH_2)$
2850-2880	C-H	$\upsilon_s(CH_2)$
2240-2270	N=C=O	υ(NCO)
1720-1740	C=O	υ(C=O), free C=O
1700-1715	C=O	υ(C=O), bonded (N-H…O=C), disordered
1670-1685	C=O	υ(C=O), bonded (N-H…O=C), ordered
1600-1610	C=C	υ(C=C), aromatic ring
1500-1550	Amide II	δ(C-N-H) + υ(C-N)
1430-1500	C-H	$\delta(CH_2)$
1410-1420	C-C	υ(C-C),aromatic ring
1360-1400	C-H	$\omega(CH_2)$
1200-1300	Amide III	δ(N-H) + δ(C-N)
1100-1120	C-O-C	υ(C-O-C), ether group (soft segment)
1050-1080	C-O-C	υ(C-O-C) , hard segment
1000-1020	C-H	r (C-H)
810-820	C-H	γ(C-H), aromatic ring
765-770	C=O	γ(C=O)

[a] υ =stretching, a=asymmetric, s= symmetric, δ= bending, ω- wagging, r=rocking γ= out of plane bending or twisting.

In addition to hydrogen bonded N-H, there exists a small peak at 3450 cm^{-1} due to free N-H vibration [162]. The free N-H or C=O groups that measured spectroscopically view as end groups of a chain of hydrogen bonded urethane groups [163]. Hydrogen bonding interaction reduces the stretching vibration frequency. Therefore, the hydrogen bonded C=O stretching band appears at lower wavenumber region than that of the free band [164]. In Figure 21, the broad carbonyl peak (amide I region) is in between 1640 and 1770 cm^{-1} with a maximum at 1698 cm^{-1} which corresponds to the region of hydrogen bonded urethane carbonyl stretching vibration.

In order to get semi quantitative information about the extent of hydrogen bonding, carbonyl stretching peak was resolved into three components. The C=O stretching band was deconvoluted as shown in Figure 22, considering peaks as Gaussian and the error associated with the fit was less than 2%. Before deconvolution, a flat baseline was chosen and baseline correction was applied by subtraction of the baseline. The representative peak positions and the integral areas associated with each carbonyl group of PU1 were shown in Table 6. The integral area results revealed that the disordered hydrogen bonded carbonyl component has the greatest contribution to the amide I region.

FTIR-ATR spectra of PU2 and PU3 were compared in Figure 23. The N-H and C=O stretching vibrations shift to lower wavenumber as the amount of diol was raised from 1.5 mole to 2 moles. The N-H band maximum was at 3277 cm^{-1} and 3257 cm^{-1} for PU2 and PU3, respectively. This shift can be attributed to the increase in extent of hydrogen bonding. Similarly, maximum of the carbonyl stretching vibration of PU2 was shifted to 1691 cm^{-1}. On the other hand, the carbonyl region of PU3 has three separate peaks at 1689 cm^{-1}, 1713 cm^{-1} and1738 cm^{-1}. These peaks corresponds to vibrations of hydrogen bonded ordered, hydrogen bonded disordered and free carbonyl bands, respectively.

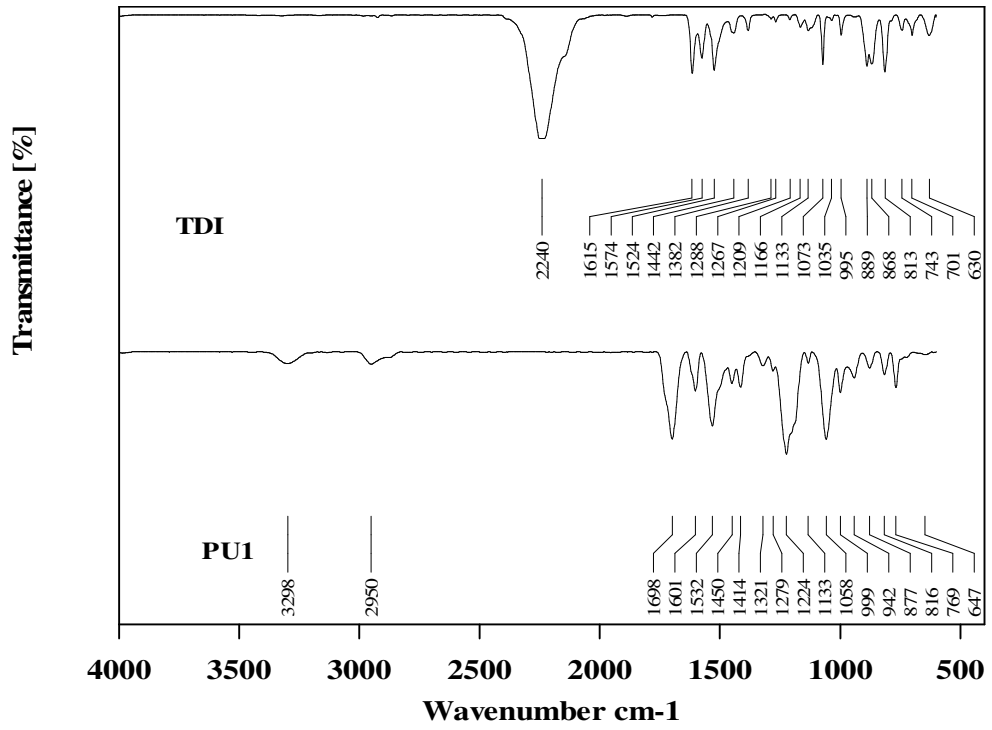

Figure 21 FTIR-ATR spectra of PU1 and TDI

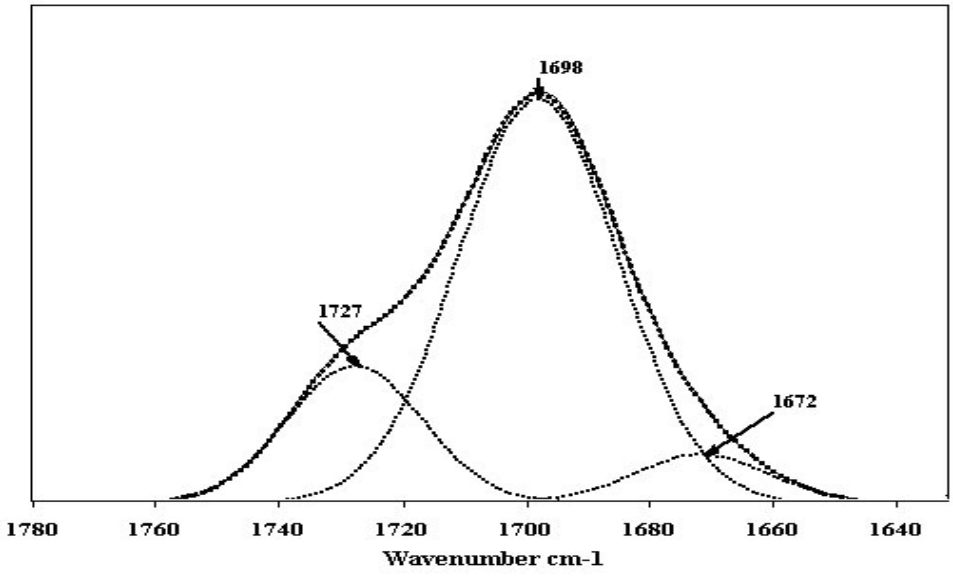

Figure 22 Deconvoluted carbonyl (C=O) region of PU1

Table 6 Deconvolution results of carbonyl peak of PU1

Frequency (cm^{-1})	Integral Area	Carbonyl Group
1672	1.42	Hydrogen bonded, strong, ordered
1698	12.49	Hydrogen bonded, weak, disordered
1727	3.74	Free

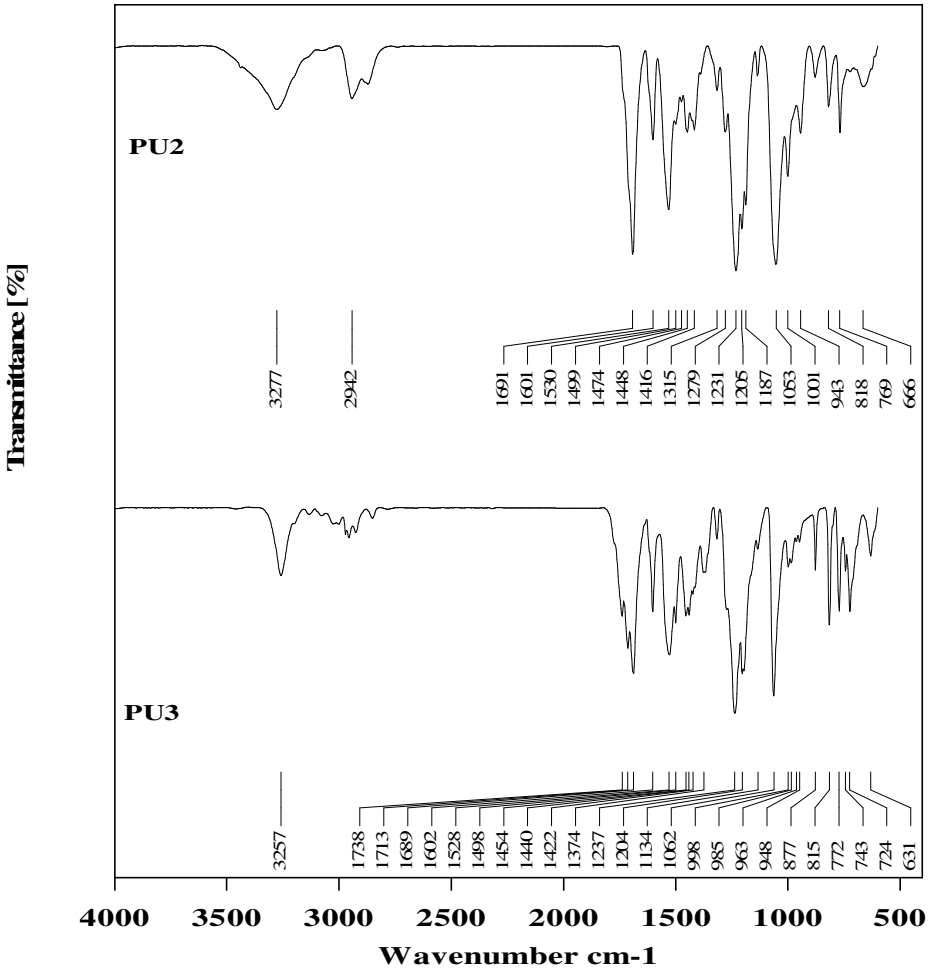

Figure 23 FTIR-ATR Spectra of PU2 and PU3

^{1}H and ^{13}C NMR Analysis Results

The indexed ^{1}H and ^{13}C NMR spectrum of PU1 was given in Figure 24 and 25, respectively. The NMR spectra of the PU2 and PU3 are similar to that of PU1 and therefore are not given here. In the ^{1}H NMR spectrum of PU1, the urethane protons (-NH in urethane) are observed at δ= 8.7, and 9.5 ppm. The NH group ortho to CH_3 will have more steric effect for H bonding (less H bonding) and also due to the electron donating nature of CH_3 will give NMR peak at higher chemical shift value. Thus, the peak at δ= 9.5 ppm is due to the N-H ortho to CH_3 and peak at δ= 8.7 ppm is due to the N-H para to CH_3. The aromatic protons from TDI appeared at δ= 7-7.8 ppm and the methyl proton was assigned to the peak at δ=2.4 ppm. Hydroxyl proton (-OH) was at δ=2 ppm and the $–OCH_2$ protons were found at δ=3.4 ppm. The CH_2 protons present in the BD were at δ=1.3 and 1.6 ppm, respectively.

^{13}C NMR spectrum of PU1 has a carbonyl peak from the urethane group at δ=153 ppm. Aromatic carbons appeared at δ=114, 125, 130, 136 and 137 ppm and were assigned to each carbon in the aromatic ring as shown in Figure 25. The ether carbon peaks were the –OCH at δ=60 and 64 ppm and $–CH_2$ at δ= 26 and 29 ppm. Methyl carbon attached to the aromatic ring was observed at δ=17 ppm. Both in ^{1}H and ^{13}C NMR spectra there were additional peaks which can be assigned to the residual solvent MEK present in the PU1.

In this type of molecules the resonance for amide groups are usually observed. This can be detected with the presence of small double bond peaks at the area of 4.5- 6.5 ppm in ^{1}H NMR and that of ^{13}C NMR at 115-130 ppm range. In the ^{1}H and ^{13}C NMR spectrum of PU1, the resonance peaks were not observed which is due to the conformation stability of the molecule.

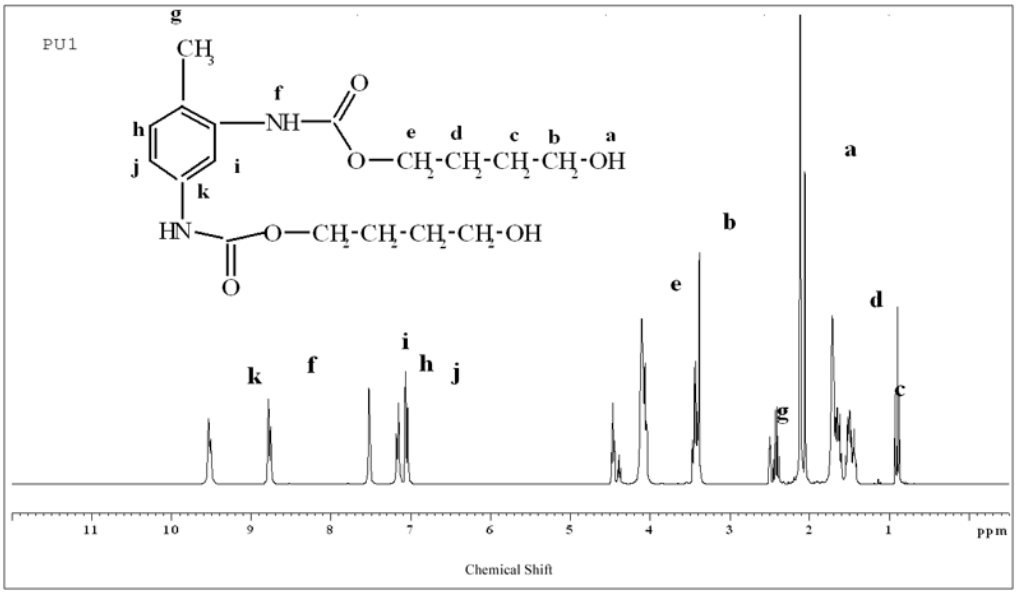

Figure 24 ^{1}H NMR spectrum of PU1

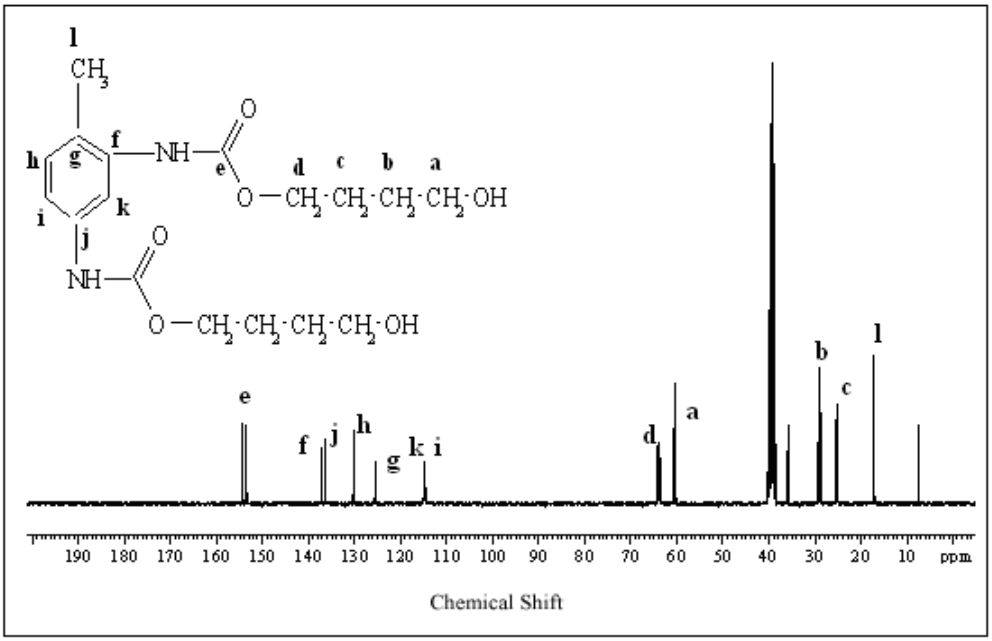

Figure 25 ^{13}C NMR spectrum of PU1

Thermal Analysis Results

Thermal stability of PU1 and PU3 in a temperature range of 30-400ºC was evaluated from the TGA data derived from the thermogravimetric analysis under N_2 atmosphere. The corresponding TGA curves of PU1 and PU3 are given in Figure 26 and 27. The derivative thermogravimetric (DTG) curves of PU1 and PU3 showed degradation in three stages. First stage, which is maximized at about 120ºC, is due to the residual solvent evaluation that might not be removed during the drying processes. The second stage is in between 125 up to 240ºC, and maximized at 205ºC. This stage corresponds to the side group linkage degradations and degradation of the small molecular weight fractions. The first stage corresponds to about 10% and second stage to about 20% weight loss. The third stage is the main chain degradation and maximized at around 290ºC. The regular trend of degradation is in between depolymerization and regular random degradation. Up to 400ºC about 5% of polymer is not degraded and this may be due to aromatization of the phenyl groups (char yield). These groups can be stable at very high temperatures. In the second stage of degradation the curve is very smooth which most probably shows that there is end group cyclization which is expected for the given structure.

TGA thermogram of PU3 shows three degradation steps again but there is an important difference in the second stage contrary to the case of PU1, in which the thermogram has a smoother change in the second stage and this ended up with a new trend at about 250ºC. However, in PU3 thermogram, the curve is continuous and does not show a noticeable change. Thus, in PU1 the end group cyclization is predominant, but not in PU3 which shows a random degradation trend.

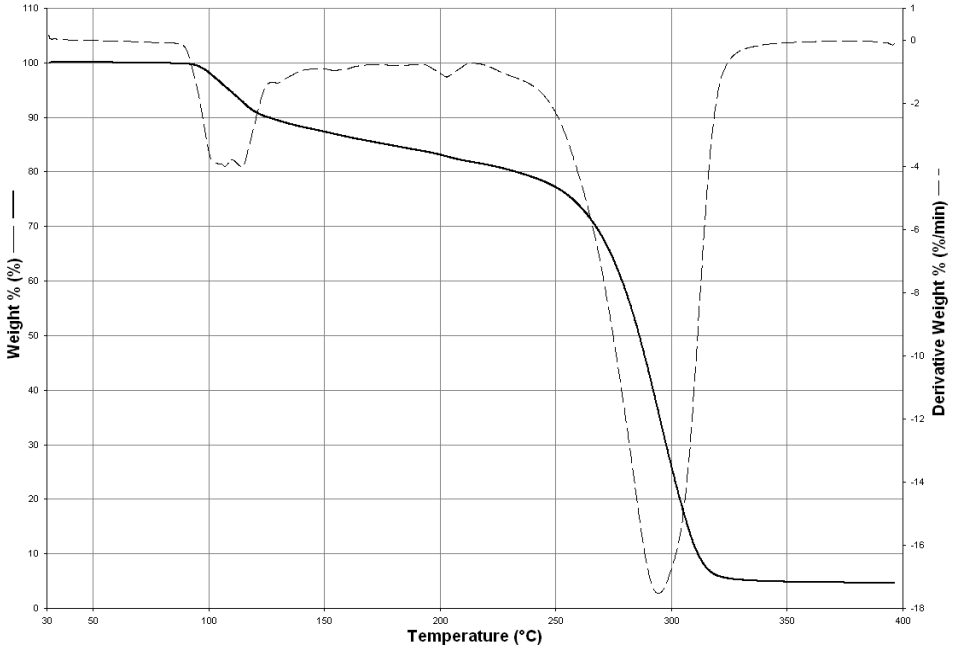

Figure 26 TGA thermogram of PU1

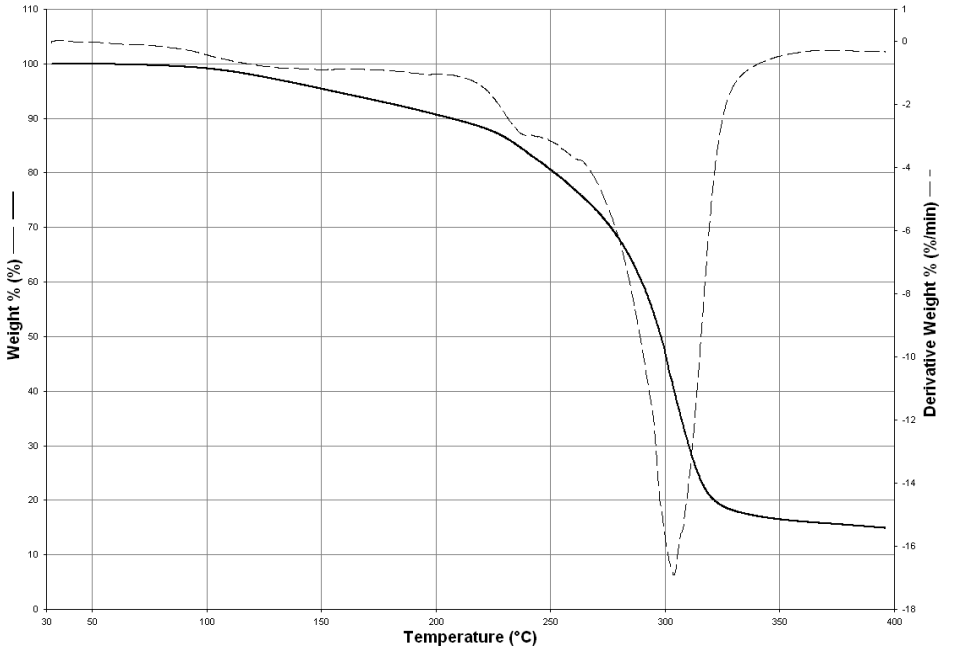

Figure 27 TGA thermogram of PU3

DSC thermogram of PU1 is given in Figure 28. The temperature range of the thermogram is in between 25-250ºC. Therefore, the expected Tg at lower temperatures is not observed in the thermogram. The exothermic curing peak centering at 97ºC showed further polymerization and the curing of the sample. This also gives a rearrangement regularity of the chain which shows a melting peak at 231ºC (liquid crystalline form in which phase separation of hard and soft segments appeared on a wide range). The DSC thermogram of PU3 is taken in the range of (-70) – $(140)^0$C and given in Figure 29. In this thermogram, Tg value is observed at -33.7ºC and the trend up to 140ºC is not changed. Thus, there is no further curing for this polymer which is also supported by second run thermogram which is identical with that of first run.

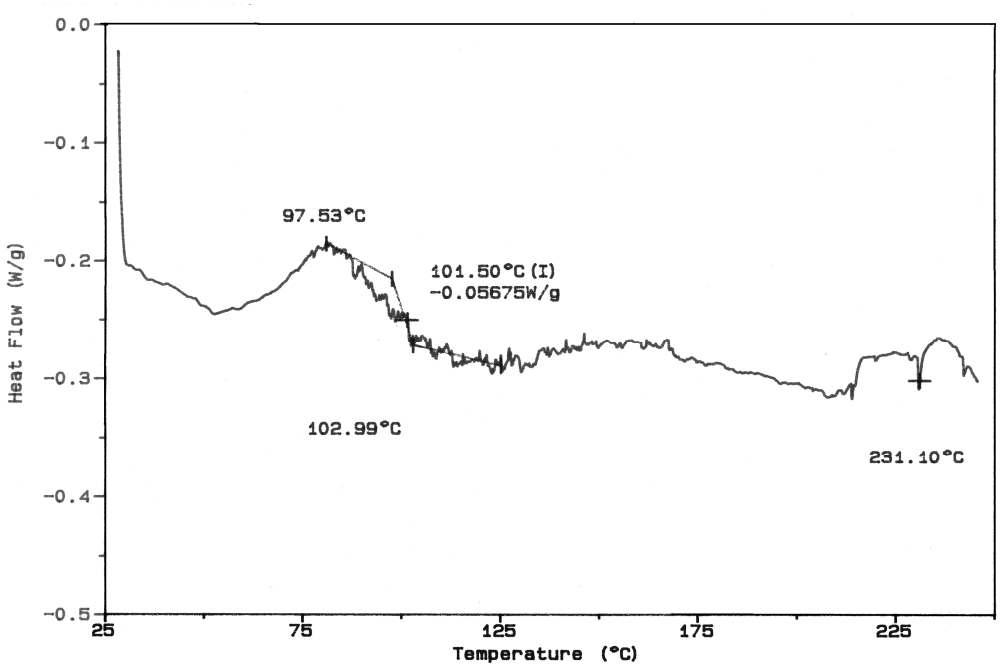

Figure 28 DSC thermogram of PU1

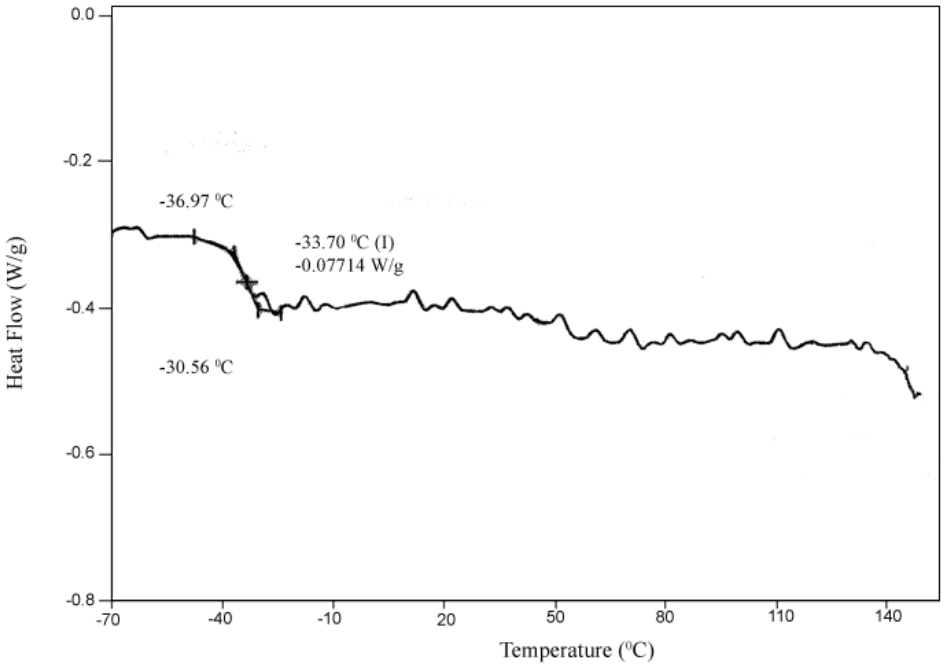

Figure 29 DSC thermogram of PU3

3.1.2 Polyurethane synthesis via prepolymer route solution polymerization

Molecular structure of the prepolymers synthesized as in the way described in section 2.2.2 have the below structure (29) and were given in Table 7. All of the polymers had an equal hydroxyl to isocyanate ratio of 1:1. The effect of soft segment molecular weight was investigated with the same diisocyanate, TDI.

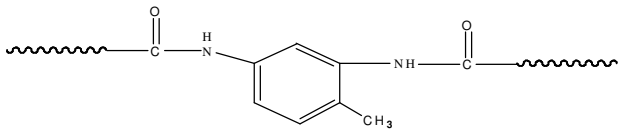

(29)

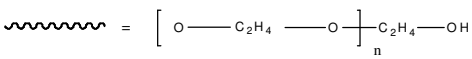

Table 7 Chemical composition of synthesized PU prepolymers

Sample Name	Chemical Composition
PU5	TDI/PEG(200)
PU6	TDI/PEG(600)
PU7	TDI/PEG(1000)
PU8	TDI/PEG(6000)

FTIR-ATR Analysis Results

The FTIR-ATR spectra of the polymers synthesized are given in Figure 30. All the polymers have N-H stretching vibration around 3300 cm^{-1}, due to the N-H bonded to the etheric oxygen present in the PEG. The amide I vibrations were on the free carbonyl vibration side and appeared at 1727 cm^{-1}. Other characteristic vibrations are located at 1601 cm^{-1}, 1535 cm^{-1}, 1225 cm^{-1}, 1094 cm^{-1}, 768 cm^{-1},due to υ(C=C), Amide II (δ(C-N-H)+υ(C-N)), Amide III (δ(N-H)+δ(C-N)), ether group υ(C-O-C) and γ(C=O) respectively. In the spectrum of both PU7 and PU8 there is a vibration band at 1966 cm^{-1} and similarly same vibration band is appeared at 1959 cm^{-1} in the FTIR-ATR spectrum of PU6. This band is attributed to the formation of lactones or lactams with the extended PEG segments.

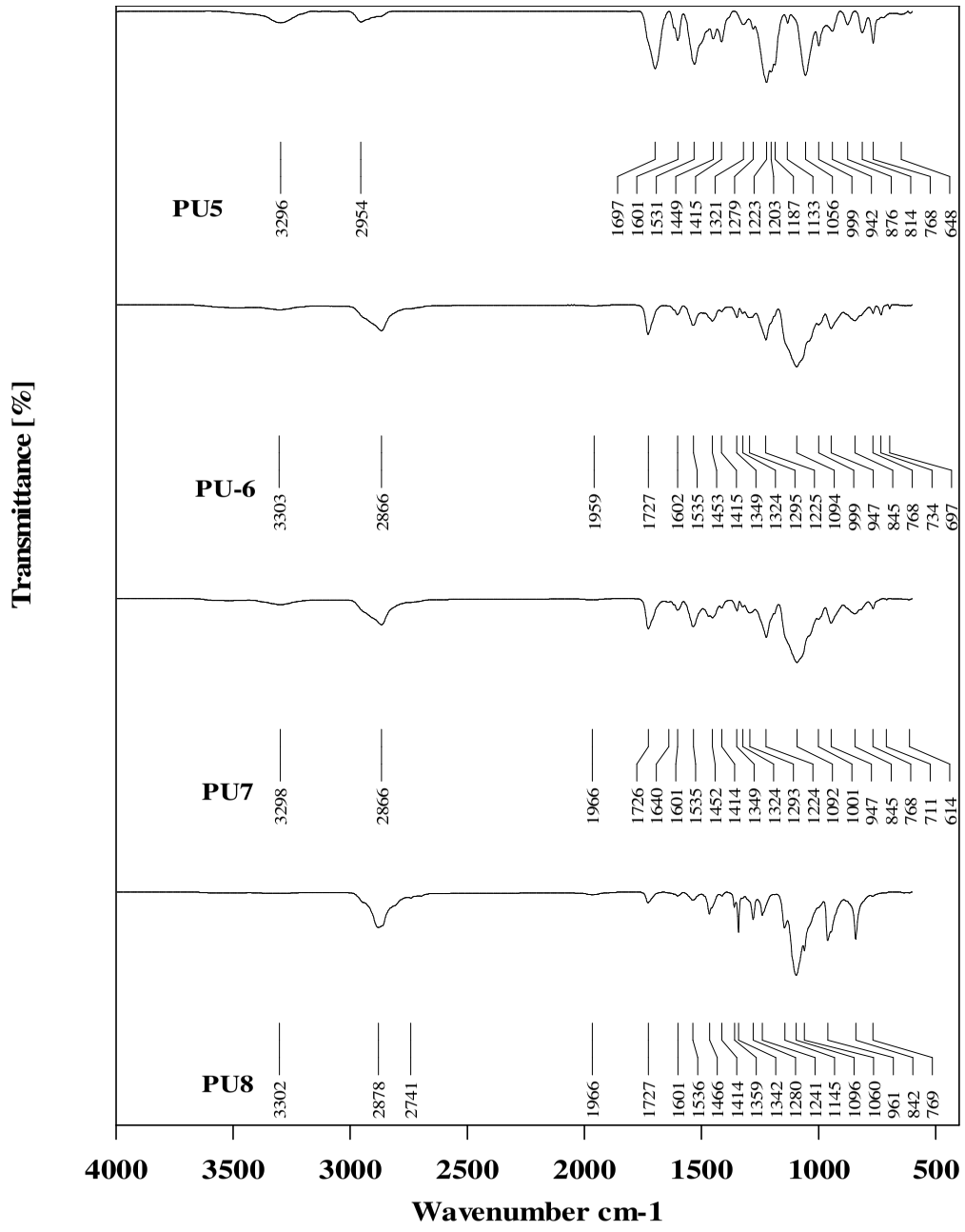

Figure 30 FTIR-ATR spectra of PU5, PU6, PU7, and PU8

^{1}H and ^{13}C NMR Analysis Results

The ^{1}H NMR spectrum of PU7 is given in Figure 31. It was observed that the chemical shifts are similar to that of PU1 (Figure 24). Main difference in PU7 proton NMR spectrum was the peak that appeared between δ=3.3-3.8 ppm which is attributed to the $–CH_2$ protons of the PEG. The urethane protons (-NH in urethane) are observed at δ= 8.9 and 9.6 ppm, aromatic protons appeared at δ= 7.0-7.6 ppm, -OH proton was at δ=4.5 ppm and $–OCH_2$ protons were at δ=3.5-3.6 , $C(O)-OCH_2$ protons were at δ=4.1- 4.3 ppm. There were peaks of the residual solvent MEK. The resonance peaks for amide groups are observed at δ=5.8-6.5 ppm in ^{1}H NMR due to the presence of small double bond peaks.

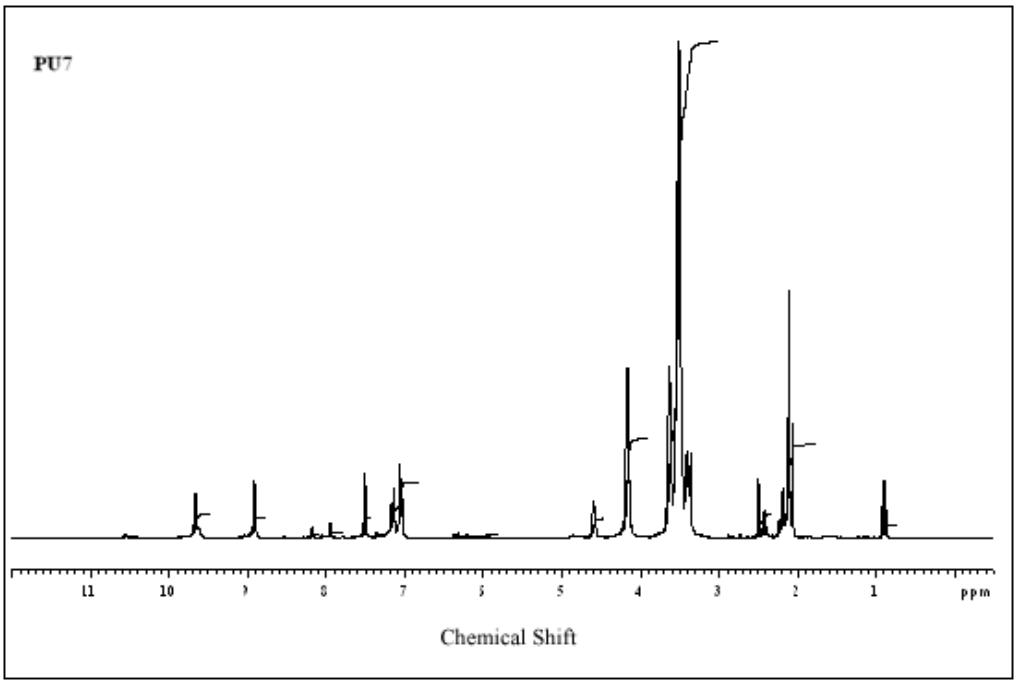

Figure 31 ^{1}H NMR spectrum of PU7

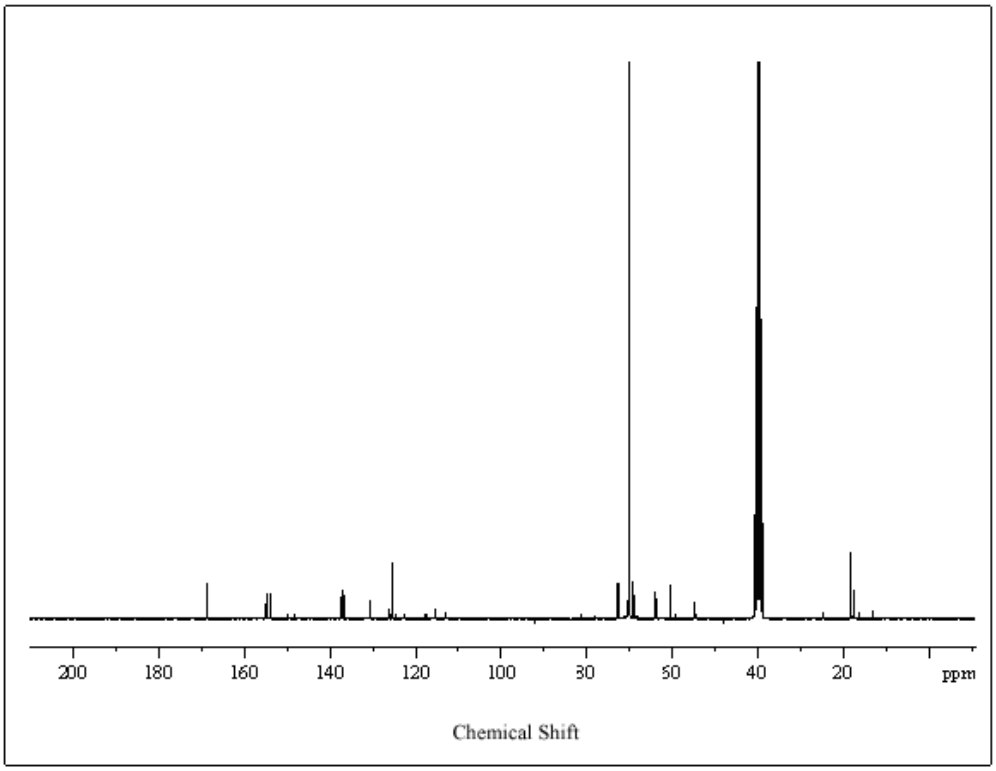

Figure 32 ^{13}C NMR spectrum of PU7

Carbon NMR spectrum of PU7 is given in Figure 32. The carbonyl peak from the urethane groups are at δ=154,155 ppm. Aromatic carbons appeared at δ=110-140 ppm. The ether carbon peaks were the –OCH at δ=60 and 64 ppm and $–CH_2$ at δ= 26 ppm. Methyl carbon attached to the aromatic ring was observed at δ=17 ppm. Both in ^{1}H and ^{13}C NMR spectra there were additional peaks which could be assigned to the residual solvent MEK present in the PU7.

Thermal Analysis Results

Thermal behavior of the urethanes was investigated with TGA thermograms. A representative curve for PU7 was given in Figure 33. The weight loss is

starting after 100ºC and continuously decreased by 5% up to 300ºC. Then the decrease rate is increased and maximized at 340ºC by weight loss reaching 20%. A new degradation trend is started at this temperature, and maximized at 410ºC up to 450ºC where the total weight loss is 90%. After 440ºC the material is stable but there might be small decreases up to high temperatures but still 10 % of material remained as char which is as explained before as caused by the aromatization. The general degradation mechanism is a random scission type degradation type.

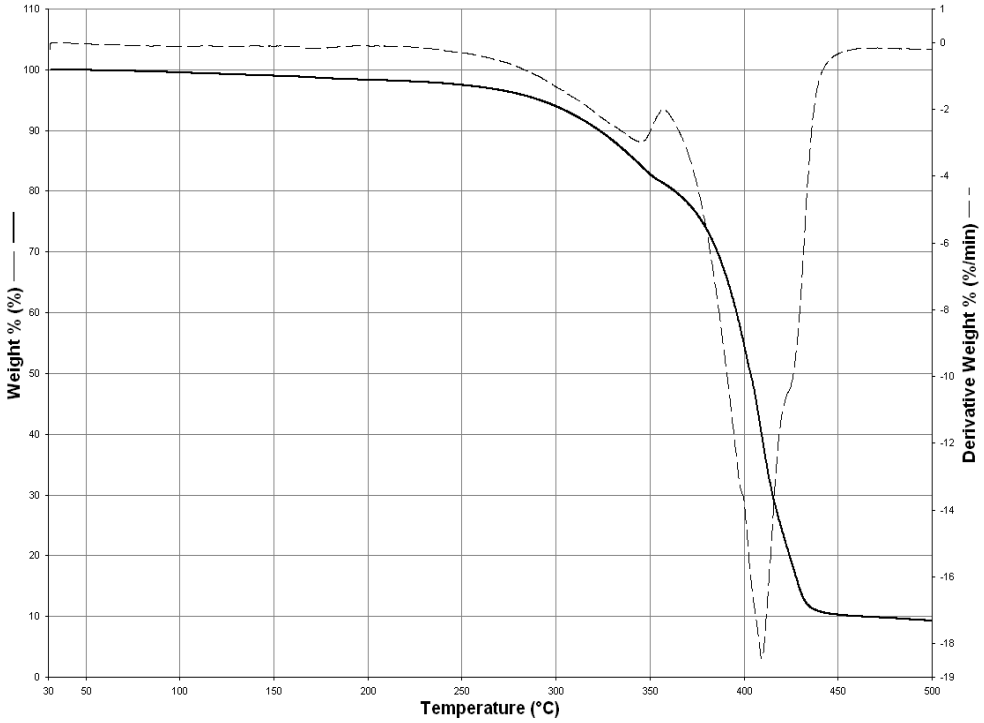

Figure 33 TGA thermogram of PU7

The DSC thermogram of PU7 (Figure 34) is almost identical with that of PU3 (Figure 29). The temperature range of the thermogram is in between (-70) - (140) ºC. Tg value is observed at -32.88ºC which is close to the Tg of PU3.

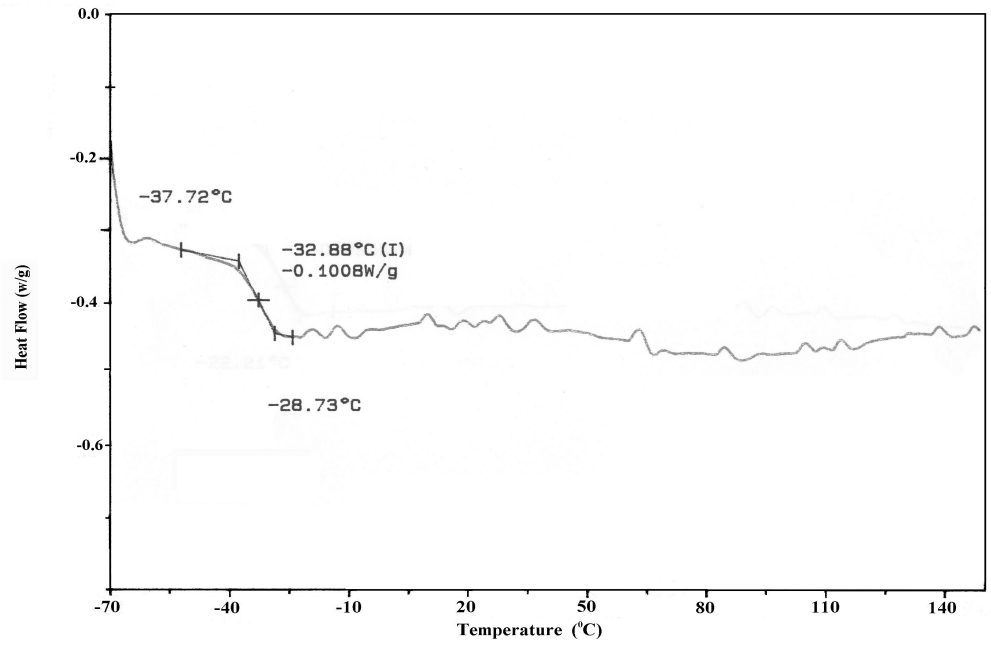

Figure 34 DSC thermogram of PU7

Mass Analysis Results

The mass thermogram of PU7 is given in Figure 35. The thermogram is recorded up to 11.0 minutes, which corresponds to the temperature range of 50-500ºC. Fragmentation takes place in four stages. Under 100ºC solvent evaporation takes place. The maximum fragmentation is at about 220-400ºC. The detailed fragmentations at 180^0 C, 250ºC and 285ºC temperatures are given

in Figure 36. The base peak at 180ºC is at m/z =43 and this peak corresponds to CHCHOH or C(=O)-N(H) (Table 8).

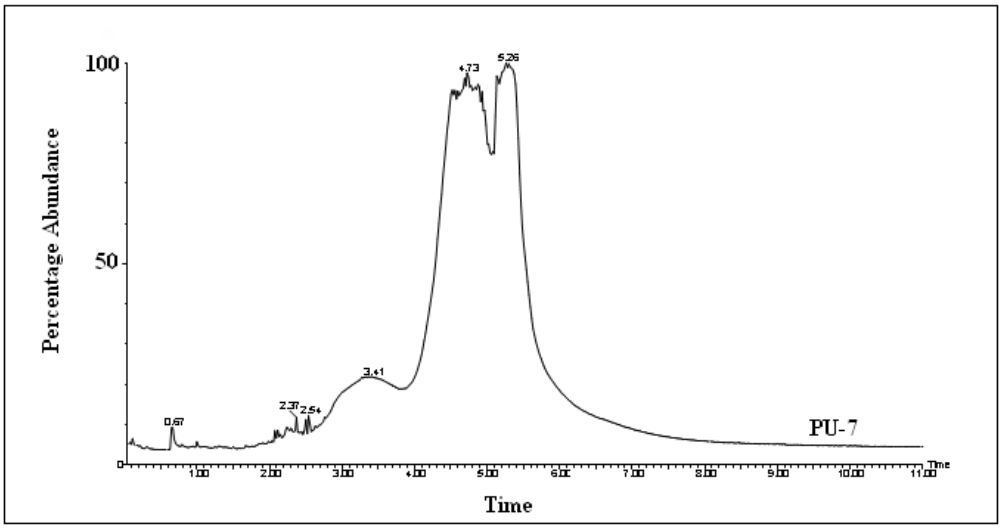

Figure 35 Mass thermogram of PU-7

Thus the degradation can be at both end of polymer chain as shown below :

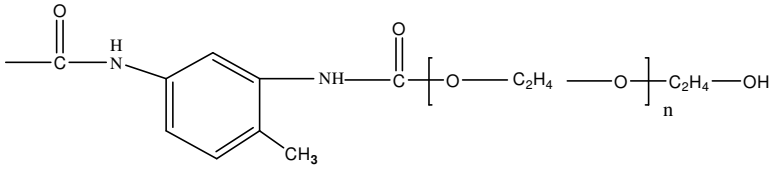

(30)

The H_2O (m/z=18) splits from the end of chain which is the result of addition of H to OH fragments during degradation. The groups CHO (m/z= 29), -

CH_2CH- (m/z= 27), are relatively strong peaks. The second strongest peak (85 %) is at m/z=72 which may be CHOCHCHOH. The other relatively strong peaks are $–CH_2CH_2$-O (m/z =44, 84%), -CH-C-O (m/z =57, 85 %). The maximum peaks at m/z =42, 45, 57 and 72 are also observed at 250ºC and 285ºC. Thus the fragmentations are maximized at this temperature, but they are similar in nature. The important fragments are tabulated in Table 8.

The fragmentation at 250ºC is due to the main chain degradation. The peak at 100 % intensity is now not m/z = 43, but m/z =31, which corresponds to $–CH_2$-OH. It is not only the end group, but also PEG degradation in main chain. It is in agreement with TGA thermogram (maximized at 410ºC) (Figure 33), where degradation rate increases at 250ºC and mechanism is random and depolymerization type. The temperature values obtained with the mass and TGA differs, because in mass spectroscopy material is subjected to degradation via electron impact and increase of temperature. The next most intense peak (78.3%) is at m/z =55 and corresponds to –CHCHOCH- group. The other intense peaks appeared at m/z = 42 (61.3%), m/z = 71 (59.1%), and m/z =174 (61.4%) which can be attributed to the groups NCO (and/or CHCHO), -N-CO-OCH, and $–CONH-C_7H_4$-NHCO respectively. The other important peaks are given in Table 8. At this temperature, the degradation rate was higher compared to 180^0 C and main chain was degraded.

At 285ºC, the backbone chain degradation was dominant. The fragments and relative intensities are much similar to those observed in 250ºC degradation temperature. However, now the intensity of the peaks at m/z = 192, 264, 304, 390 are relatively high. These peaks are mostly isocyanate fragments. The peaks and fragments are given in Table 8. There is no cyclization of main chain and the degradations at this temperature are random.

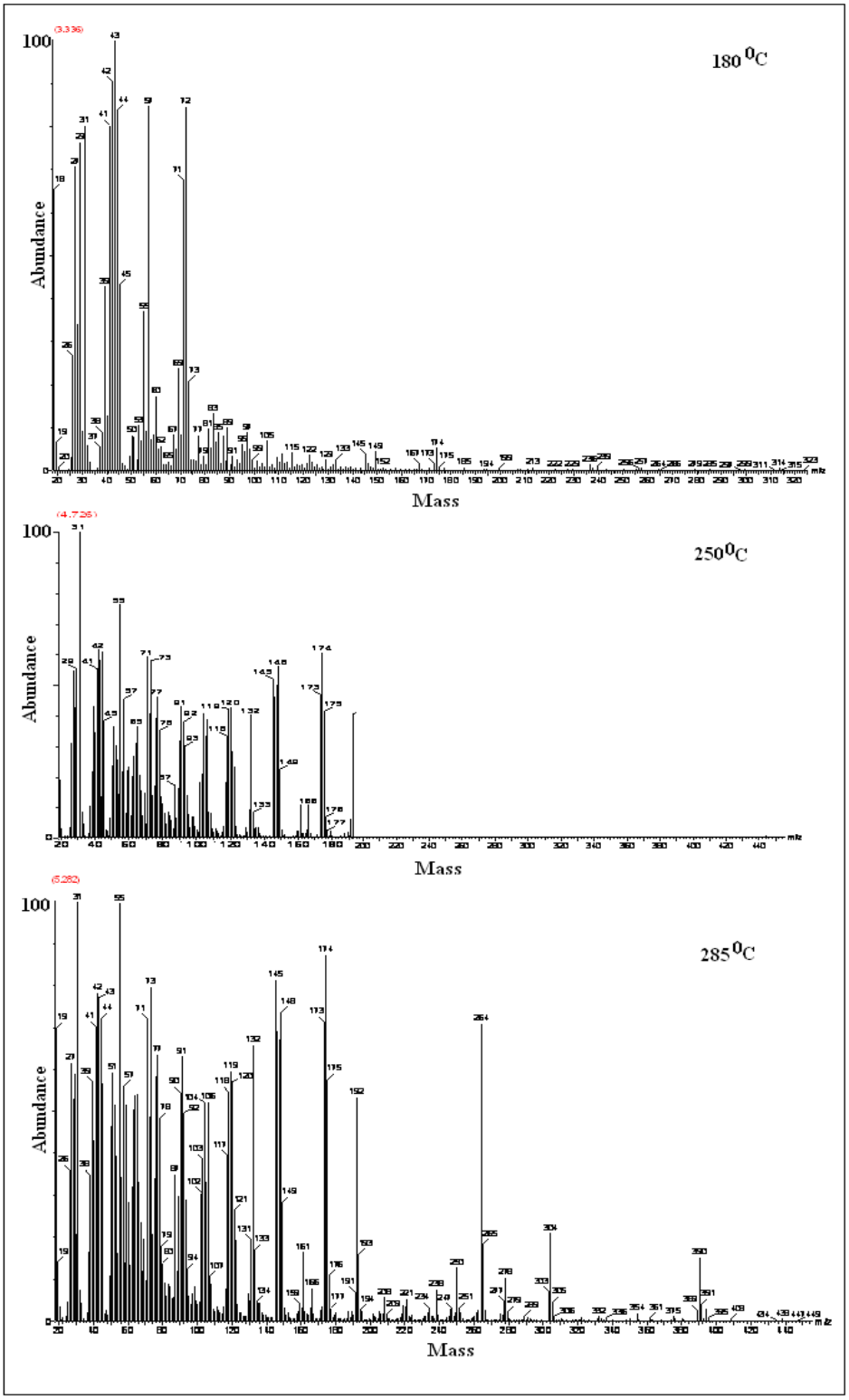

Figure 36 Mass thermogram fragments of PU7 at 180ºC, 250ºC and 285ºC

Table 8 The relative abundance (intensity %) of the peaks and their fragments for PU7

m/z	Fragment	Intensity (%) 180°C	Intensity (%) 250°C	Intensity (%) 285°C
18	H_2O	67,2	52,2	14,1
26	CN C_2H_2	28,3	31,0	36,2
27	C_2H_3	72,1	55,1	62,1
28	CO	33,0	42,5	53,9
29	CHO C_2H_5	76,0	54,9	59,1
31	CH_3O CH_2OH	81,0	100	100
41	C_2HO C_3H_5	81,2	55,2	71,2
42	C_3H_4 C_2H_2O	92,1	61,3	77,9
43	CNO C_2OH_3 CHNO	100,0	57,5	76,8
44	C_2H_4O	84,2	60,8	72,5
45	C_2H_5O	44,3	37,2	56,1
55	C_3H_3O	38,7	78,3	99,2
57	C_2HO_2	85,0	46,8	55,9
60	C_3H_5O	18,1	23,2	28,1
69	C_3HO_2 C_4H_5O	23,5	14,5	19,1
71	$C_3H_3O_2$ C_3H_5NO	68,2	59,1	73,2
72	$C_3H_4O_2$	85,0	40,5	49,5
73	$C_3H_5O_2$	20,0	57,8	80,0
77	C_6H_5	9,3	46,7	64,3
81	C_4HO_2	11,0	7,8	8,7
87	C_7H_3 $C_4H_7O_2$	3,1	16,1	35,0

Table 8 (cont'd)

m/z	Fragment	Intensity (%) 180°C	Intensity (%) 250°C	Intensity (%) 285°C
89	C_7H_5	12,0	15,4	30.1
91	C_7H_7 C_6H_5N	4,5	44,2	63,9
95	$C_5H_3O_2$	8,4	7,1	5,9
97	$C_5H_5O_2$	10,3	5,9	6,7
104	C_7H_6N	8,1	42,3	53,3
115	$C_6H_{11}O_2$	6,2	1,9	4,1
122	$C_7H_6O_2$	5,2	23,4	18,9
132	C_8H_7NO	2,1	40,1	65,2
145	$C_6H_9O_4$	5,0	51,3	82,1
149	$C_9H_5O_2$	6,6	23,0	28,4
169	$C_9H_8N_2O_2$	0,4	0,5	0,3
174	$C_8H_{15}O_4$	6,1	61,2	88,7
176	$C_8H_{16}O_4$	0,02	6,2	11,0
185	$C_9H_8NO_2$	1,3	0,4	0,03
192	$C_9H_8N_2O_3$	0,07	42,3	54,3
265	$C_{12}H_{14}N_2O_5$	0,23	-	72,1

3.1.3 Isocyanate Terminated Prepolymer synthesis

The molecular formula of the polymer synthesized in section 2.2.3, from the reaction of PEG with an excess TDI, is given below (31). Chemical compositions of the PUNCO's were given in Table 9. Prepolymers labeled with the numbers 1, 2, and 3 which correspond to the diisocyanate used (TDI, HDI and MDI), respectively. DBTDL was added as a catalyst only in reactions

of MDI and HDI, since the relative reactivity of the TDI is greatest and leads to sudden viscosity increase and finally gelation occurred in the system.

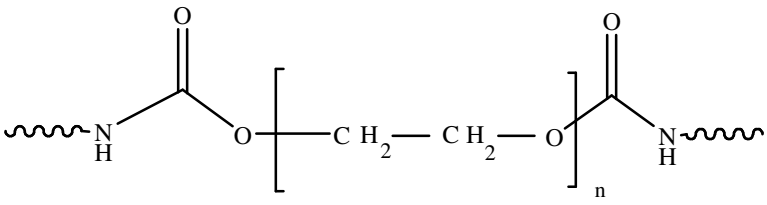

(31)

Table 9 Abbreviations of isocyanate terminated prepolymers

Sample Name	**Chemical Composition**
PUNCO1	TDI/PEG
PUNCO2	HDI/PEG
PUNCO3	MDI/PEG

FTIR-ATR Analysis Results

FTIR-ATR spectra of synthesized prepolymers are given in Figure 37. The FTIR-ATR spectra of PUNCO1, PUNCO2, and PUNCO3 showed differences mostly at the carbonyl and N-H vibration frequency regions. PUNCO3 carbonyl frequency appeared at 1705 cm^{-1}, whereas PUNCO1 and PUNCO2 at 1726 and 1715 cm^{-1}. This result may be attributed to the difference in hydrogen bonding capacity of the aliphatic and the aromatic isocyanates. The N-H

vibration frequencies of PUNCO1 and PUNCO3 are at 3300 cm^{-1}, which correspond to the bonded N-H to the etheric oxygen (-N-H…O). On the other hand, the peak maximum of PUNCO2 is at 3332 cm^{-1} indicating the bonded N-H to the carbonyl oxygen (N-H…O=C). All of the three spectra exhibit characteristic urethane vibration bands as described in Table 5.

Even though isocyanate is in excess, the isocyanate peak at about 2270 cm^{-1} is not observed in Figure 37. This is because isocyanate is very reactive and any species in the reaction mixture can add and block the group easily.

NMR Analysis Results

The ^{1}H and ^{13}C NMR spectra of PUNCO polymers are given in Figure 38 and 39 for PUNCO2 prepolymer (aliphatic diisocyanate used). Unlike to the polymers synthesized from the aromatic isocyanates (PUNCO1 and PUNCO3), the –NH protons are shifted and detected as a broad peak at δ=7.3 ppm. The hydroxyl proton (-OH) due to the resonance was at δ=4.65 ppm and the $–OCH_2$ protons were present at δ=4.1 ppm. The CH_2 protons present in the HDI were between δ=1.3-1.6 ppm and at δ=2.9 ppm.

Urethane carbonyl peak (C=O) was at δ=155 ppm in the ^{13}C NMR spectrum. The ether carbon peaks ($-OCH_2$) were at about δ= 68 ppm and $–CH_2$ peaks were at δ= 63 ppm. HDI carbons were appeared at δ= 25-29 ppm. NMR spectra of PUNCO2 did not exhibit any resonance peaks and this is due to the conformation stability of the molecule.

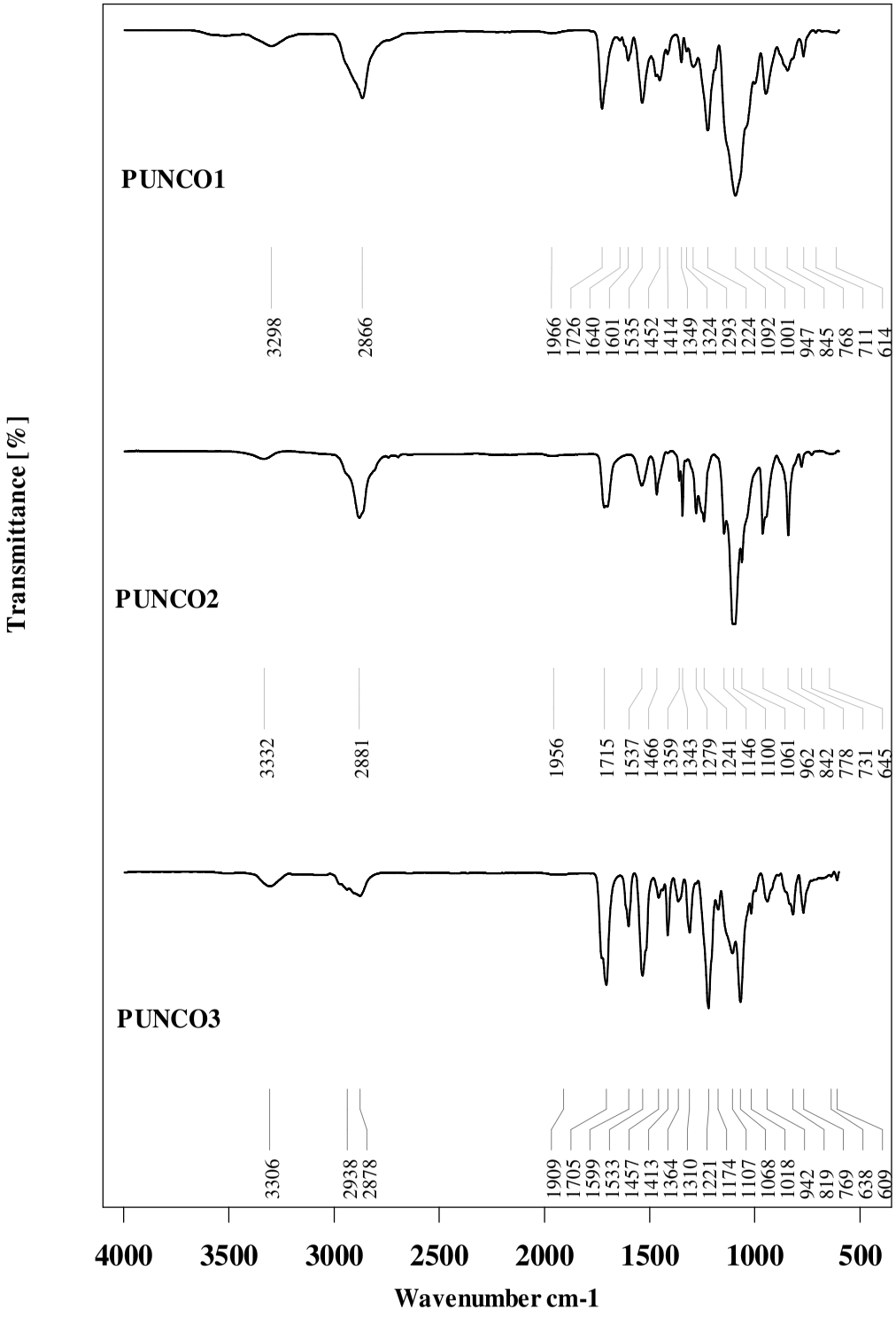

Figure 37 FTIR-ATR spectra of PUNCO polymers

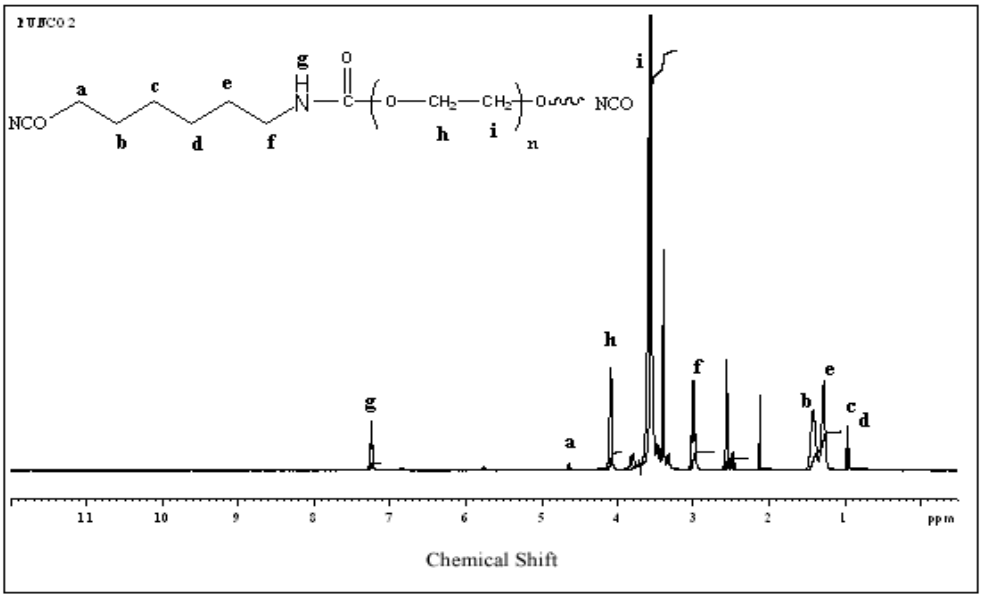

Figure 38 ^{1}H NMR Spectrum of PUNCO2

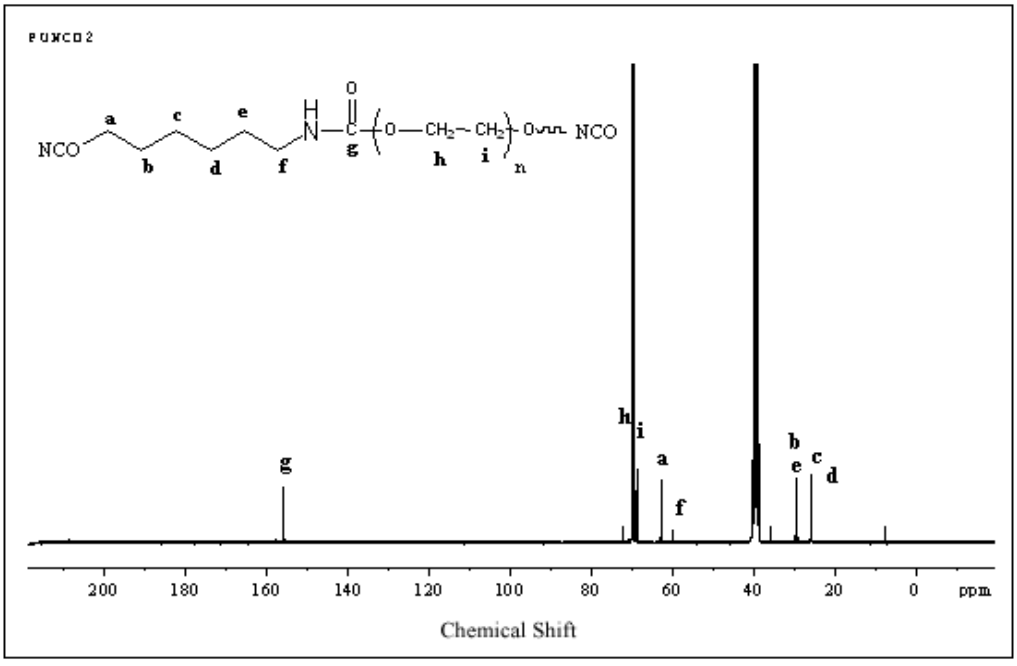

Figure 39 ^{13}C NMR Spectrum of PUNCO2

Thermal Analysis Results

TGA spectra of PUNCO1 and PUNCO2 are represented in Figures 40 and 41, respectively. The TGA thermogram of PUNCO1 showed a three-stage decomposition, one of which was due to the remained solvent at 110ºC. The other degradation stages follow each other and exist between 260ºC and 400ºC. There is a 15% char yield due to the presence of aromatization. On the other hand PUNCO2 (Figure 41) was thermally stable (more stable than aromatic PUNCO1), so that it has the only main decomposition at 420ºC and almost all the polymer was decomposed at this temperature. The char yield observed at 450ºC is 3%. The degradation mechanism for PUNCO2 is random degradation with some depolymerization.

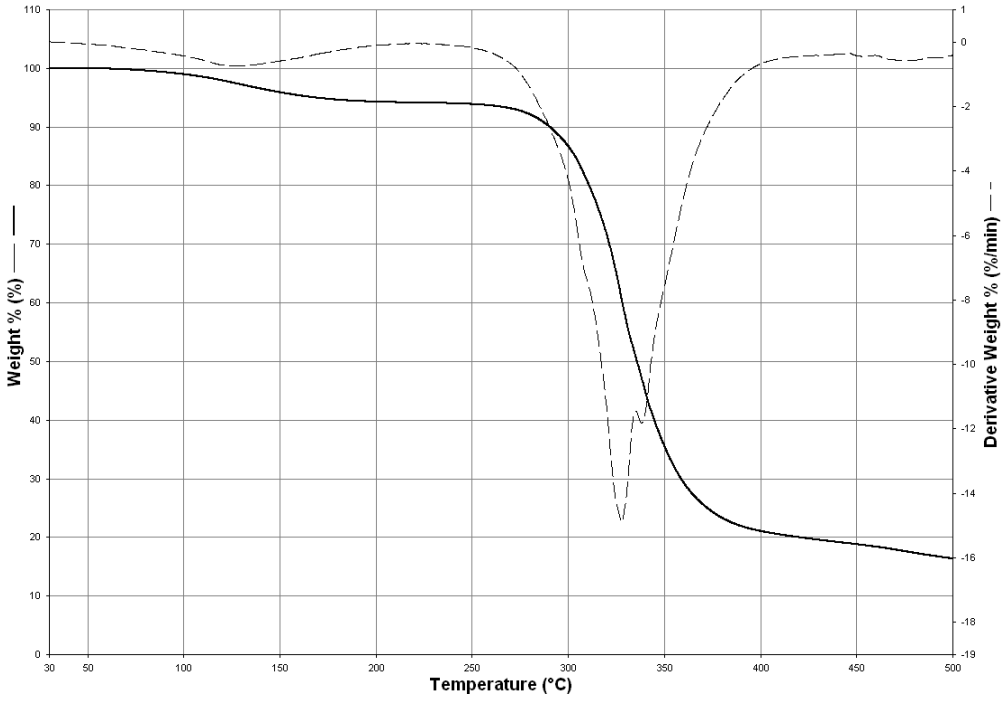

Figure 40 TGA thermogram of PUNCO1

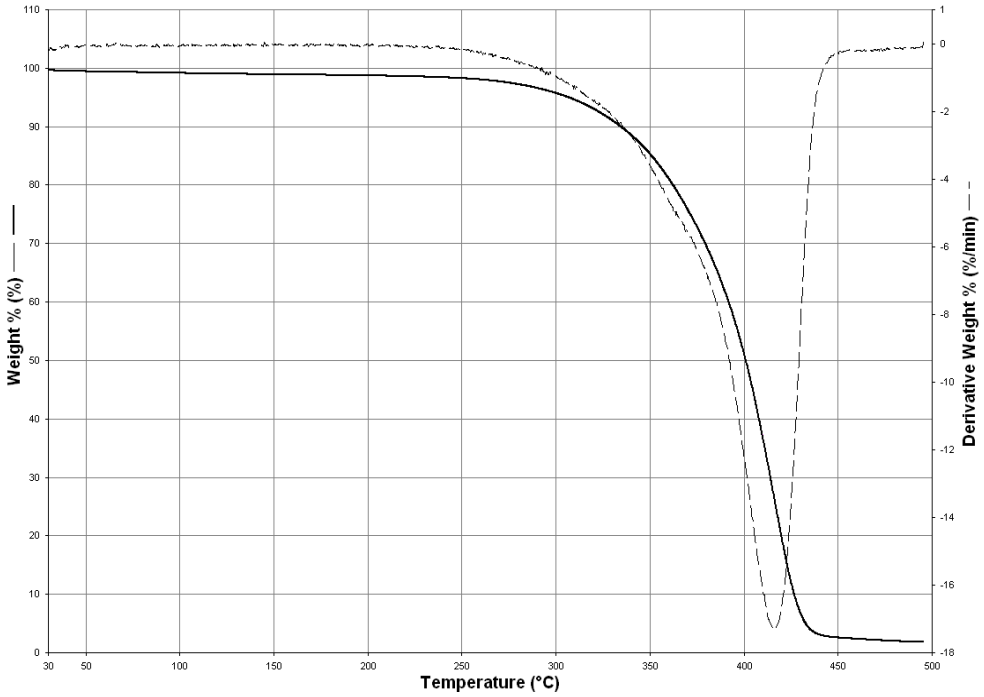

Figure 41 TGA thermogram of PUNCO2

DSC thermogram of PUNCO1 is given in Figure 42 in between -70 to 140ºC. At higher temperatures, the material decomposes giving gasses harmful to the instrument. Tg is observed at 20ºC. The heat capacity change at Tg value is 0.456 J/ g.^{0}C. The DSC thermogram of PUNCO2 is given in Figure 43. The thermogram is much different from that of PUNCO1. In this case, the Tg value is observed at -42ºC with a heat capacity change of 0.205 J/gºC. The Tg value of PUNCO2 is lower than that of PUNCO1 due to the presence of aromatic group (hard segment domination) in PUNCO1, whereas PUNCO2 was synthesized from flexible aliphatic chain. At higher temperatures, polymorphic structures (liquid crystal property) are observed. The melting points (Tm) of these polymorphs are at 26.02ºC and 37.45ºC respectively. The enthalpy of

fusion for each melting peaks are 7.6 J/g and 47.5 J/g respectively. This is unusual for the polyurethane type polymers that gives liquid crystal structures and due to the presence of aliphatic group (no phenyl groups) which gives linear chain with hard and soft segments.

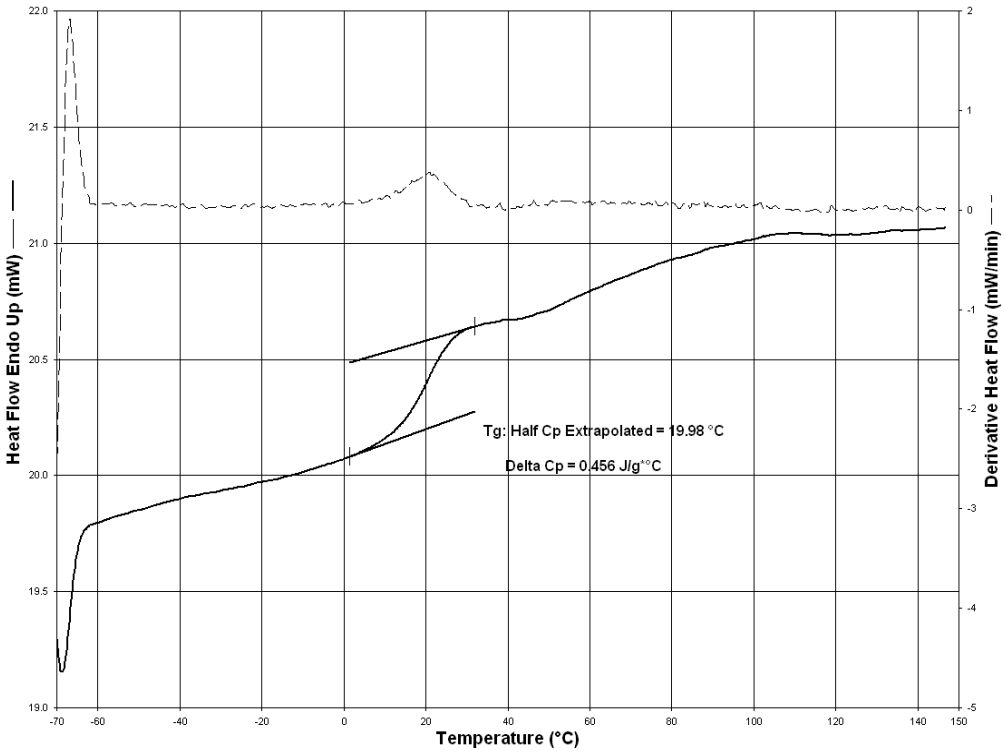

Figure 42 DSC thermogram of PUNCO1

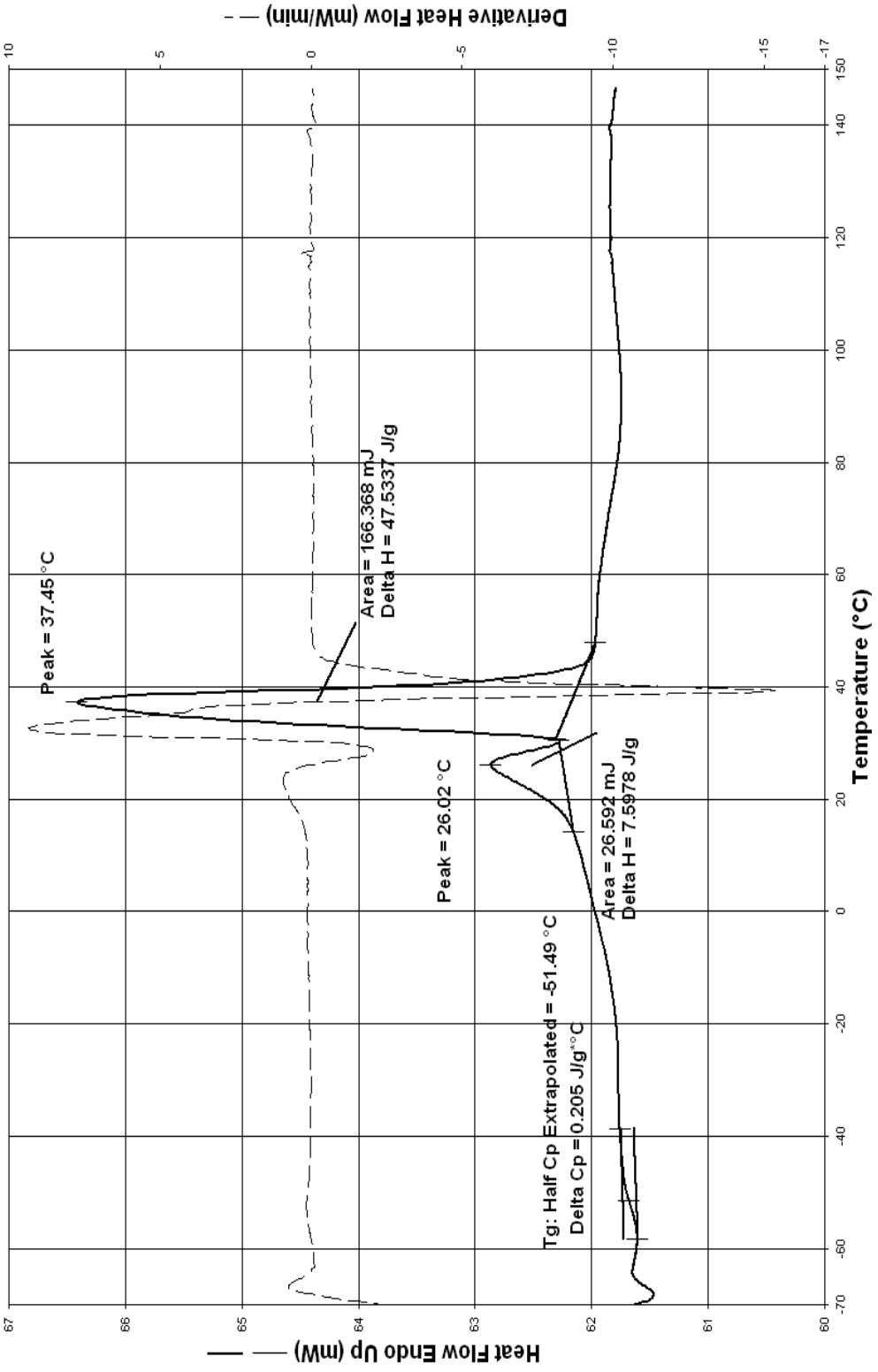

Figure 43 DSC thermogram of PUNCO2

3.1.4 Hydroxyl Terminated Prepolymer Synthesis

Several model of hydroxyl terminated prepolymers as shown by the formula (32) were prepared as explained in section 2.2.4 and chemical composition of the prepolymers are given in Table 10.

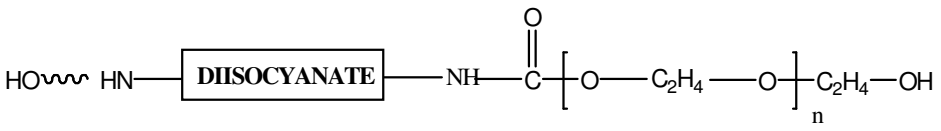

(32)

Table 10 Abbreviations of hydroxyl terminated prepolymers

Sample Name	Chemical Composition
PUOH1	TDI/PEG
PUOH2	HDI/PEG
PUOH3	MDI/PEG

FTIR-ATR Analysis Results

FTIR-ATR spectra of PUOH prepolymers are shown in Figure 44. Characteristic urethane FTIR-ATR vibrations appeared in each spectrum, especially vibrations at amide I region (1680-1715), confirmed the urethane formation. Main vibration frequencies of each type of prepolymer are tabulated in Table 11. The remaining vibration frequencies resemble to those of the bands appeared in PU1, PU7 and PUNCO polymers as explained before. It should be noted that the carbonyl vibration frequency of PUOH2 and PUOH3

appeared at the range of disordered and limited hydrogen bonded urethane carbonyl vibration band where as the same band of PUOH1 is at free carbonyl side. N-H vibration frequency of the PUOH2 and PUOH3 prepolymers showed a hydrogen bonded structure between N-H of urethane and the carbonyl oxygen. On the other hand, N-H group of PUOH1 is hydrogen bonded to the etheric oxygen.

The C=C stretching band is not present in the PUOH2 spectrum which was synthesized from aliphatic isocyanate, as expected. This band appeared almost at the same frequency for the prepolymers synthesized from aromatic diisocyanates (1600 cm^{-1}).

Table 11 Characteristic FTIR-ATR vibration bands of PUOH prepolymers.

	Frequency (cm^{-1})		
Group Assignment	**PUOH1**	**PUOH2**	**PUOH3**
υ(C=O)	1722	1713	1706
υ(N-H)	3298	3334	3310
υ(C=C)	1601	-	1600
δ(C-N-H) + υ(C-N)	1536	1536	1534
δ(N-H) + δ(C-N)	1224	1241	1221
υ(C-O-C) ether group	1101	1102	1107
υ(C-O-C) hard segment	1065	1061	1069

NMR Analysis Results

The ^{1}H and ^{13}C NMR spectra of PUOH1 are given in Figure 45 and 48, respectively. The urethane protons (-NH in urethane) are observed at δ= 8.9, 9.7 ppm. The aromatic protons from the TDI appeared at δ= 7-7.6 ppm and the methyl proton was assigned to the peak at δ=2.5 ppm. Hydroxyl proton (-OH) was at δ=4.4 ppm and the $–OCH_2$ protons were found at δ=4.3 ppm. The CH_2 protons of PEG were at δ=3.2-3.7 ppm. Carbonyl peak from the urethane group was at δ=153 ppm in carbon NMR spectrum. Aromatic carbons appeared between δ=114-137 ppm and were assigned to each carbon in the aromatic ring as shown in Figure 48. The ether carbon peaks were (–OCH) at δ=68 ppm and $–CH_3$ at δ= 17 ppm.

The indexed ^{1}H NMR spectra of PUOH2 and PUOH3 are given in Figure 46 and 47, respectively. The urethane protons appeared at δ= 7.2-7.3 for PUOH2 and at δ=9.7ppm for PUOH3. Phenyl protons of the aromatic ring of PUOH3 are observed at δ=7.1- 7.4 ppm. There exists small double bond peaks from the resonance of amide groups at the area of 5.5- 6.3 ppm in proton NMR of PUOH2.

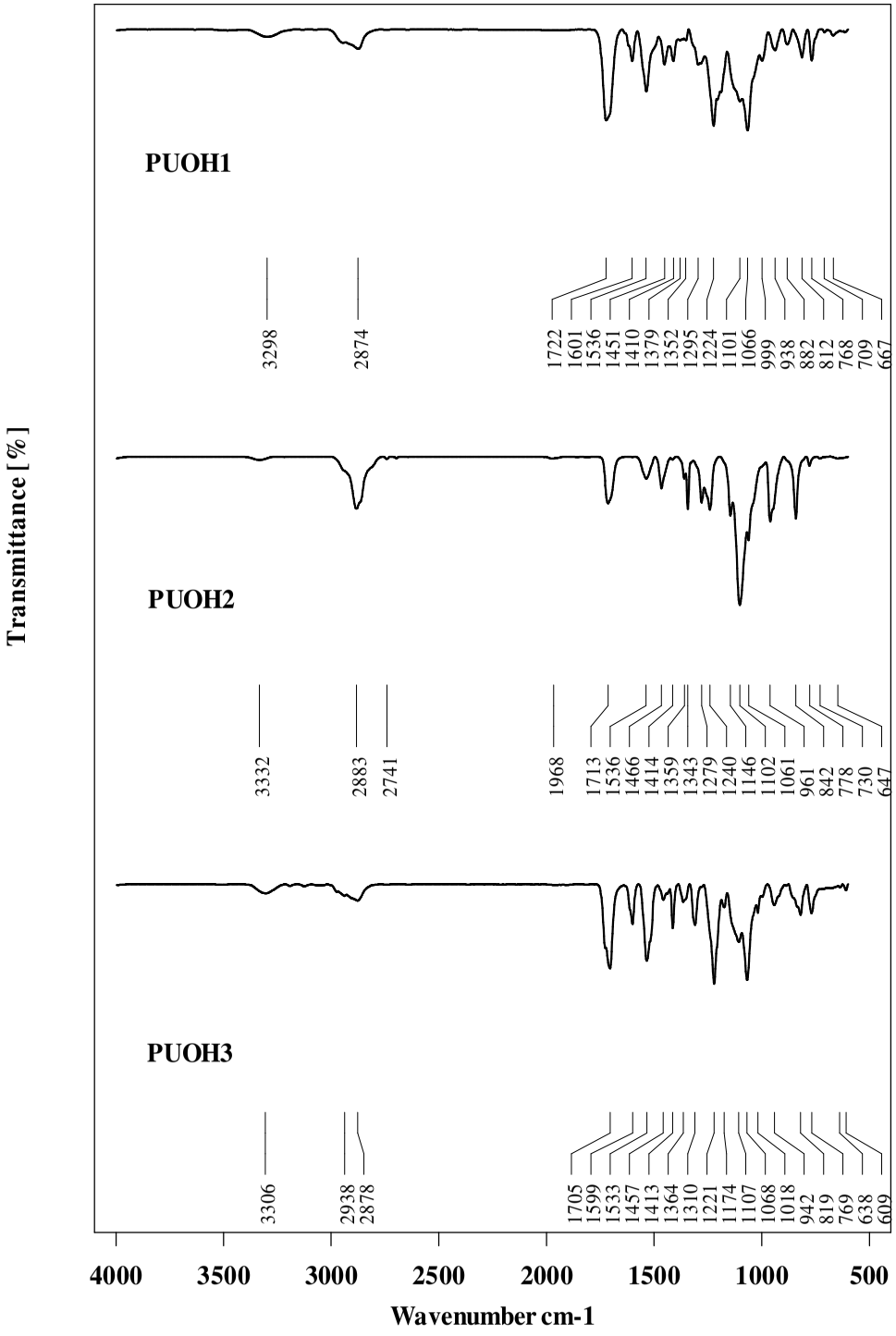

Figure 44 FTIR-ATR spectra of PUOH polymers

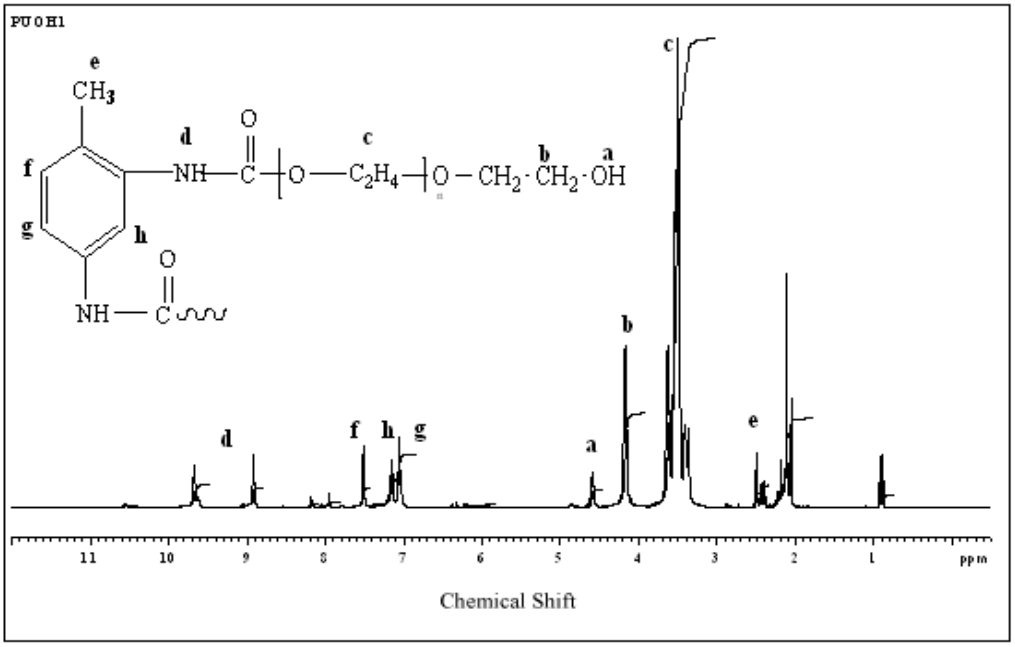

Figure 45 ^{1}H NMR spectrum of PUOH1

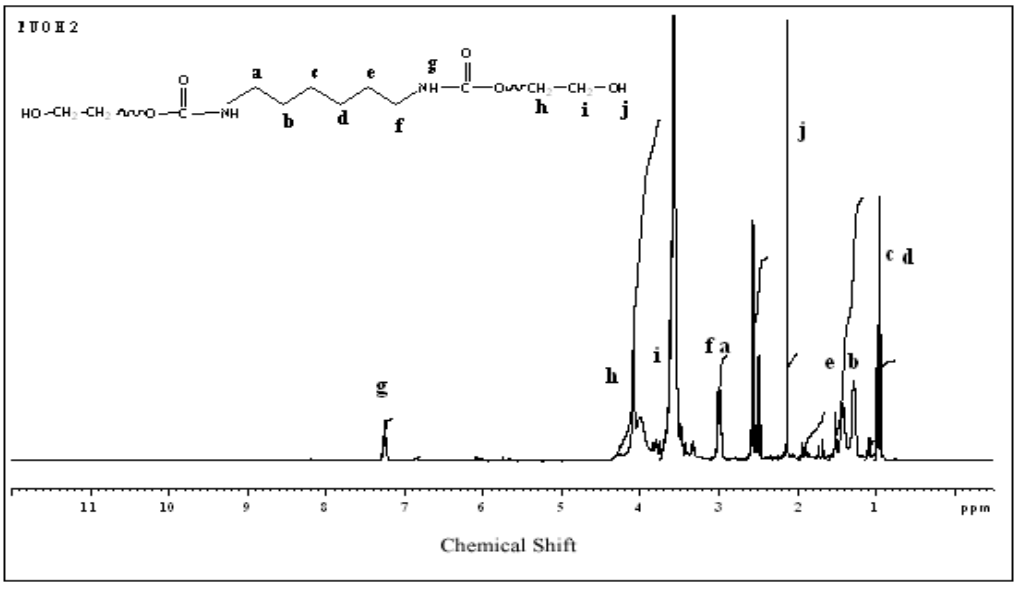

Figure 46 ^{1}H NMR of PUOH2

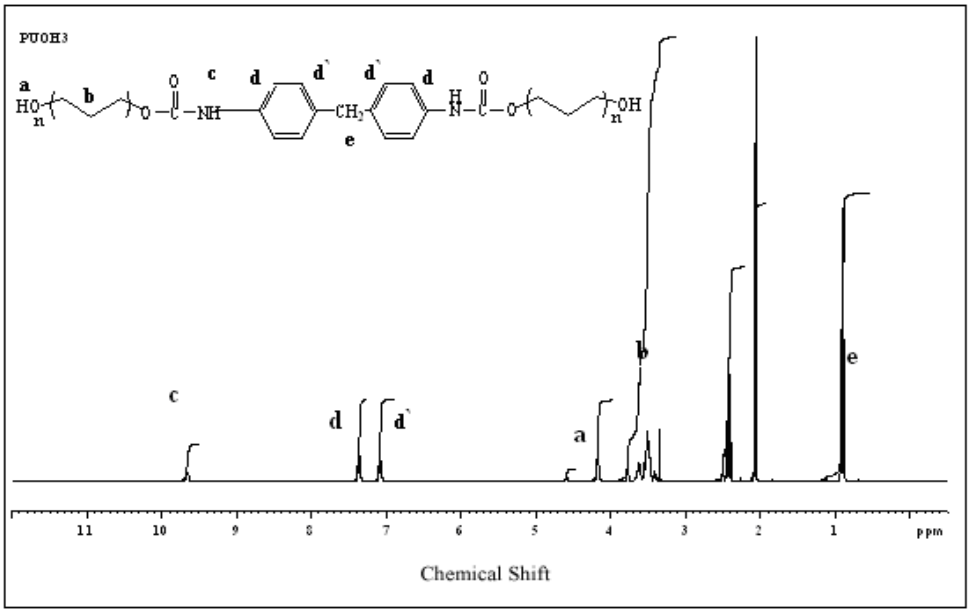

Figure 47 ^{1}H NMR of PUOH3

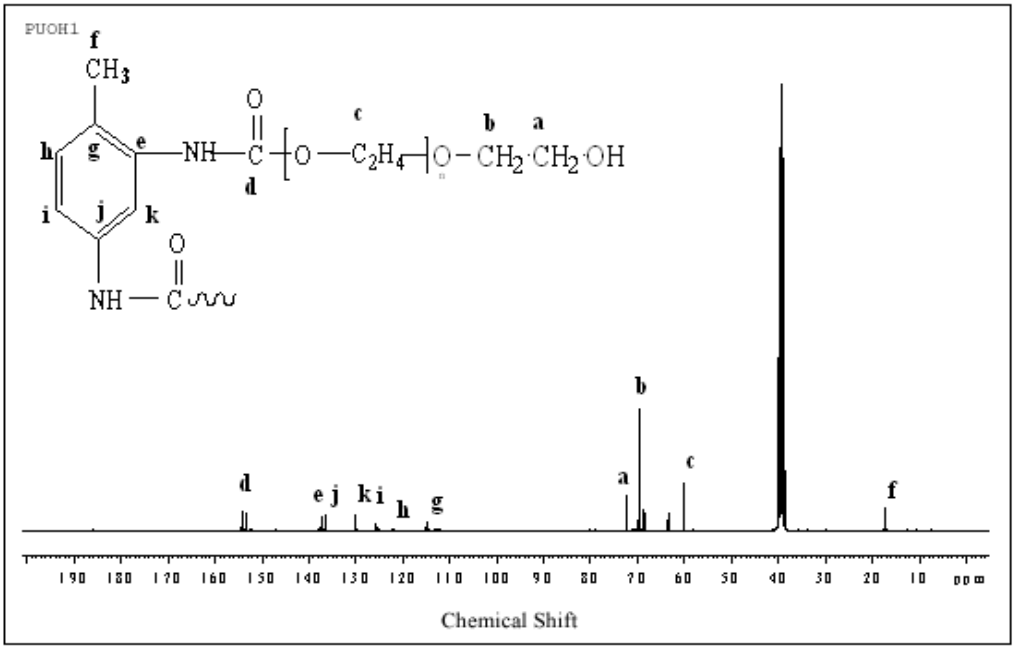

Figure 48 ^{13}C NMR Spectrum of PUOH1

Thermal Analysis Results

TGA curves of polymers PUOH1 and PUOH2 are provided in Figure 49 and 50, respectively. TGA thermogram of PUOH1 showed a smooth decrease starting from 100ºC with a weight loss of 10% up to 280ºC. Then there is an increasing rate of degradation, which is maximized at 325ºC with a weight loss of 83%. The char yield is high and about 15%, as expected. This decomposition could be considered as of random scission type with fluctuations due to the limited amount of end group cyclizations.

The thermogram of PUOH2 showed random type degradation. Main degradation was maximized at 420ºC and has a shoulder at 375ºC. The shoulder with a 30% weight loss can be attributed to the side groups where as total weight loss of 97% was due to the main decomposition of the molecule. There remained 3 % char yield.

DSC thermogram of PUOH2 is given in Figure 51 and in a temperature range between -70 to 140ºC. Two Tg values are observed at -57.4ºC and -6.54ºC which corresponds to the soft and hard domains, respectively. This result is in agreement with the FTIR-ATR vibration frequencies given in Table 11. The heat capacity changes at Tg values are 0.108 and 0.079 J/ gºC. The melting point (Tm) of the PUOH2 is 43.87ºC with an enthalpy of fusion 114.71 J/g. The presence of Tm shows the Tm of the hard segment in liquid crystal phase. However, for the soft segment there is no distinct Tm but a shoulder, which indicates the melting point of soft segment at about 20ºC.

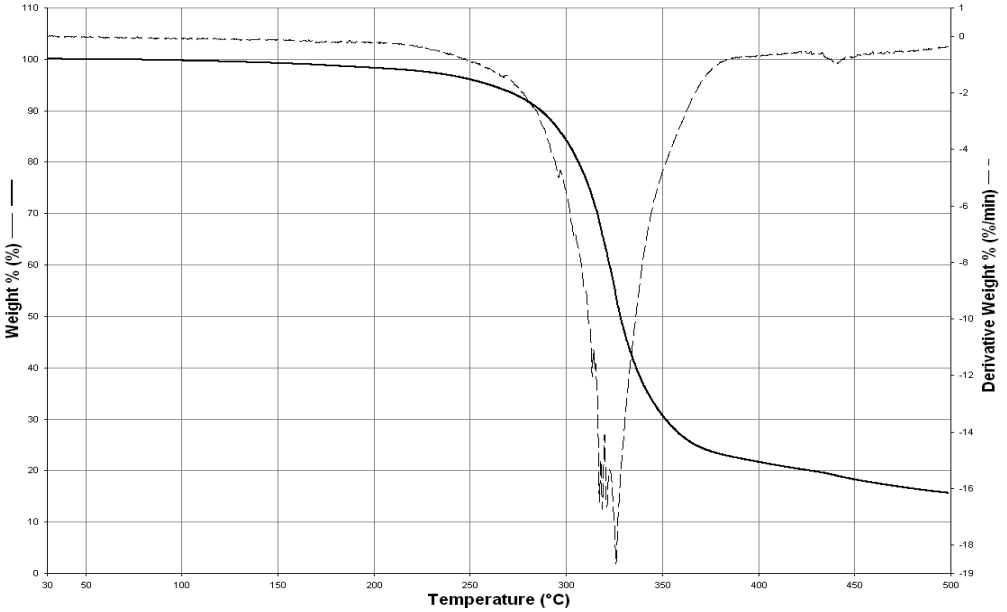

Figure 49 TGA thermogram of PUOH1

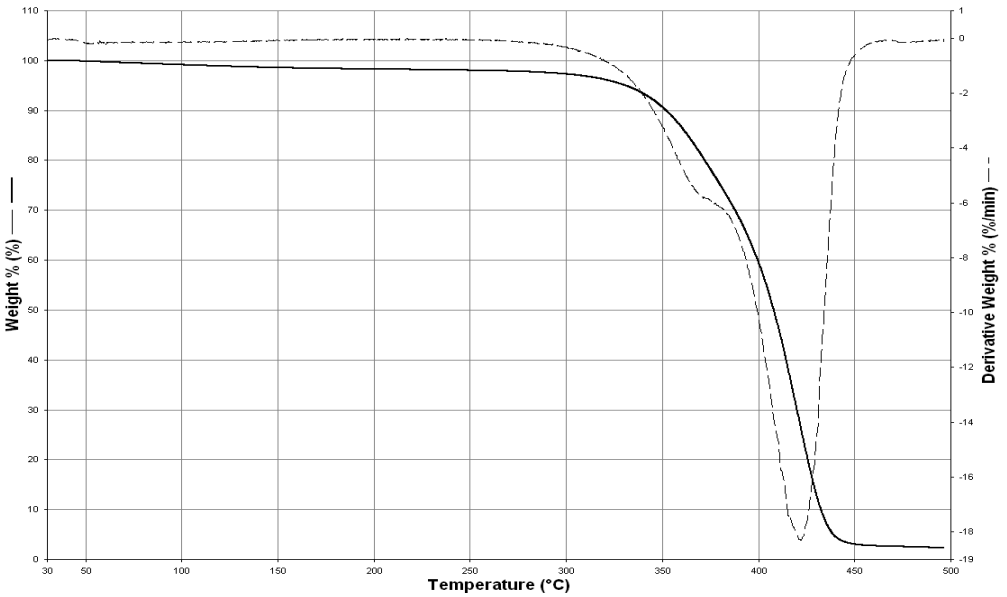

Figure 50 TGA thermogram of PUOH2

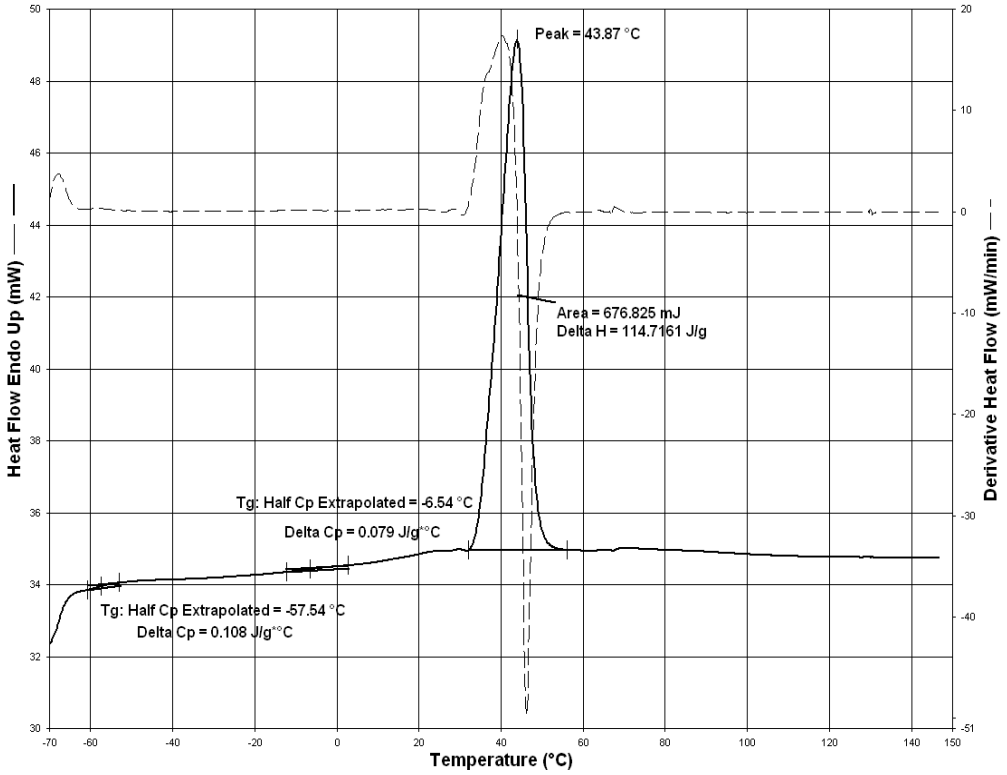

Figure 51 DSC thermogram of PUOH2

3.2 Urethane Acrylate synthesis

3.2.1 Synthesis of Acrylate End capped Isocyanate Terminated Polyurethane

The chemical compositions of the acrylate end capped polymers are given in Table 12. Acrylate end capping was achieved by two acrylate monomers; MMA and HEMA.

Molecular weights of the obtained PUNCOA polymers are given in Table 11. The molecular weight of PUNCOMMA2 could not be measured due to the solubility problem in THF and DMF. Mn and Mw of PUNCOMMA1 are 3518

and 3714 g/mol with a Pd of 1.056, which shows a narrow molecular weight distribution (Appendix B). PUNCOHEMA1 polymer has similar type of distribution with Pd of 1.037. On the other hand, the PUNCOMMA3 polymer has a relatively high Pd value of 3.95 with a Mn and Mw value of 5474 and 21629 g/mol, respectively. This large difference could be attributed to the formation of PMMA homopolymer together with urethane acrylate polymer.

Table 12 Abbreviation of PUNCOA polymers

Sample Name	Chemical Composition	Mn (g/mol)	Mw (g/mol)	Pd
PUNCOMMA1	TDI/PEG/MMA	3518	3714	1.056
PUNCOMMA2	HDI/PEG /MMA	-	-	-
PUNCOMMA3	MDI/PEG/MMA	5474	21629	3.95
PUNCOHEMA1	TDI/PEG/HEMA	3171	3289	1.037

FTIR-ATR Analysis Results

FTIR-ATR spectra of PUNCOA polymers are given in Figure 52. Carbonyl vibration frequencies are at 1727, 1715, 1705, 1706 cm^{-1} and N-H vibrations appeared at 3298, 3339, 3308, 3305 cm^{-1} for PUNCOMMA1, PUNCOMMA2, PUNCOHEMA1, PUNCOHEMA3 polymers, respectively. Hydrogen bonding effect is dominant in HEMA added polymers as shown by the frequency values

obtained for carbonyl vibrations. Almost all the PUNCOA polymers have NH…O type hydrogen bonding except PUNCOMMA2, which has a NH…C(=O) type bond. Common vinyl group vibration bands are mostly found at 1643, 940-980, and 814 cm^{-1}. HEMA containing polymers have vibration frequencies at 814 cm^{-1}. Characteristic urethane vibrations explained in Table 5 are also present in the spectra shown in Figure 52. All the polymers have bands at 940-980 cm^{-1}, whereas vibration band at 1640 cm^{-1} is only present in PUNCOMMA2. Vibration at 1640 cm^{-1} cannot be seen clearly in other PUNCOMMA polymers due to overlapping of the C=C stretching vibration of the aromatic groups present in the diisocyanate. Therefore, FTIR is not a good method for distinguishing vinyl groups due to the presence of aromatic groups. The presence of these groups can be explained better with the NMR spectroscopy.

NMR Analysis Results

As representative spectra for PUNCOA polymers, the ^{1}H and ^{13}C NMR of PUNCOMMA2 are given in Figures 53 and 54, respectively. Characteristic protons were labeled on the proposed structure that was attached to the Figures. Proposed structures and the observed chemical shifts of the protons are in good agreement with each other. Urethane protons appeared at δ= 9.7 ppm, vinylic protons are at δ =5.7 and 5.8 ppm, -CH_2 protons of PEG are at δ = 3.2-3.7 ppm and –OCH_2 protons are at δ = 4.1-4.2 ppm range. In the carbon NMR, C=C are at δ = 115 ppm, carbonyl peaks are at δ = 149, 156 and 158 ppm, NH-C at δ = 60-62 ppm, -CH_2 appeared at 25-29 ppm and PEG carbons were at δ = 68 ppm.

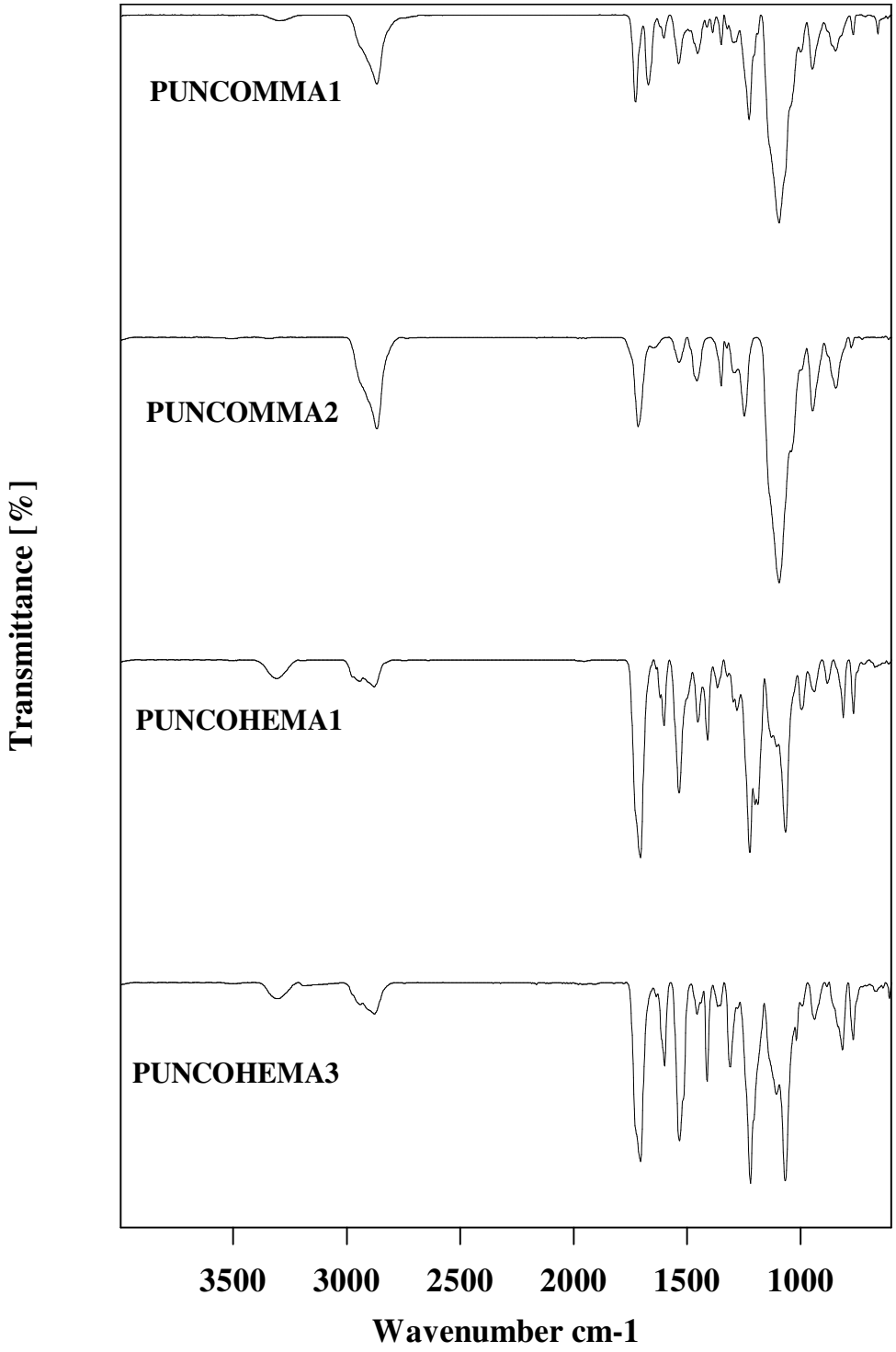

Figure 52 FTIR-ATR Spectrum of PUNCOA polymers

The ^{1}H NMR of PUNCOHEMA1 is given in Figure 55. During end capping with HEMA, the $-OCH_2CH_3$ group was eliminated therefore it is expected that the NMR spectrum of PUNCOHEMA1 has a quiet similar characteristic with that of PUNCOMMA1. –NH protons of the urethane group were present in the spectrum at δ = 8.9 and 9.7 ppm. The aromatic ring protons of TDI were in the range of δ = 7.0-7.6 ppm. The double bond protons in HEMA structure is observed at δ = 5.8 and 6.4 ppm.

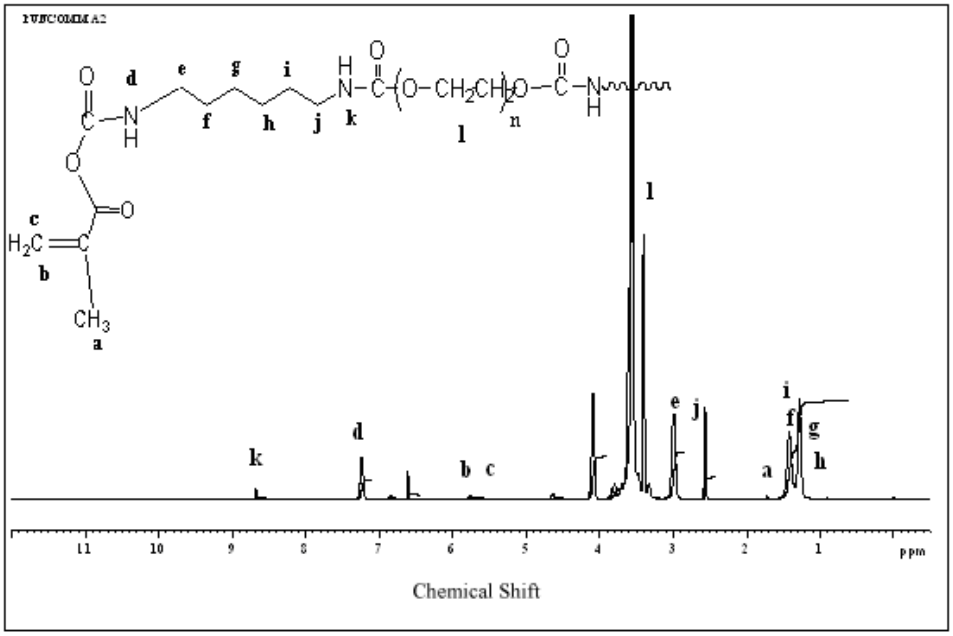

Figure 53 ^{1}H NMR Spectrum of PUNCOMMA2

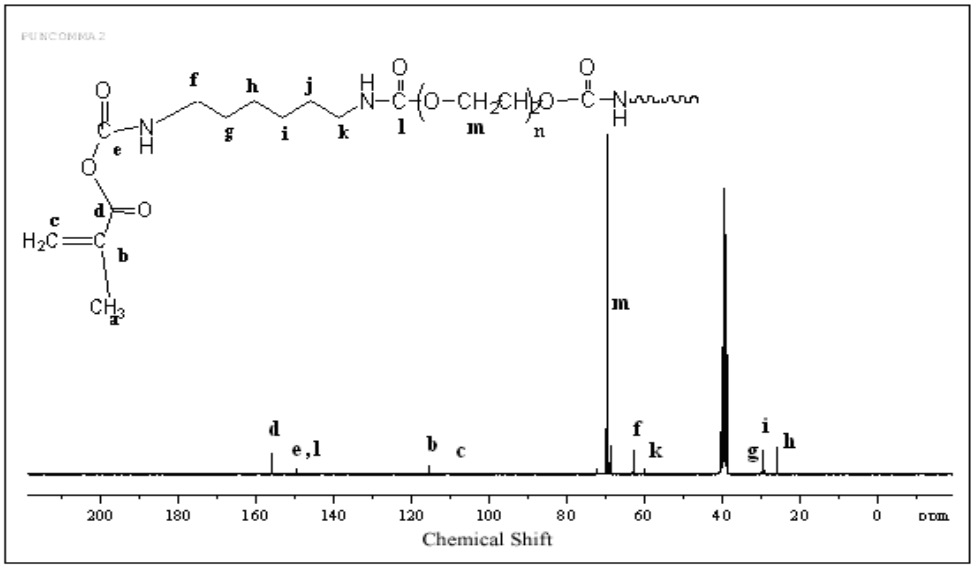

Figure 54 ^{13}C NMR Spectrum of PUNCOMMA2

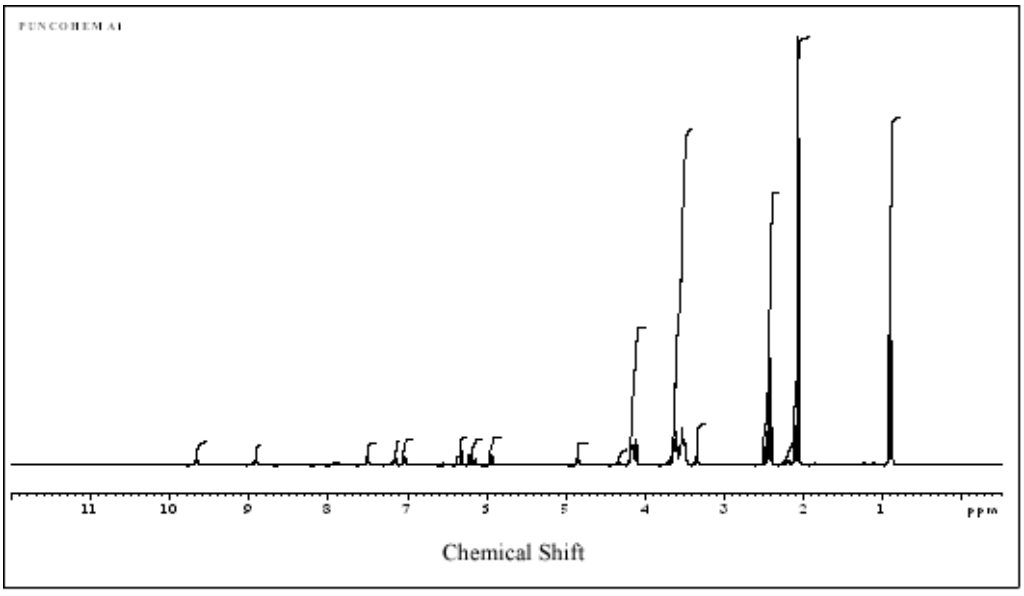

Figure 55 ^{1}H NMR Spectrum of PUNCOHEMA1

Thermal Analysis Results

TGA thermograms of polymers synthesized in section 2.2.5 were given in Figure 56-59. The TGA thermogram of PUNCOMMA1 has a two stage degradation process. First stage started at 50ºC and reached to 10% weight loss up to 225ºC. This stage corresponds to the degradation of the side groups present in the polymer. Main degradation is maximized at 325ºC and lead to a total weight loss of 95%. The remaining char yield of 5% was due to the presence of thermally stable aromatic groups.

The TGA thermogram of PUNCOMMA3 showed that the first degradation stage was started at 100ºC and end up at 260ºC with a weight loss of 8%. Main degradation which is maximized at 330ºC with a weight loss of 90% end up with 10% char yield. The comparison of the TGA thermogram of PUNCOMMA2 with the other TGA thermogram of PUNCOA polymers containing aromatic isocyanate groups gave that the aliphatic diisocyanate caused the resulting polymer to be much more thermally stable. Thus, PUNCOMMA2 polymer undergoes a main degradation at 420ºC and has a char yield of 2 % at 450ºC.

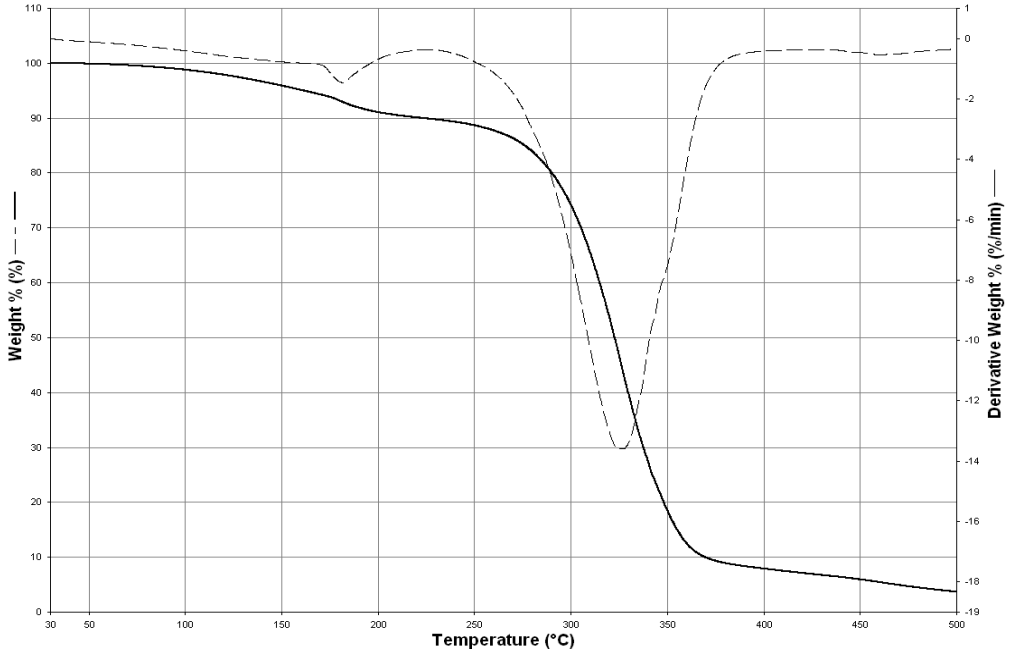

Figure 56 TGA thermogram of PUNCOMMA1

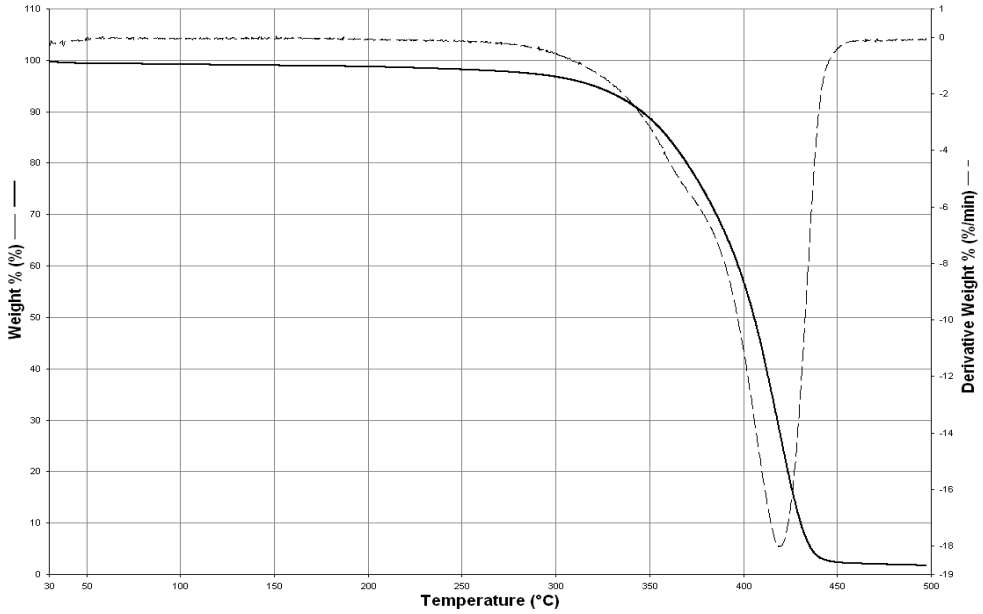

Figure 57 TGA thermogram of PUNCOMMA2

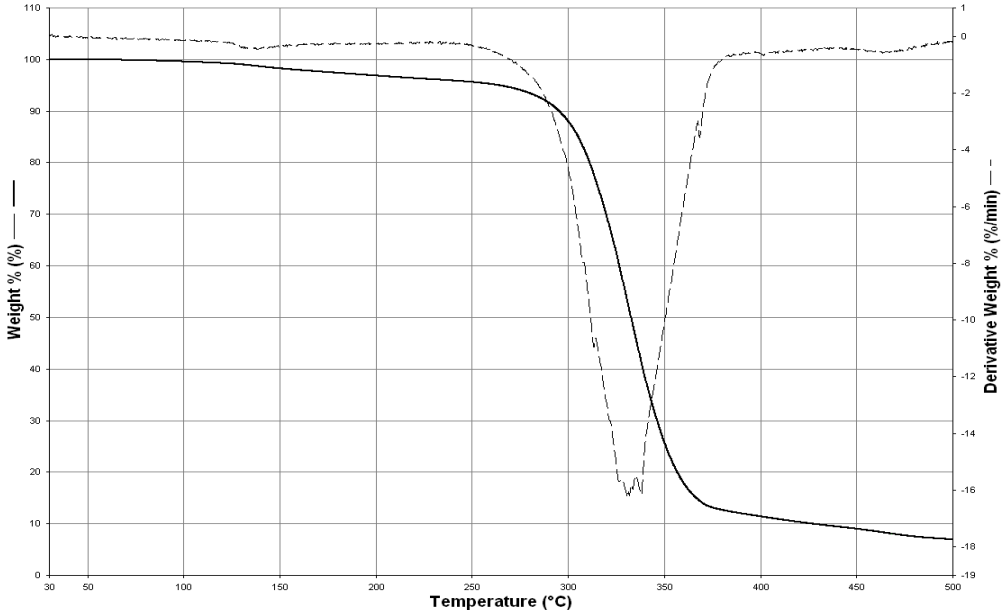

Figure 58 TGA thermogram of PUNCOMMA3

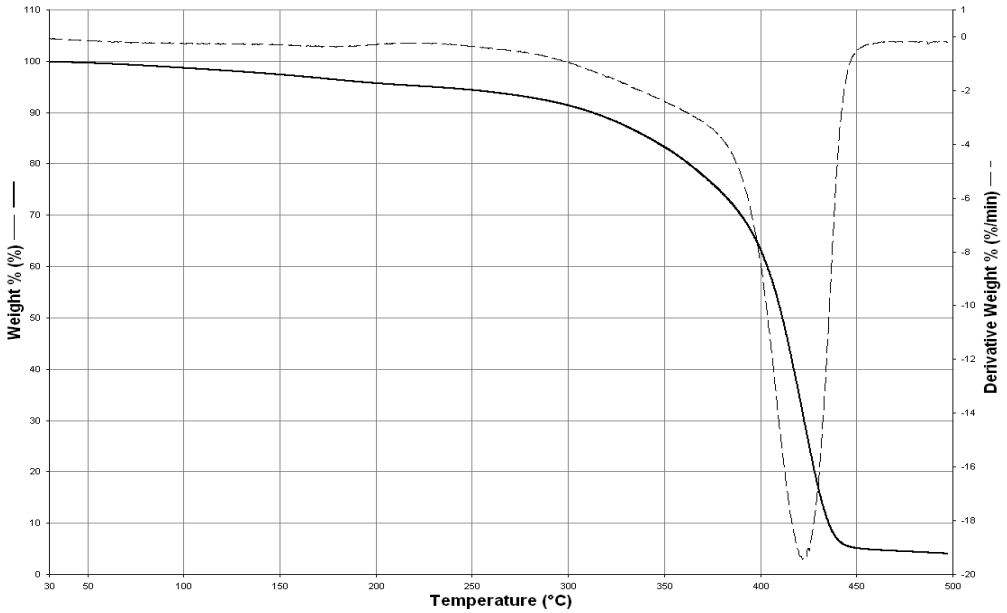

Figure 59 TGA thermogram of PUNCOHEMA1

DSC thermogram of the PUNCOMMA1, PUNCOMMA2, and PUNCOMMA3 are given in Figures 60, 61, and 62, respectively. There exists one Tg value for the polymers PUNCOMMA1 at 17.0ºC (Figure 60) and PUNCOMMA3 at 7.06ºC (Figure 62) and the corresponding heat capacity change at Tg value is 0.274 J/gºC and 0.552 J/gºC . On the other hand, PUNCOMMA2 has two Tg values at -48.46ºC and -4.39ºC (Figure 61). The observed Tg values correspond to the transitions of soft/hard domains present in the urethane and acrylate end groups. Heat capacity changes at Tg values are 0.341 and 0.237 J/gºC respectively. Tm of the observed polymorphic structures is at 26.85ºC and 41.31ºC with an enthalpy of fusion of 0.90 J/g and 72.85 J/g respectively.

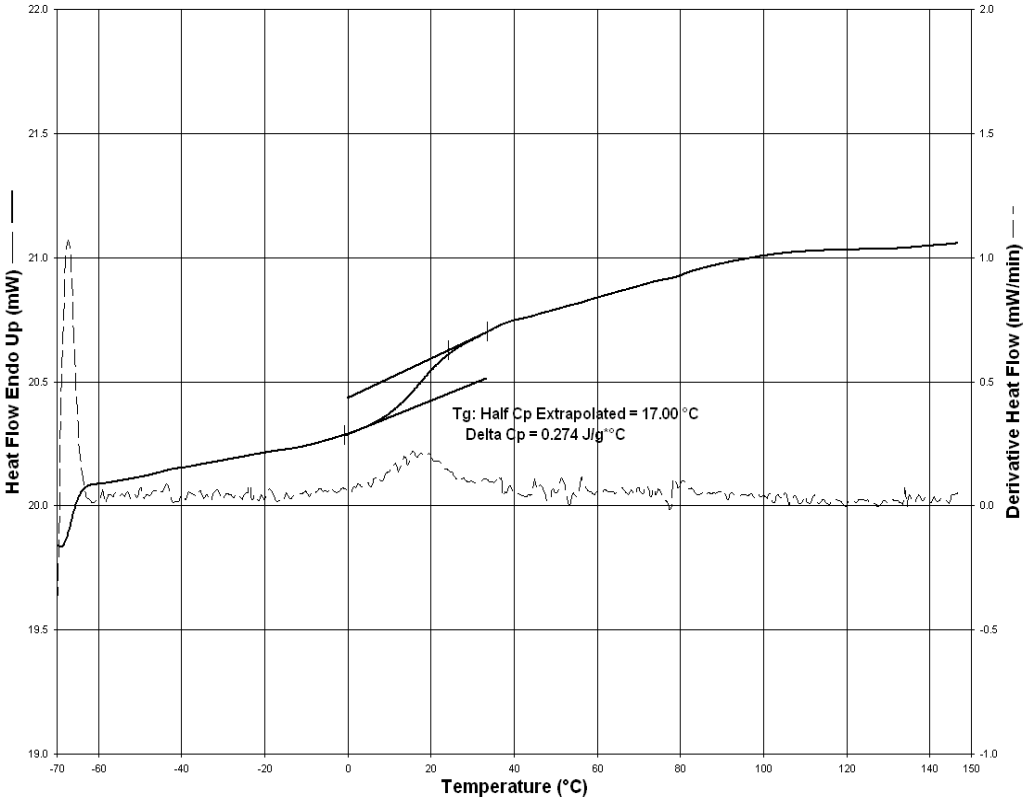

Figure 60 DSC thermogram of PUNCOMMA1

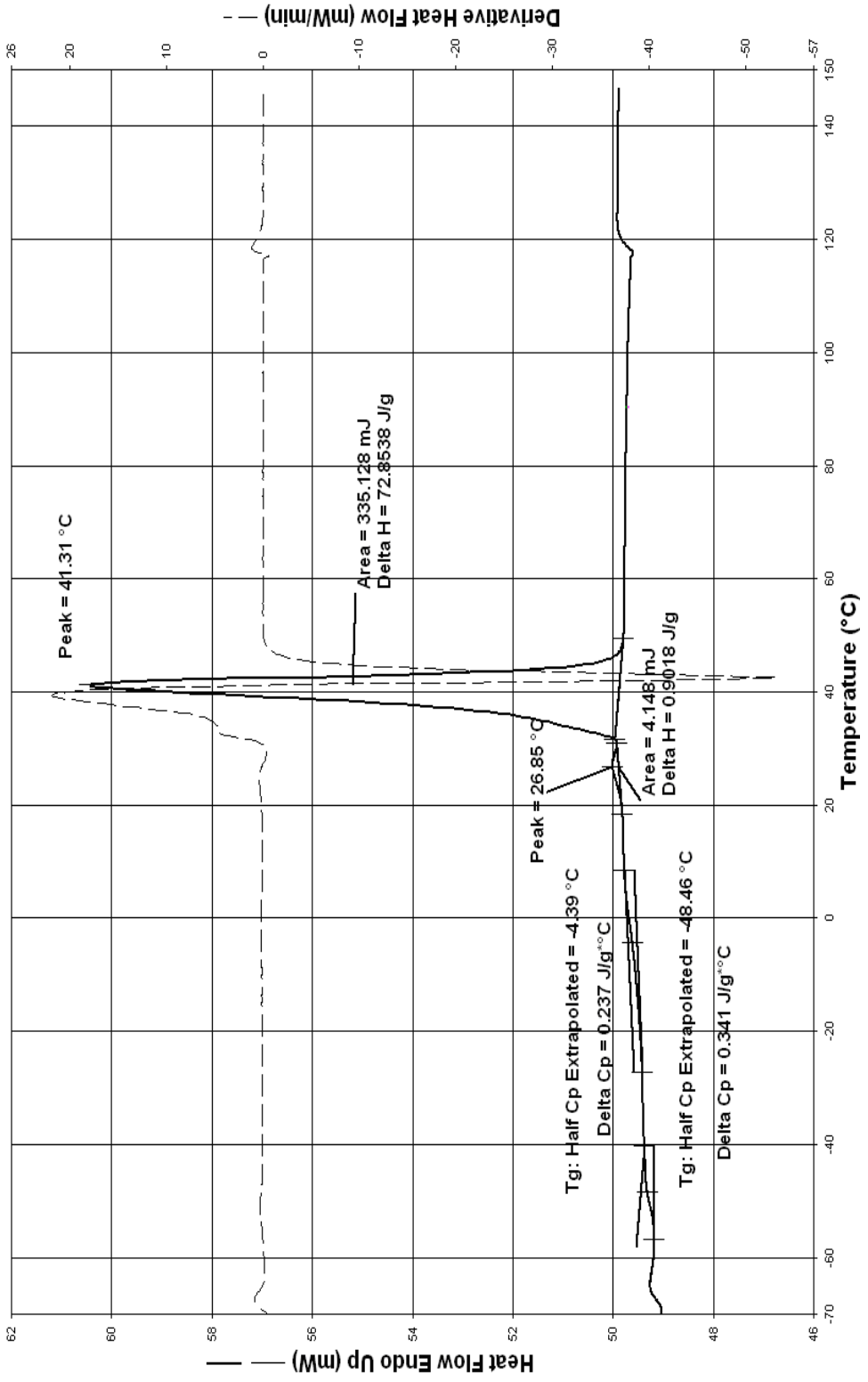

Figure 61 DSC thermogram of PUNCOMMA2

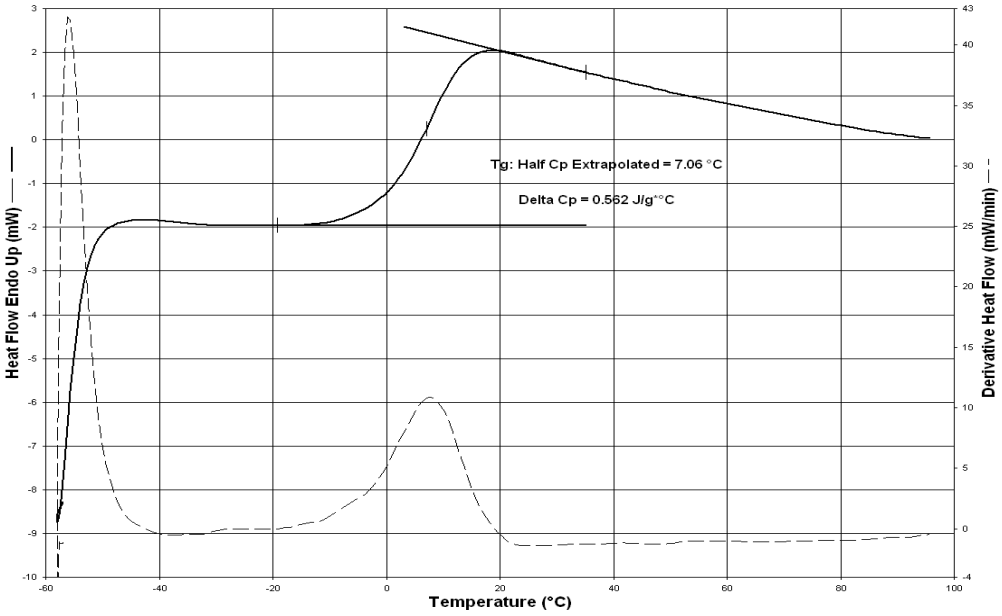

Figure 62 DSC thermogram of PUNCOMMA3

Mass Analysis Results

The mass thermogram of PUNCOHEMA1 is given in Figure 63 and that of PUNCOMMA3 in Figure 64, respectively. There are important differences between two thermograms. PUNCOHEMA1 is fragmented at a narrow temperature range and most of the fragmentation is the main chain fragmentation. The narrow distribution shows that the polymer obtained is linear with a high conversion leaving very small amount of monomers in the mixture. The fragmentation of PUNCOMMA3 is in a wider temperature range with several side group linkage fragmentation. These fragments might also be unpolymerized fractions that were degraded in between 100-200ºC.

The fragmentations at 200ºC, 250ºC, and 270ºC are given in Figure 65. The base peak at 200ºC is m/z = 55, which corresponds to –C(O)-C(CH_3)-. It is most probable that firstly the end vinyl group lost CH_2 group, then the ester group is splitted off. The following most intense peaks are -CH_2-C_6H_3-N- (m/z =99 and 85,6%) and –C_6H_3-CH_2- (m/z = 89 and 74,8%). The other peaks are shown in Table 13 and they are similar to other fragments given in Table 8.

At 250ºC the base peak is $C_6H_9O_4$ (m/z =145 and 100%) and second most intense peak is CH_2OH (m/z =31 and 94,6%). Although it is expected to have a mechanism based on the end group cyclization, it is interesting that further fragmentation is mostly peculiar to the isocyanate group (hard segment). Fragmentation is of random type and observed peaks are the same with the peaks observed at previous fragmentation. All the peaks are tabulated in Table 13.

At 270ºC the base fragment is CH_2CH_2-O-C(O)-NH- (m/z =87 and 100%). The other intense peaks are m/z = 145 (82.2 %), 174 (79,1%) etc. The other peaks are tabulated in Table 12.

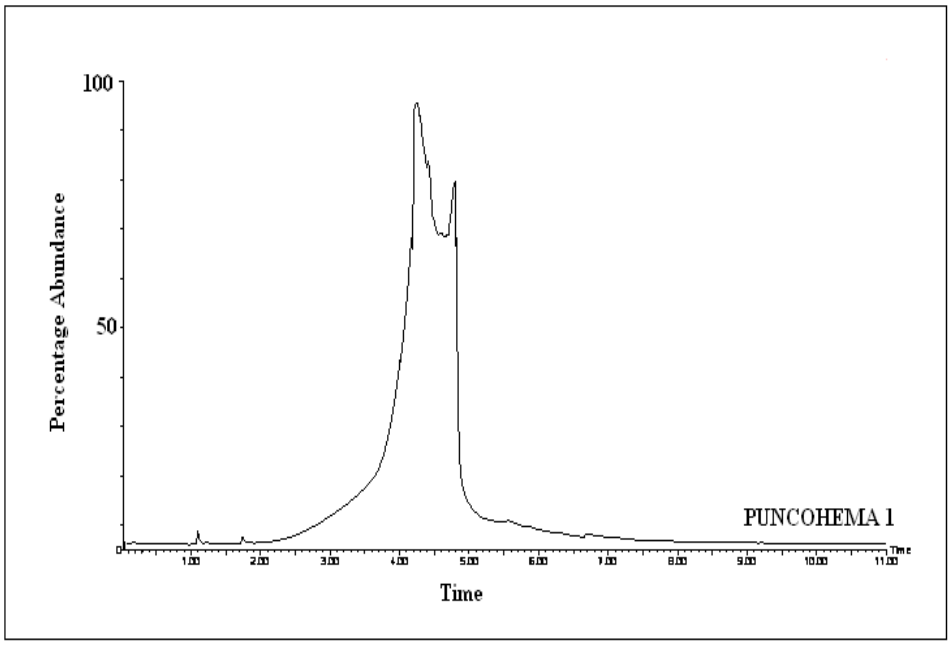

Figure 63 Mass thermogram of PUNCOHEMA1

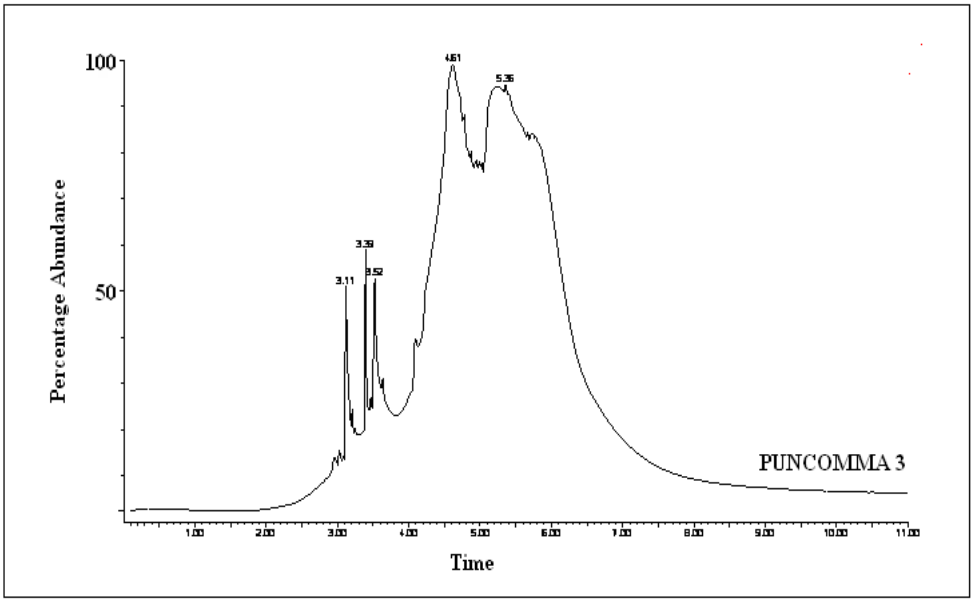

Figure 64 Mass thermogram of PUNCOMMA3

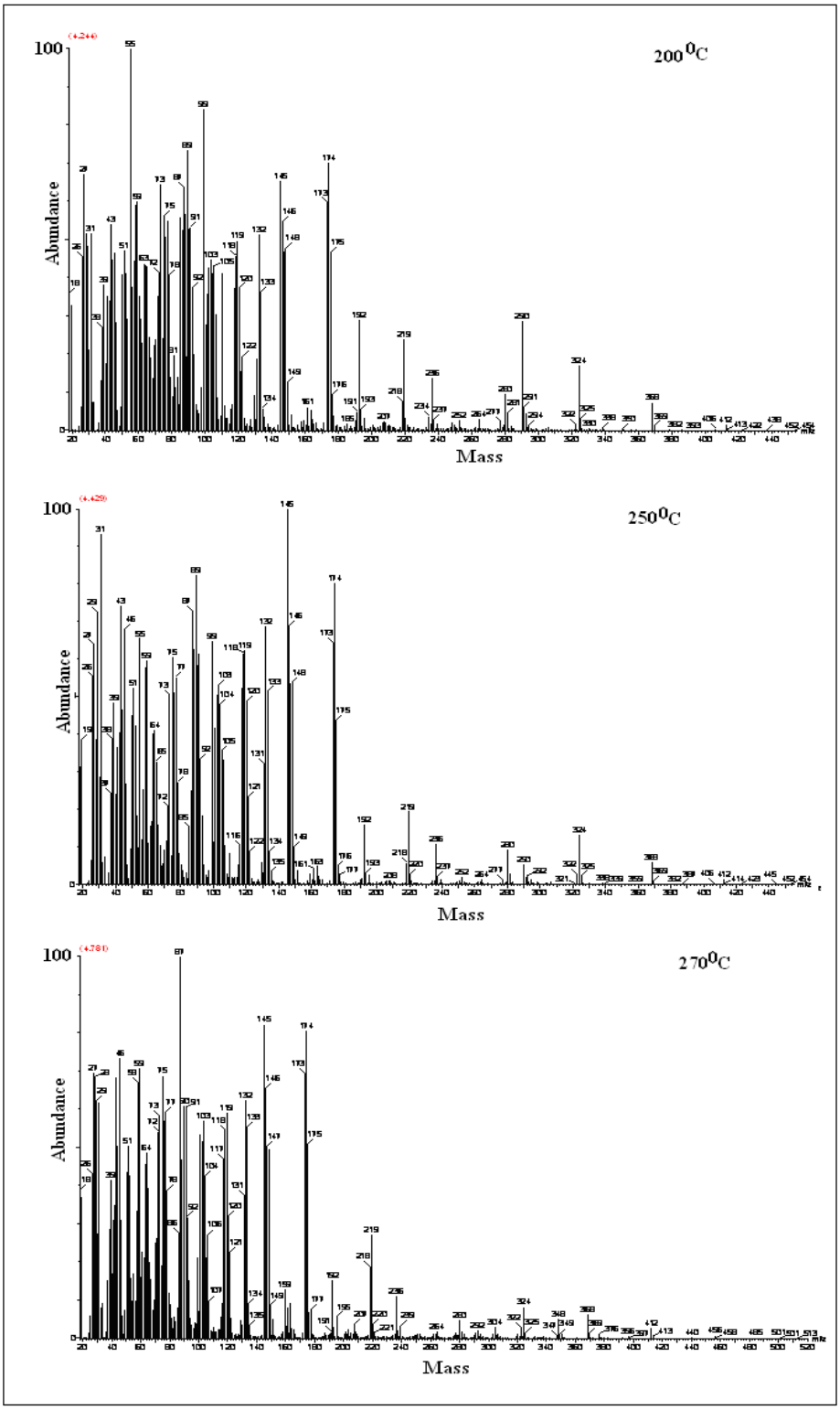

Figure 65 Fragments of PUNCOHEMA1 at 200ºC, 250ºC and 270ºC.

Table 13 The relative abundance (Intensity %) of the peaks and their fragments for PUNCOHEMA1.

m/z	Fragment	Intensity (%) 200ºC	Intensity (%) 250ºC	Intensity (%) 270ºC
18	H_2O	36,1	31	37,9
26	CN C_2H_2	45,2	56	43,1
27	C_2H_3	68,2	68,9	69,4
28	CO	52,3	37,8	67,8
29	CHO C_2H_5	48,1	73	62,7
31	CH_3O CH_2OH	52,3	94,6	61,3
39	C_3H_3	38,8	48,2	42,3
41	C_2HO C_3H_5	35	36	31,8
42	C_3H_4 C_2H_2O CNO	34,5	40	35,0
43	C_2OH_3 CHNO	54,5	75	67,9
44	CO_2	45,2	46,8	50,2
45	C_2H_5O	46,7	47,2	30,2
55	C_3H_3O	100	66,3	17,1
57	C_2HO_2	45	25,9	33,9
60	C_3H_5O	35	11,5	16,0
69	C_3HO_2 C_4H_5O	22,5	6,1	11,1
71	$C_3H_3O_2$ C_3H_5NO	34,9	12,5	25,5
72	$C_3H_4O_2$	42,3	22,2	54,3
73	$C_3H_5O_2$	64,7	50	57,8
75	$C_3H_6O_2$	57	61,9	68,2
77	C_6H_5	55,3	56,6	58,8
81	C_4HO_2	20	4,3	5,6

Table 13 (cont'd)

m/z	Fragment	Intensity (%) 200°C	Intensity (%) 250°C	Intensity (%) 270°C
85	$C_4H_5O_2$	6,7	16,7	7,8
87	C_7H_3 $C_4H_7O_2$	64,2	74,1	100
89	C_7H_5	74,8	83,2	45,3
91	C_7H_7 C_6H_5N	53,4	62,5	61,3
95	$C_5H_3O_2$	6,3	3	3,9
99	C_7H_5N	85,6	65,3	22,3
104	C_7H_6N	42,0	48,2	42,5
118	$C_6H_{12}O_2$	46,3	62,7	54,7
122	$C_7H_6O_2$	20	8,4	5,5
129	$C_6H_9O_3$	8,2	6,4	5,0
132	C_8H_7NO	52,4	69,0	62,5
145	$C_6H_9O_4$	65,2	100	82,2
149	$C_9H_5O_2$	13,5	10,3	8,6
174	$C_8H_{15}O_4$	70,2	82,4	79,1
175	$C_8H_{16}O_4$	47,5	44,8	51,0
176	$C_8H_{16}O_4$	8,2	4,9	6,9
185	$C_9H_8NO_2$	3,2	0,6	0,07
192	$C_9H_8N_2O_3$	28,7	17,5	15,3
205	$C_9H_5N_2O_4$	1,6	1,2	1,4
265	$C_{12}H_{14}N_2O_5$	1,5	0,6	0,3
290	$C_{12}H_{14}O_4$	29,1	5,1	0,8
324	$C_{10}H_8N_2O_3$	17,8	15,3	8,9

The fragmentation for PUNCOMMA3 at 168ºC, 250ºC and 315ºC is given in Figure 66. The baseline at 168ºC is m/z = 72 and other peaks very close to the base line are m/z = 57 and 45. The other peaks are similar to the peaks obtained for other polymers. At 250ºC, the base peak is m/z =87 and other intense peaks are m/z = 59, 75 and 174. These are the same fragments obtained in other fragmentations. At 315ºC the base peak is m/z = 45 and others are at m/z =69, 89 and 174 etc. The results are tabulated in Table 14.

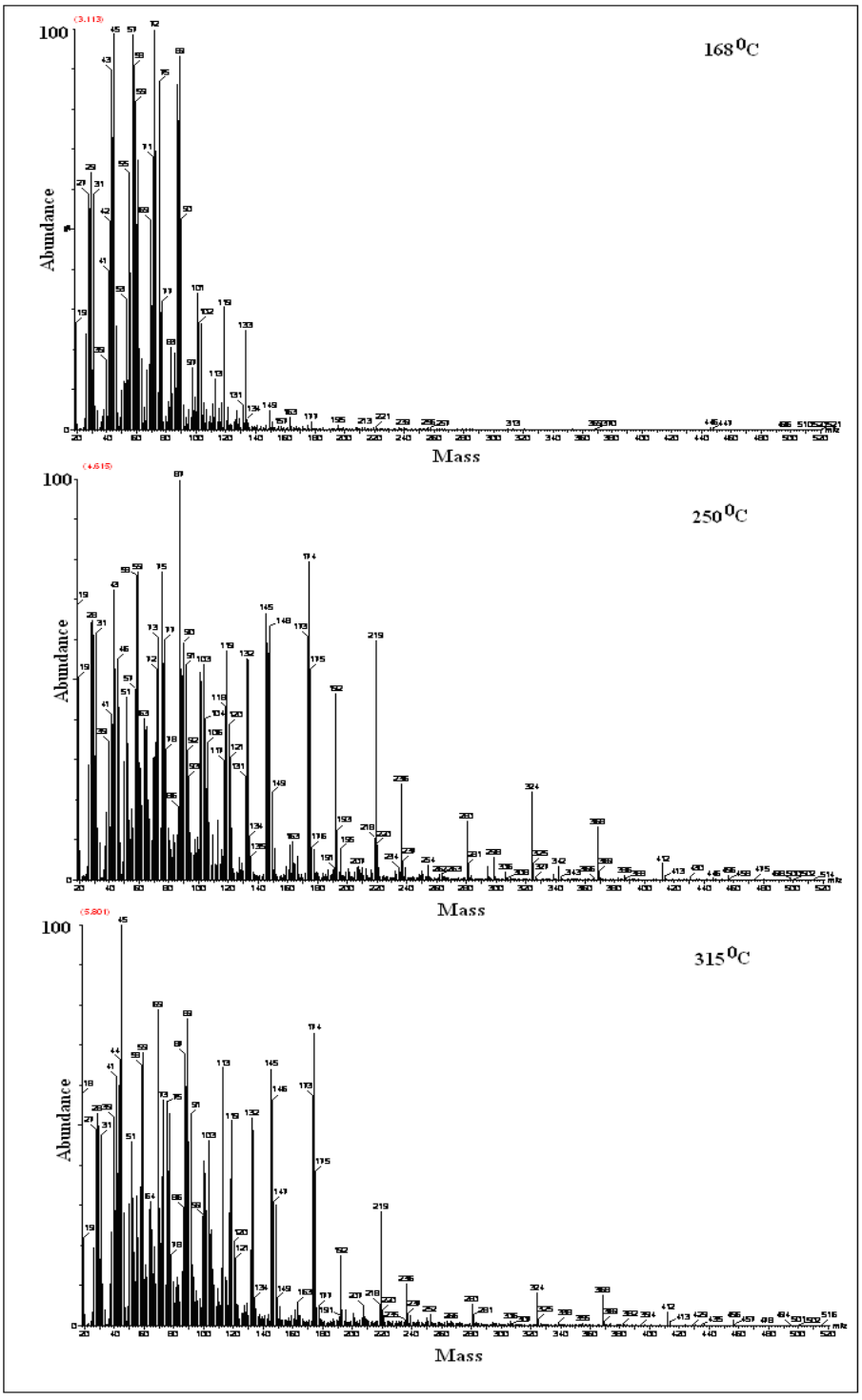

Figure 66 Fragments of PUNCOMMA3 at 168ºC, 250ºC and 315ºC

Table 14 The relative abundances of the peaks and their fragments for PUNCOMMA3.

m/z	Fragment	Intensity (%) 168°C	Intensity (%) 250°C	Intensity (%) 315°C
18	H_2O	57,5	68,5	57,1
26	CN C_2H_2	24,6	27,8	19,6
27	C_2H_3	58,0	63,8	48,0
28	CO	55,0	64,5	52,5
29	CHO C_2H_5	64,6	61,1	50,0
31	CH_3O CH_2OH	57,5	61,8	47,4
41	C_2HO C_3H_5	39,1	42,1	62,2
42	C_3H_4 C_2H_2O	52,4	38,0	38,2
43	CNO C_2OH_3 CHNO	90,3	72,5	59,8
44	CO_2	72,8	52,5	66
45	C_2H_5O	98,2	53,4	100
55	C_3H_3O	64,2	17,5	32
57	C_2HO_2 C_3H_5O	98,0	48,2	35,1
58	C_3H_5OH	92,1	76,0	64,9
59	C_3H_6OH	82,4	77,1	68,4
60	C_3H_5O	52,5	29,3	12
69	C_3HO_2 C_4H_5O	52,5	30,4	77,9
71	$C_3H_3O_2$ C_3H_5NO	67,9	34,1	29,1
72	$C_3H_4O_2$	100	52,5	37,3
73	$C_3H_5O_2$	69,0	60,0	55,5
75	C_6H_3	86,2	77,1	55,1

Table 14 (cont'd)

m/z	Fragment	Intensity (%) 168°C	Intensity (%) 250°C	Intensity (%) 315°C
77	C_6H_5	32,3	60,0	52,5
87	C_7H_3 $C_4H_7O_2$	86,5	100	67,8
89	C_7H_5 C_6H_3N	93,8	51,7	76,2
90	C_7H_6	52,5	59,0	45,8
91	C_7H_7 C_6H_5N	5,5	53,6	52,8
95	$C_5H_3O_2$	4,1	6,1	7,8
97	$C_5H_5O_2$	15,2	11,2	12,5
104	C_7H_6N	3,9	40	23,2
113	$C_5H_5O_3$	13,0	15,0	64,7
119	C_7H_5NO	31,3	57,0	51,8
122	$C_7H_6O_2$	1,6	13,5	5,2
132	C_8H_7NO	2,6	55,0	52,4
133	C_8H_8NO	24,8	55,1	47,8
145	$C_6H_9O_4$	1,8	66,2	64,7
149	$C_9H_5O_2$	4,8	22,5	7,3
154	$C_{12}H_{10}$	1,0	2,3	1,5
163	$C_{12}H_5N$	3,8	11,5	6,2
169	$C_{12}H_{11}N$	0,1	2,5	1,5
174	$C_8H_{15}O_4$	0,5	80,0	73,9
192	$C_9H_8N_2O_3$	0,4	47,5	17,7
205	$C_9H_5N_2O_4$	0,3	2,5	2,9
219	$C_{10}H_7N_2O_3$	0,5	60,0	29,0
241	$C_{15}H_{15}NO_2$	0,03	1,0	1,1
265	$C_{12}H_{14}N_2O_5$	0,01	1,8	1,0

3.2.2 Synthesis of Acrylate End capped Hydroxyl Terminated Polyurethane

The compositions of the PUOHA polymers synthesized in section 2.2.6 are given in Table 15. Acrylate end capping was achieved with two types of acrylate, MMA and HEMA.

Table 15 Chemical composition and molecular weights of PUOHA polymers.

Sample Name	**Chemical Composition**	**Mn (g/mol)**	**Mw (g/mol)**	**Pd**
PUOHMMA1	TDI/PEG/MMA	4749	9820	2.068
PUOHMMA2	HDI/PEG/MMA	6234	13907	2.23
PUOHMMA3	MDI/PEG/MMA	5493	39486	7.19
PUOHHEMA1	TDI/PEG/HEMA	2590	2661	1.027

Molecular weights and the Pd values of PUOHA polymers are given in Table 15, and molecular weight distributions are given in Appendix B. MMA end capped polymers have much higher Mn and Mw values compared to that of HEMA end capped polymer PUOHHEMA1. The Pd value of PUOHMMA3 is 7.19. PUOHMMA2 has the highest Mn and Mw value.

Obtained polymers were not purified therefore it is possible that they may contain some fractions of acrylate homopolymers in the final product. This gives rise to the difference between Mn and Mw as well as Pd. However, the observed differences are not too big, and therefore they could be acceptable. In future work, the polymer obtained will be purified to obtain much better products.

FTIR-ATR Analysis Results

FTIR-ATR spectra of the acrylate end capped hydroxyl terminated polyurethanes are given in Figure 67. All the polymers have the characteristic vibration bands of urethane. NH stretching vibration maxima of PUOHMMA1, PUOHMMA3 and PUOHHEMA1 appeared at 3295-3310 $cm^{-1}$and these bands showed the presence of strong hydrogen bonding. This result was also consistent with the vibration frequency of the carbonyl band that is at 1705-1710 cm^{-1}. On the other hand, the N-H vibration for PUOHMMA2 is at the free NH side and carbonyl vibration frequency is recorded at 1716 cm^{-1} that is close to the free carbonyl vibration band. All the polymers except PUOHMMA2 have a C=C vibration band at 1602 cm^{-1} due to the aromatic ring present in the diisocyanate structure. Vinyl group stretching vibration band is shown at 1636 cm^{-1} for PUOHHEMA1.

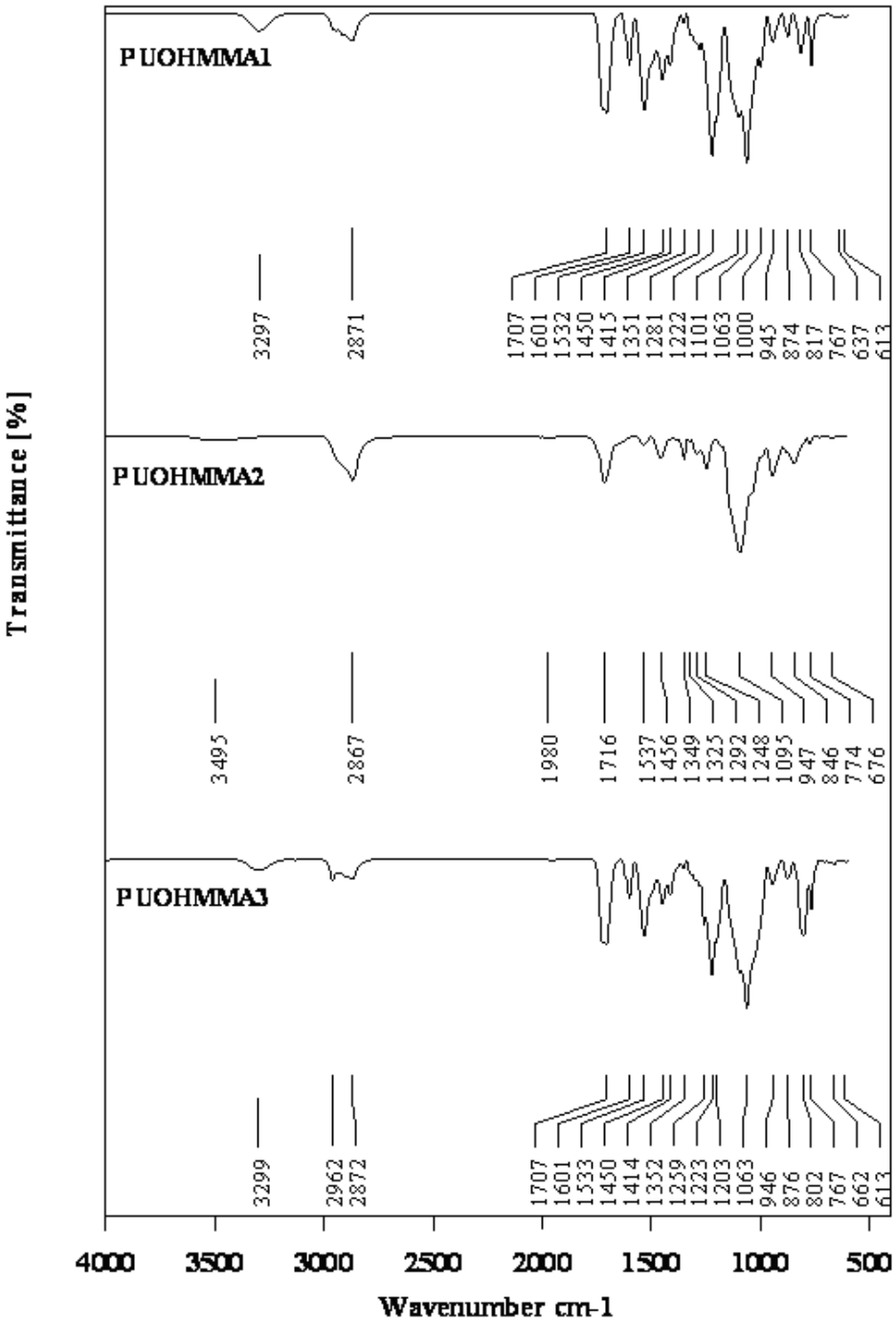

Figure 67 FTIR ATR Spectrum of PUOHA polymers

NMR Analysis Results

The ^{1}H and ^{13}C NMR spectra of PUOHMMA1 are given in Figure 68 and 69, respectively. Urethane protons (-NH in urethane) are observed at δ= 8.9, 9.8 ppm, aromatic protons are appeared at δ= 6.9-7.9 ppm, the methyl proton is assigned to the peak at δ=0.9 ppm, hydroxyl proton (-OH) is at δ=2 ppm and the $–OCH_2$ protons are found at δ=3.4 ppm. Vinylic protons of MMA are observed at δ=5.7, 5.9 ppm. In the ^{13}C NMR spectrum, there are two carbonyl peaks at δ=153,154 ppm that corresponds to the urethane and acrylic carbonyl. Aromatic carbons and the carbons of the vinylic end group appeared at δ=114, 122, 125, 130, 136 and 137 ppm. The ether carbon peaks (–OCH) are at δ=63 and $–CH_2$ at δ= 29 ppm. Methyl carbon attached to the aromatic ring was observed at δ=17 ppm.

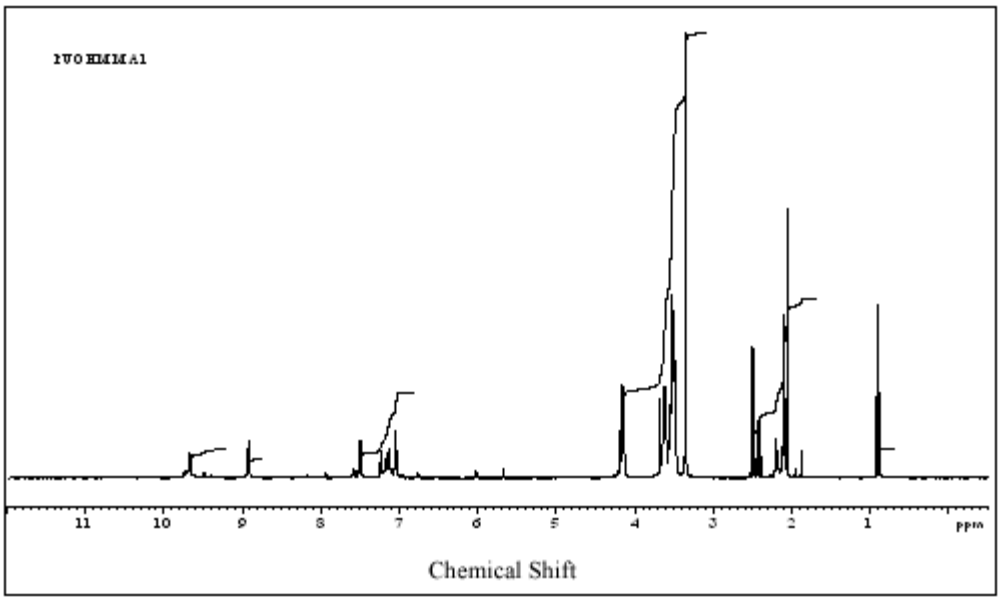

Figure 68 ^{1}H NMR spectrum of PUOHMMA1

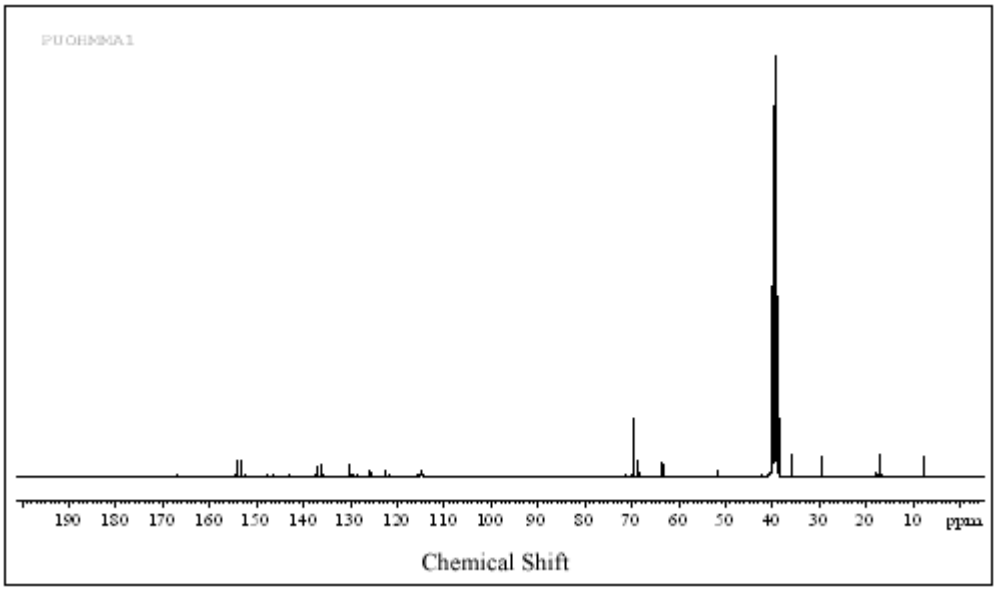

Figure 69 ^{13}C NMR Spectrum of PUOHMMA1

The ^{1}H and ^{13}C NMR spectrum of PUOHHEMA1 is given in Figure 70 and 71, respectively. Characteristic chemical shifts for the protons present in the polymer structure are observed at δ= 8.9, 9.6 ppm for NH protons, at δ= 6.9-7.6 ppm for aromatic protons, at δ=5.7 - 6.4 ppm for vinylic protons of HEMA, at δ=2.1 ppm for hydroxyl proton (-OH). In the ^{13}C NMR spectrum, there are three carbonyl peaks at δ=153,154 and 165 ppm that correspond to the urethane and acrylic carbonyl carbons. Vinylic carbons are present at δ=114-130 ppm, which were very close to aromatic carbons.

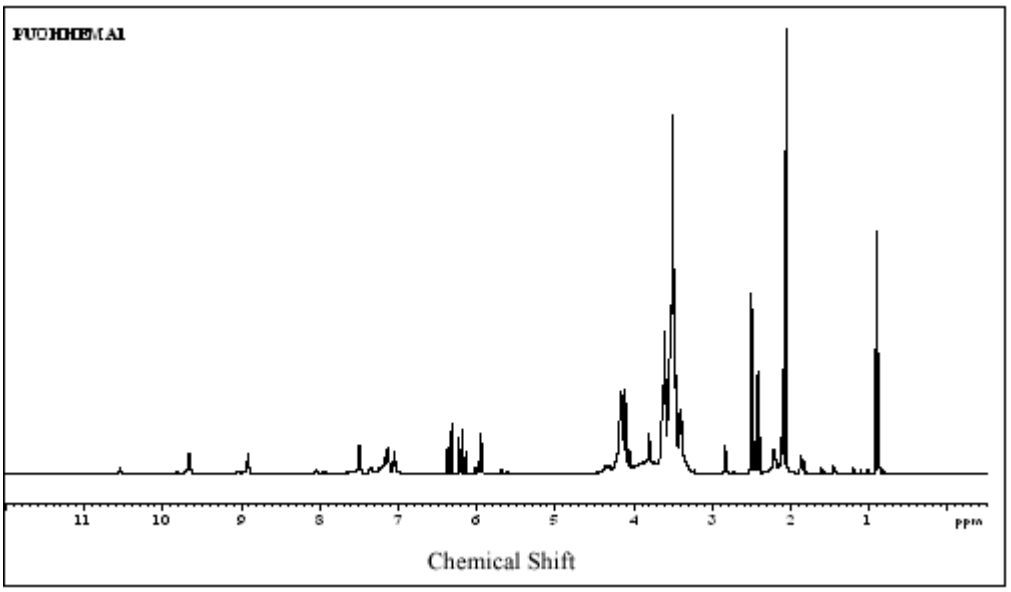

Figure 70 ^{1}H NMR Spectrum of PUOHHEMA1

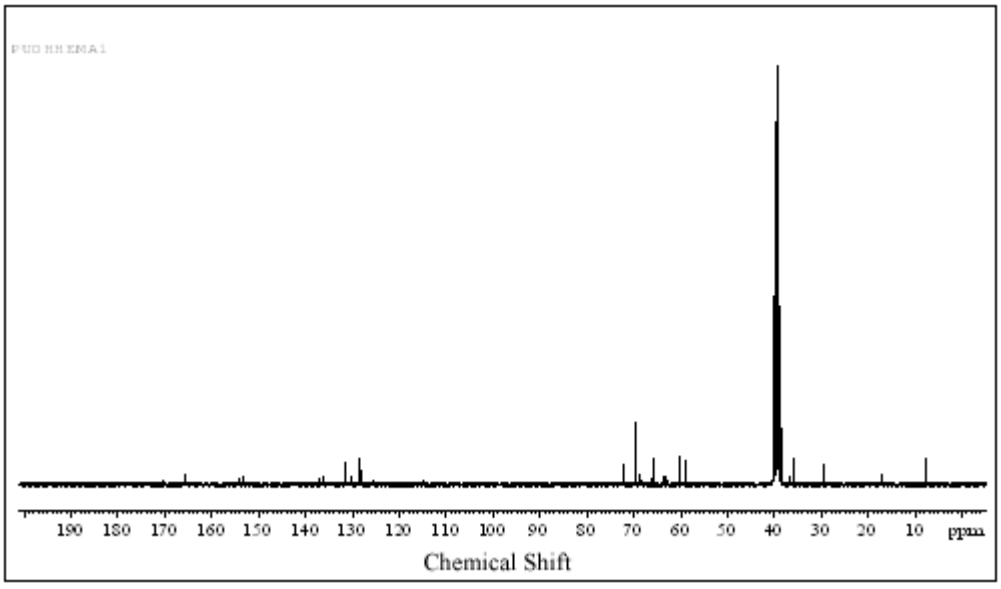

Figure 71 ^{13}C NMR Spectrum of PUOHHEMA1

Thermal Analysis Results

Thermal analysis of PUOHA polymers were carried out by TGA, DSC and Mass spectroscopy. The TGA thermograms of these polymers are given in Figures 72-74. All the polymers have two main degradation stages that are described in Table 16.

Table 16 TGA results of PUOHA polymers.

Polymer	**Degradation Stage**	**Temperature (°C)**	**Weight Loss (%)**
PUOHMMA1	1 2	130 350 (multiple peaks)	10 90
PUOHMMA2	1 2	410 430	45 40
PUOHMMA3	1 2	216 410	6 93
PUOHHEMA1	1 2	200 430	30 95

PUOHMMA1 is degraded within two steps (Figure 72). First degradation with a weight loss of 10 % is up to 130ºC might be attributed to the solvent removal and it is followed by a second degradation maximized at 350ºC (in the range of 300-375ºC) with a total weight loss of 90 %. In the second stage, there are fluctuations that might be due to end group cyclization. General trend of thermogram resembles to that of PUOH1 (Figure 49). In this case, acrylate

ends lead to a much higher thermally stable polymer. Thermal degradation of PUOHMMA1 could be considered as a depolymerization mechanism type.

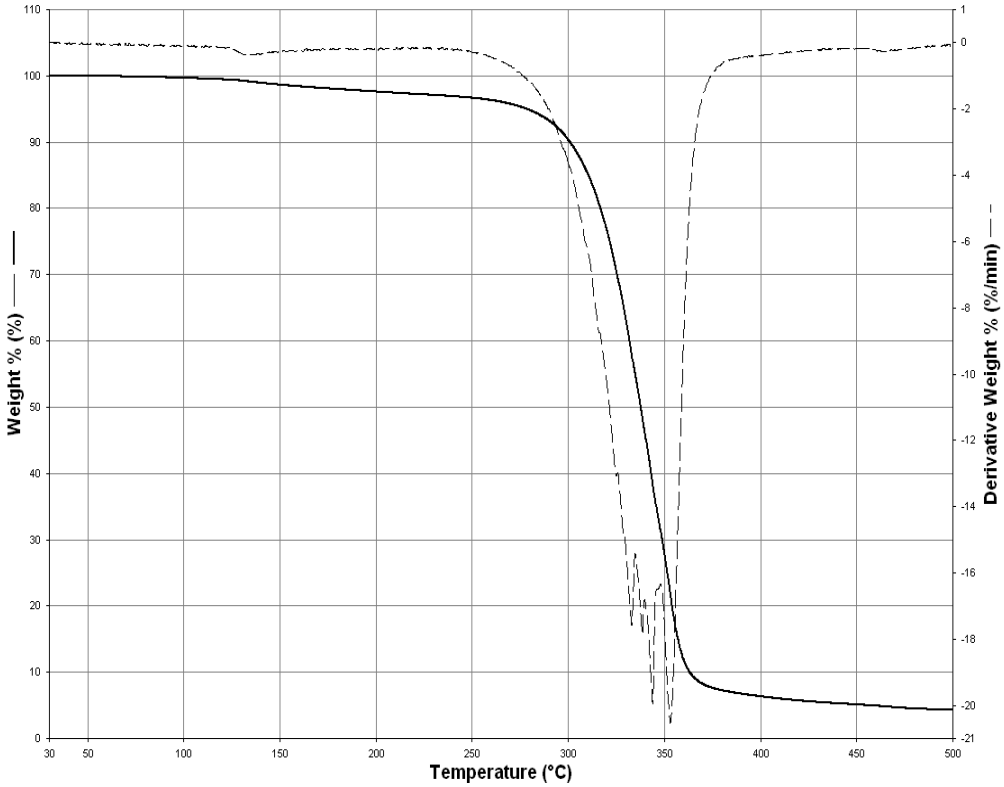

Figure 72 TGA thermogram of PUOHMMA1.

Thermal degradation of PUOHMMA2 shown in Figure 73 was started at 30ºC up to 310ºC with a smooth decrease that leads to a weight loss of 10% and continued by acceleration up to 400ºC with a weight loss of about 32%. Then rate of degradation is increased and maximized at 420ºC with a shoulder at 410ºC due to decomposition of side groups. Total weight loss in stage two is

96%. Random scission type degradation behavior with some depolymerization is also observed in PUOHMMA2 thermogram.

In the thermal degradation of PUOHMMA3 represented in Figure 74, showed the same trend as it was observed in PUOHMMA1 thermogram. However, there is no shoulder in the main peak decomposition. A smooth decrease by 10 % due to possible end group cyclization is observed at 216ºC and main chain degradation with a total weight loss of 93% is maximized at 410ºC.

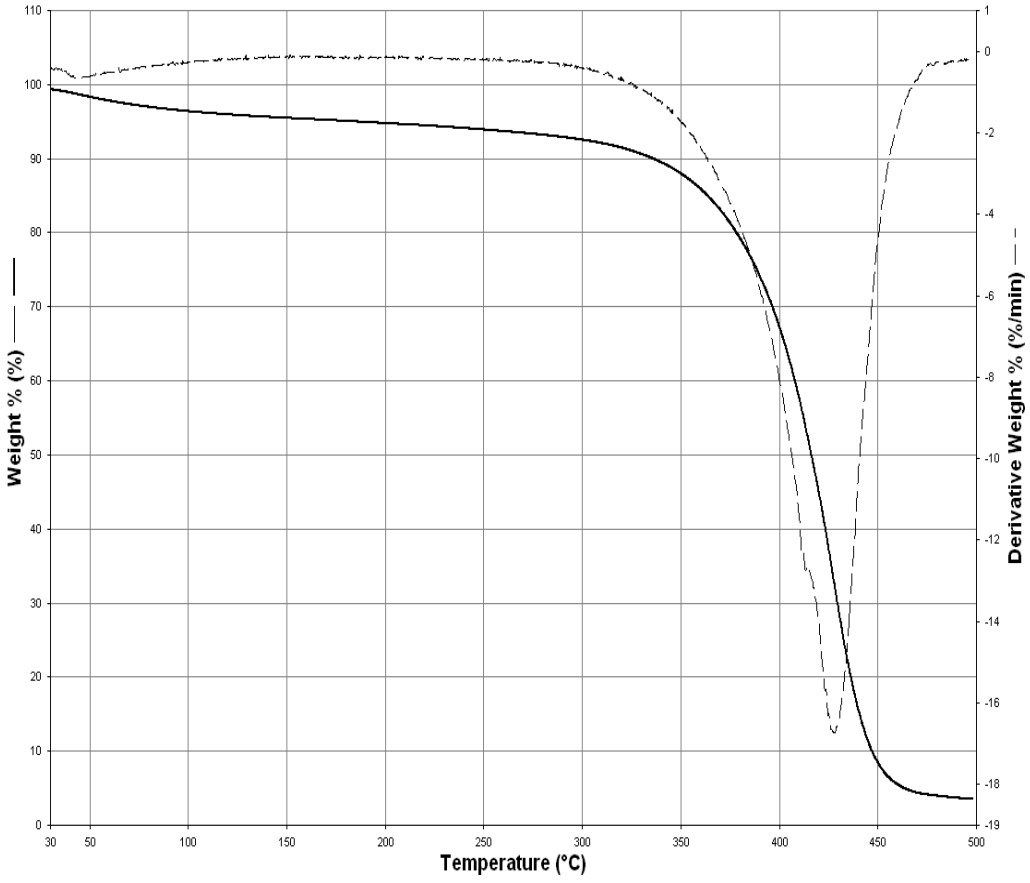

Figure 73 TGA thermogram of PUOHMMA2

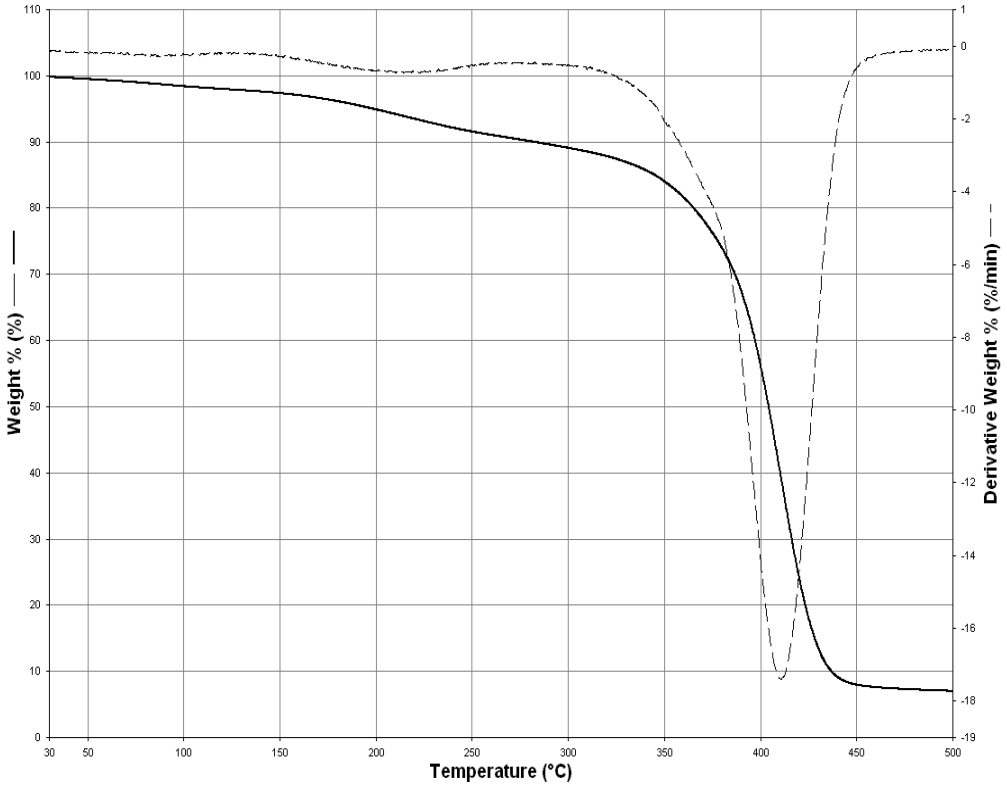

Figure 74 TGA thermogram of PUOHMMA3

PUOHHEMA1 decomposition (Figure 75) starts from the beginning, continues up to 200ºC, and ends with a weight loss of 30% due to side group degradation. This degradation can be regarded as a linkage type. This first degradation stage is followed by a random degradation with fluctuations due to the end group cyclization and second stage is continued up to 430ºC and ended with a total weight loss of 95%. The TGA thermogram of PUOHHEMA1 has a similar characteristic with typical TGA thermogram of polyHEMA. Therefore, it is possible to have considerable amount of homopolymer HEMA. Similarly, PUOHMMA3 thermogram shows more depolymerization type degradation, which is typical of polyMMA homopolymers.

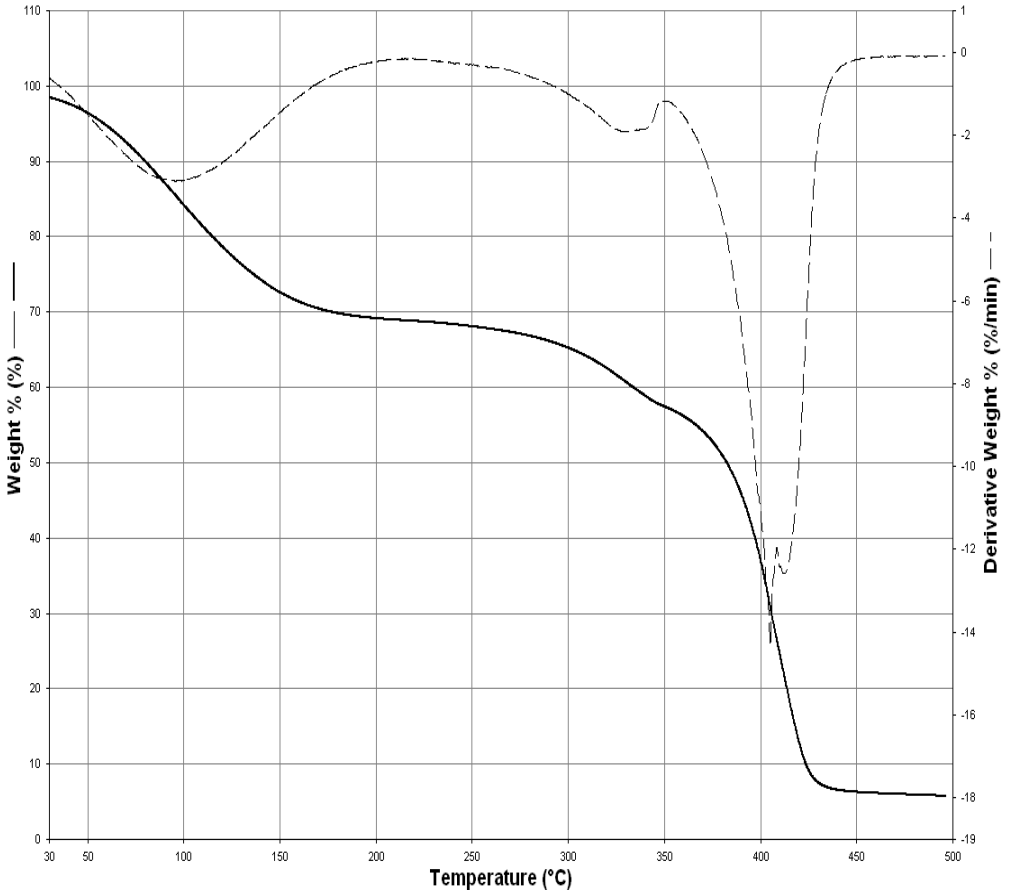

Figure 75 TGA thermogram of PUOHEMA1

The DSC thermograms of PUOHMMA1, PUOHMMA2, and PUOHMMA3 are given in Figure 76, 77 and 78, respectively. Thermograms were recorded at a temperature range of (-70) - 150^{o}C. In this temperature range PUOHMMA1 exhibited a Tg value of 13.31ºC with a heat capacity of 0.563 J/g ^{o}C. The single Tg value of sample showed the phase mixing of the sample rather than phase separation.

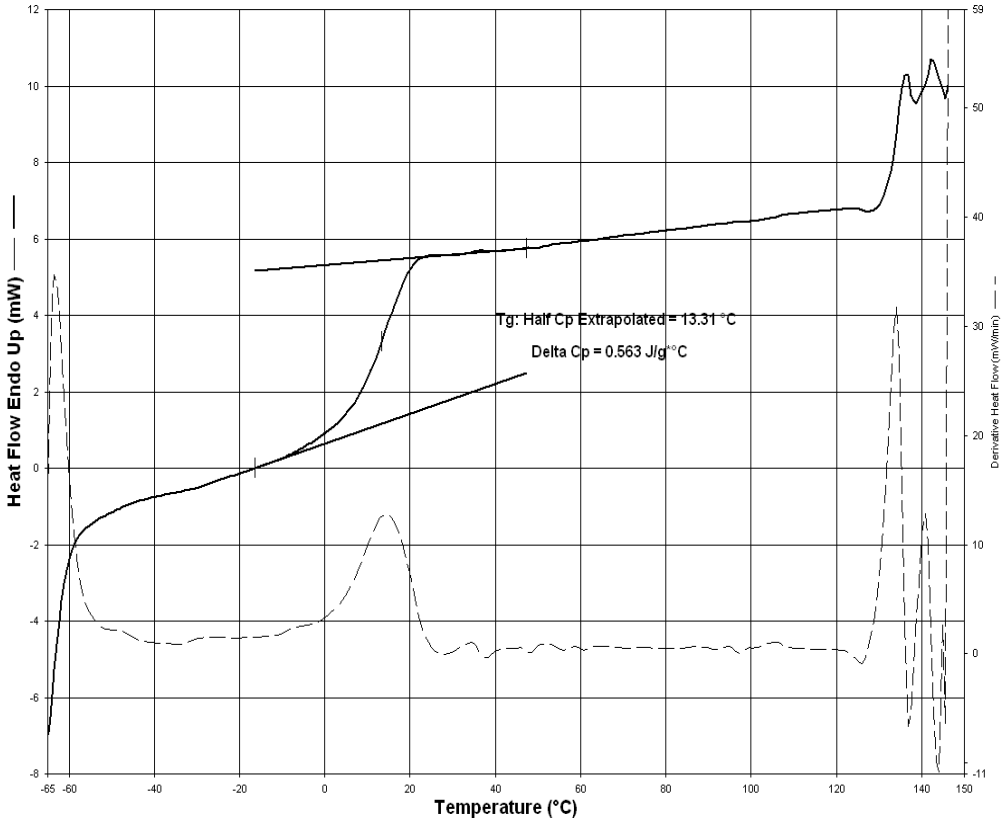

Figure 76 DSC thermogram of PUOHMMA1.

The DSC thermogram of PUOHMMA2 is shown in Figure 77. At -54.76ºC, Tg of the polymer was recorded with a heat capacity change of 0.45 J/g ºC. The crystallization peak is observed at -29.79ºC. There are two Tm values, which are at 22.94ºC and 33.47ºC due to the polymorphic structures present. The enthalpy of fusion for the crystallization is -13.8, for melting 41.7 and 5.6 J/g respectively. Results of the DSC data showed that, there exists a phase mixing and a liquid crystal formation in the polymer. The obtained Tm values indicate the presence of liquid crystal, whereas the observed single Tg value is the indication of phase mixing (no phase separation).

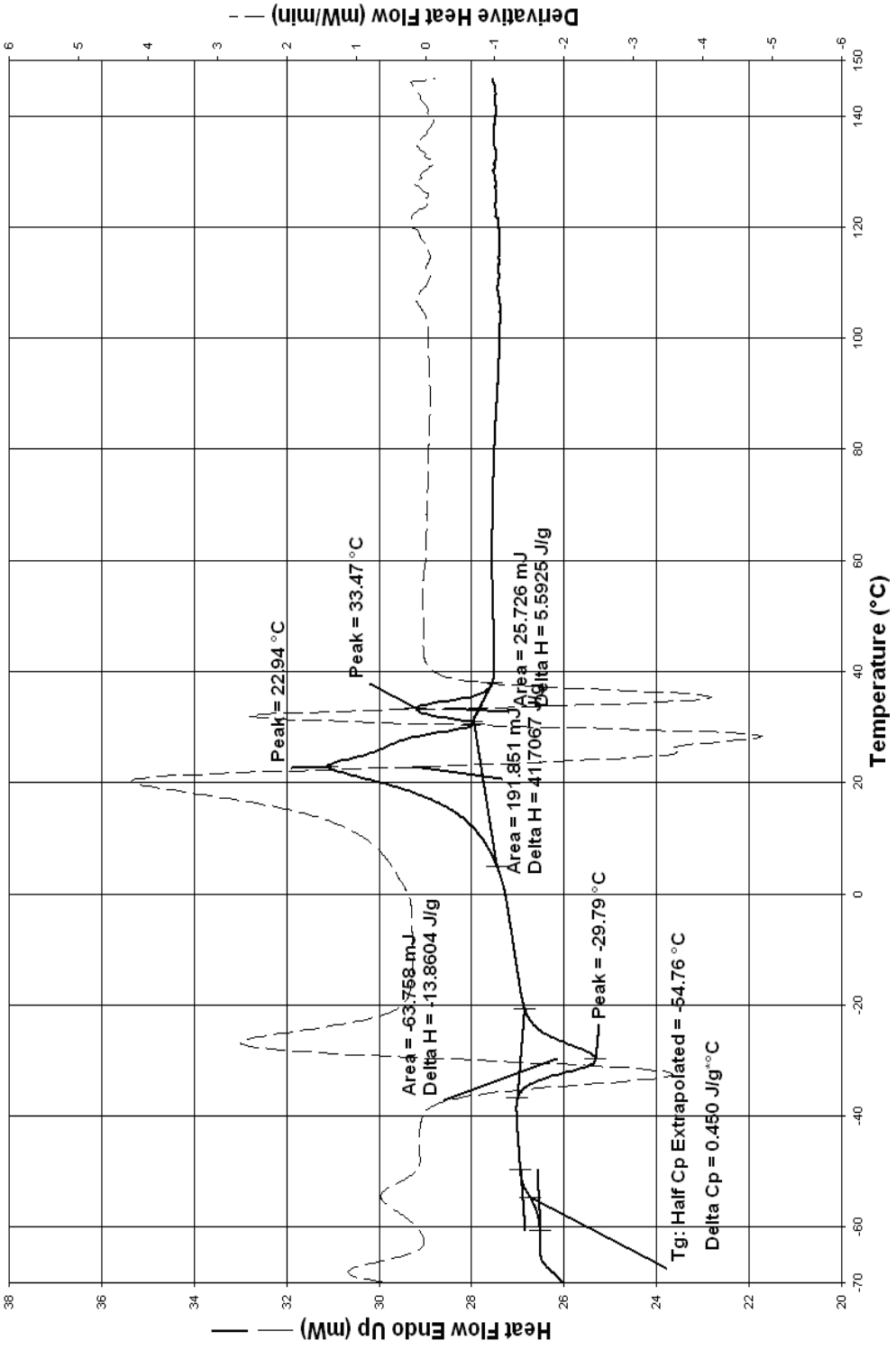

Figure 77 DSC thermogram of PUOHMMA2

The Tg values observed for PUOHMMA3 are at -45.61ºC, -25.04ºC and 9.05ºC as given in Figure 78. The negative Tg values may correspond to the transitions of soft and hard segments present in the acrylate end capped polyurethane, whereas the positive one may be due the homopolymer of acrylate (oligomer). The molecular weight of the homopolymer can be calculated with the above equation as 3049 g/mol.

$$Tg = Tg^{\infty} - \frac{K}{Mn} \qquad (K= 4.3\times10^{5} \text{ and } Tg^{\infty} =423)$$

Mn = 3049 g/mol (homopolymer)

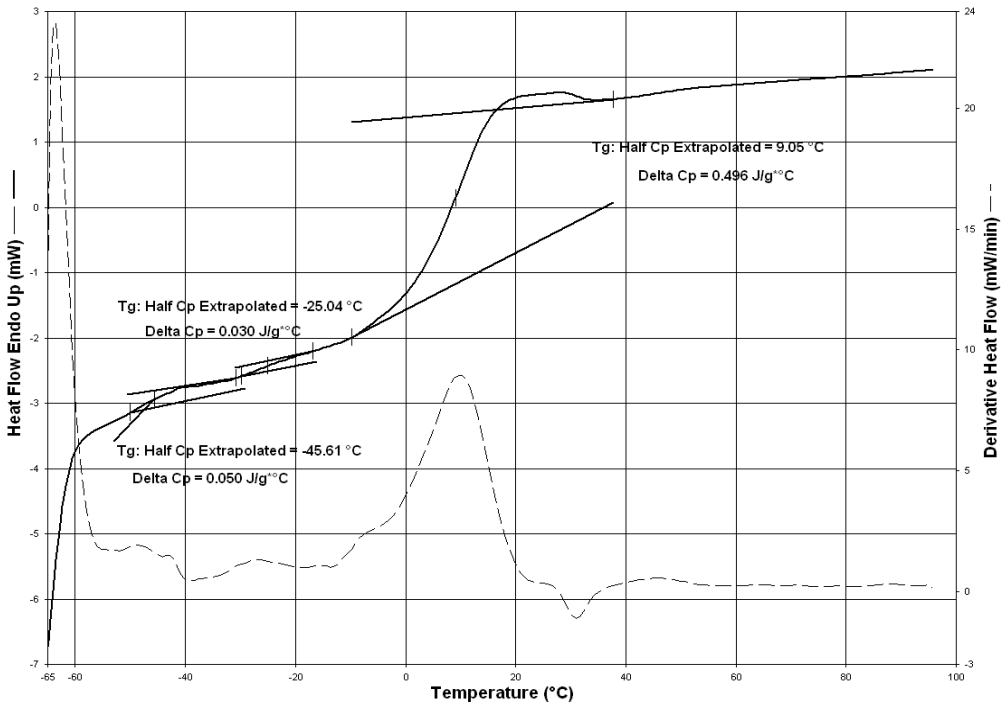

Figure 78 DSC thermogram of PUOHMMA3

Mass Analysis Results

The mass thermograms of PUOHMMA1 and PUOHMMA3 are given in Figures 79 and 81, respectively. Fragments of PUOHMMA1 at 154ºC, 250ºC, and 304ºC are given in Figure 80. The details of the fragments obtained at these temperatures are tabulated at Table 17.

PUOHMMA1 mass thermogram fragmentation at 154ºC gave three most intense peak at m/z = 18, 43, and 45 (base peak) that are due to the fragments of H_2O, CHNO(or CHCHOH) and CH_2CH_2OH, respectively. It is obvious from the fragmentation thermogram that at this temperature low mass fragments, which might be the soft segments of the urethane part, were splitted off.

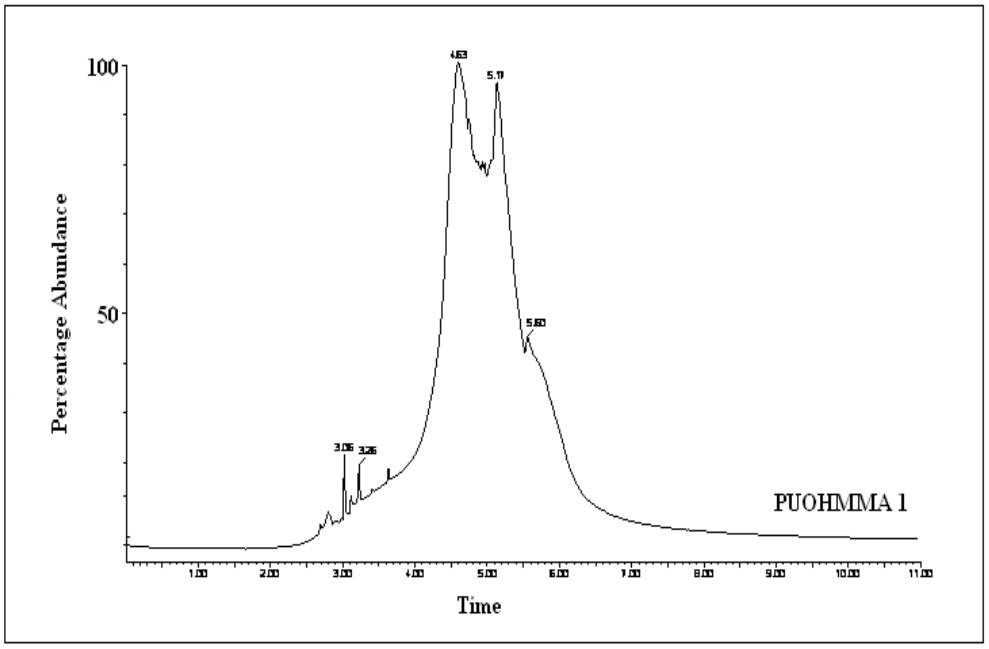

Figure 79 Mass thermogram of PUOHMMA1.

In addition to the above intense mass fragments, m/z =28, 29, 57, 72 and 89 are also relatively predominant. These masses are due to the groups CO, CHO/C_2H_5, C(O)CHO, C(O)-CH_2CH_2O and C_7H_5.

Although the most intense peak at 250ºC is m/z = 87, most of the fragments appeared to have abundance value close to the base fragment. Among them m/z =43 (CHNO or CHCHOH), 59 (CO-CH_2-OH), 103 (CH_3-C_6H_2-N), 119 (C_6H_4-CO-O), 132 (CH_3-C_6H_3-NH-C(O), 145 (CH_2=C(CH_3)-C(O)O-OC_2H_4-O), 174 (CH_2=C(CH_3)-C(O)O-OC_2H_4-O-C(O)) , 219 (O-C(O)-NH-C_6H_3(CH_3) – NH-C(O)O-CH_2) are important.

The m/z values obtained at 304ºC have same fragments with varying abundance percentages. Base peak is at m/z= 45 which is the same as in temperature 154ºC. Also at m/z =174, $C_8H_{15}O_4$ decomposition is dominant. All the fragments are tabulated in Table 17 for three different temperatures.

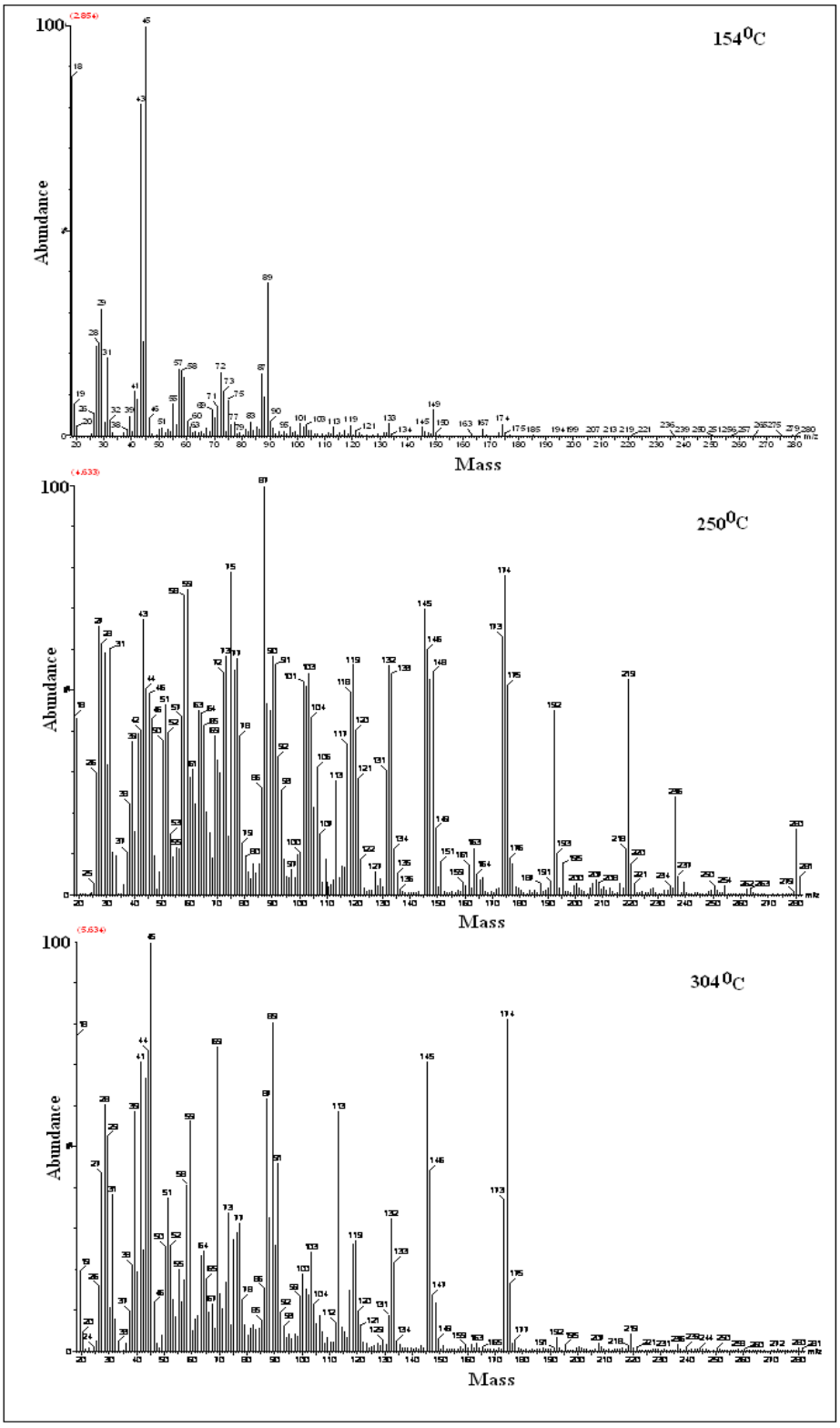

Figure 80 Fragments of PUOHMMA1 at 154ºC, 250ºC and 304ºC

Table 17 The relative abundances of the peaks and their fragments for PUOHMMA1.

m/z	Fragment	Intensity (%) 154°C	Intensity (%) 250°C	Intensity (%) 304°C
18	H_2O	97,2	45,0	78,2
26	CN C_2H_2	5,1	30,0	15,2
27	C_2H_3	22,2	66,1	43,2
28	CO	22,6	62,2	60,2
29	CHO C_2H_5	31,6	58,2	54,2
31	CH_3O CH_2OH	18,5	60,6	38,4
41	C_2HO C_3H_5	10,8	40,1	70,1
42	C_3H_4 C_2H_2O	8,8	41,2	25,2
43	CNO C_2OH_3 CHNO	80,8	67,6	67,2
44	CO_2	24,2	50,2	75,2
45	C_2H_5O	100	-	100
46	C_2H_6O	4,2	49,8	12,5
51	C_2H_7O	2,0	47,5	37,6
55	C_3H_3O	8,2	12,1	20,2
58	$C_2H_2O_2$	15,6	74,0	40,2
59	$C_2H_3O_2$	14,8	75,0	56,2
60	C_3H_5O	3,8	28,8	5,8
69	C_3HO_2 C_4H_5O	6,2	39,1	75,2
71	$C_3H_3O_2$ C_3H_5NO	7,4	30,0	10,1
72	$C_3H_4O_2$	15,2	54,6	17,2
73	$C_3H_5O_2$	11,0	56,7	35,4

Table 17 (cont'd)

m/z	Fragment	Intensity (%) 154°C	Intensity (%) 250°C	Intensity (%) 304°C
75	$C_3H_6O_2$	8,4	78,5	27,2
77	C_6H_5	3,8	56,0	32,0
81	C_4HO_2	2,1	5,2	7,1
87	C_7H_3 $C_4H_7O_2$	15,1	100	63,4
89	C_7H_5	38,4	45,3	80,8
91	C_7H_7 C_6H_5N	2,6	56,2	56,3
95	$C_5H_3O_2$	2,5	5,2	5,0
97	$C_5H_5O_2$	1,2	6,4	5,1
103	C_7H_5N	3,3	55,0	25,2
104	C_7H_6N	1,2	44,4	12,9
115	$C_6H_{11}O_2$	0,6	7,5	5,9
119	$C_7H_4O_2$	2,8	56,4	27,0
132	C_8H_7NO	0,8	56,2	33,3
145	$C_6H_9O_4$	3,2	71,4	65,8
149	$C_9H_5O_2$	5,2	17,5	3,9
174	$C_8H_{15}O_4$	3,8	78,4	80,2
176	$C_8H_{16}O_4$	0,2	8,9	2,5
185	$C_9H_8NO_2$	0,002	2,0	1,1
192	$C_9H_8N_2O_3$	-	45,2	4,6
205	$C_9H_5N_2O_4$	0,008	3,4	3,0
219	$C_{10}H_{10}N_2O_4$	0,012	53,8	5,0
279	$C_{12}H_{15}N_2O_5$	0,4	1,2	0,03

The mass thermogram of PUOHMMA3 is given in Figure 81. The thermogram is recorded up to 500ºC. Detailed fragments at 132, 264, and 353ºC are shown in Figure 71 and most intense mass fragments are given in Table 18.

Main fragments of PUOHMMA3 is given on the below structure (33). Acrylate group cleavage (m/z= 41,69) is prominent and reached to a maximum abundance value at high temperatures as shown on Figure 82. The m/z = 41 and 69 are the main peaks at temperatures 264 and 353ºC . At low temperatures (132ºC), H_2O was splitted off from the end of the chain and has a % abundance of 56,2 %.

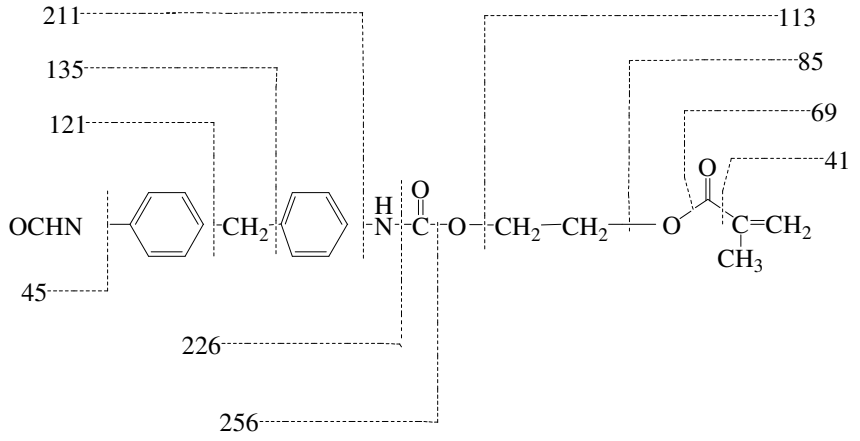

(33)

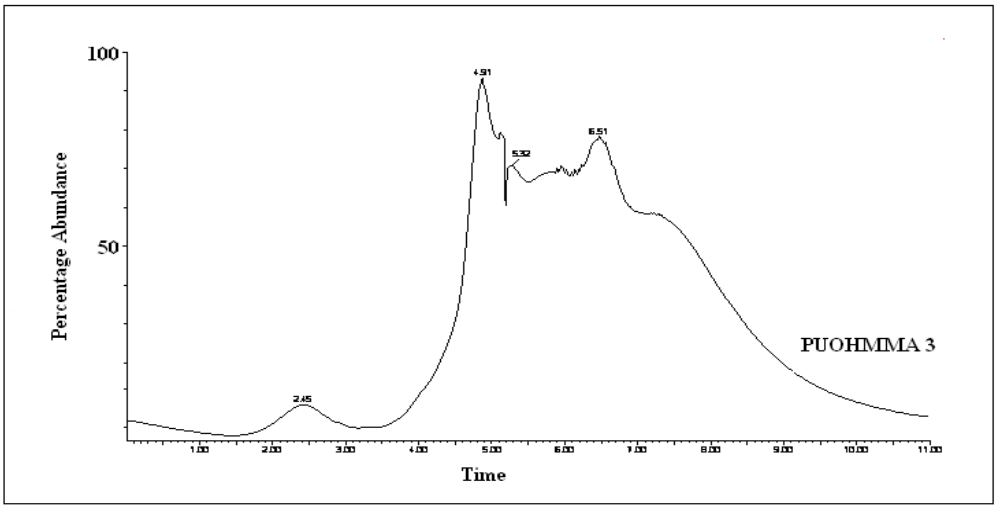

Figure 81 Mass thermogram of PUOHMMA3

Table 18 The relative abundances of the peaks and their fragments for PUOHMMA3.

m/z	Fragment	Intensity (%) 132°C	Intensity (%) 264°C	Intensity (%) 353°C
18	H_2O	56,2	40,0	55,0
26	CN C_2H_2	6,3	18,0	28,2
27	C_2H_3	20,1	41,8	52,4
28	CO	13,4	42,2	57,8
29	CHO C_2H_5	16,6	44,8	66,2
31	CH_3O CH_2OH	10,4	38,6	60,0
39	C_3H_2	34,0	59,5	55,0
41	C_2HO C_3H_5	13,2	72,3	74
42	C_3H_4, CNO, C_2H_2O	5,0	38,6	47,5

Table 18 (cont'd)

m/z	Fragment	Intensity (%) 132°C	Intensity (%) 264°C	Intensity (%) 353°C
43	C_2OH_3 CHNO	24,8	56,8	73,4
44	CO_2	12,5	55,0	48.8
45	C_2H_5O	72,5	87,5	48,2
55	C_3H_3O	13,4	44,2	54,2
57	C_2HO_2	14,1	42,1	54,8
60	C_3H_5O	12,5	13,2	18,0
69	C_3HO_2 C_4H_5O	6,6	100	100
71	$C_3H_3O_2$ C_3H_5NO	6,6	55,4	60,0
73	$C_3H_5O_2$	27,5	62,5	75,4
78	C_6H_6	100	43,6	6,4
87	C_7H_3, $C_4H_7O_2$	7,5	69,0	79,0
89	C_7H_5	6,0	85,2	45,1
91	C_7H_7 C_6H_5N	8,0	26,8	26,4
97	$C_5H_5O_2$	2,2	35,4	17,6
104	C_7H_6N	1,2	48,0	13,4
105	$C_4H_9O_3$	3,6	73,1	50,2
113	$C_5H_9O_2$	100	2,7	75,8
123	C_7H_7NO	88,8	5,0	15,8
135	C_9H_9NO	0,0005	9,4	14,2
169	$C_9H_8N_2O_2$	-	6,5	4,1
185	$C_9H_8NO_2$	-	2,5	4,7
206	$C_9H_6N_2O_4$	-	44,8	4,2
211	$C_{14}H_{11}NO$	-	2,7	5,0
250	$C_{15}H_6N_2O_2$	-	80,0	12,1
256	$C_{15}H_{10}N_2O_2$	-	1,8	2,5

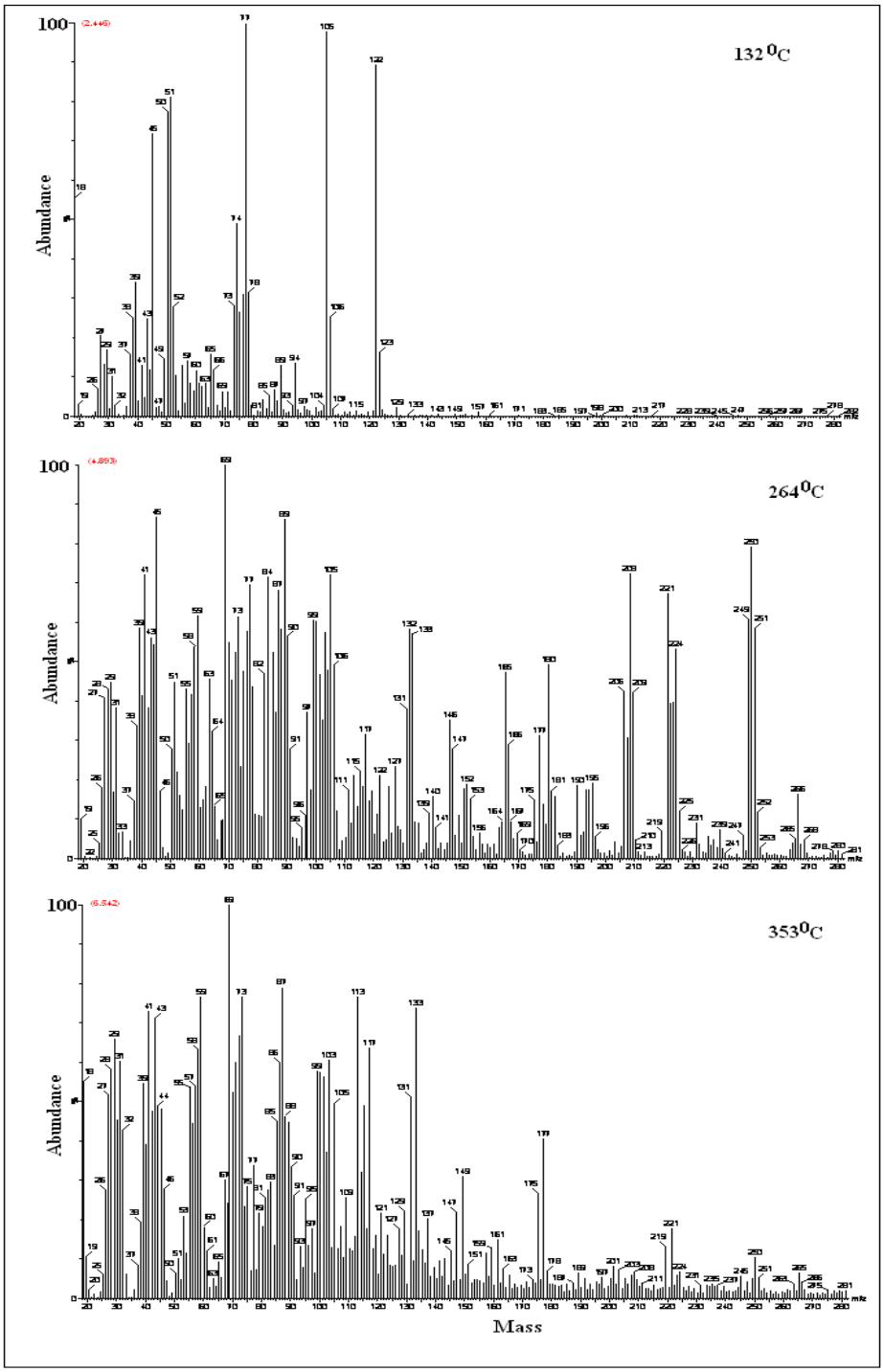

Figure 82 Fragments of PUOHMMA3 at 132ºC, 264ºC and 353 ºC

Rheological Investigation

In order to obtain the molecular interpretation of the viscoelastic behavior, some of the synthesized polymers were investigated by rheometer. Actually, the samples analyzed are uncured prepolymers and their molecular weights were found to be low and gel point is not observed at this level. At relatively low temperatures, these samples are fluids in which desired viscoelastic properties are on the viscous part rather than plastic part. Thus, the highest temperature used in rheological experiments was 120ºC.

Temperature dependence of storage and loss modulus at a frequency of 10 rad/s is given in Figure 83 and 84, respectively. G` is a measure of stiffness of the material. At low temperatures, we would expect the stiffness to relate to changes in the stored elastic energy on deformation, which are associated with small displacements of the molecules from their equilibrium positions. On the other hand, at high temperatures, the molecular chains are flexible and they can adopt conformations, which lead to maximum entropy. Therefore, the storage modulus values of all polymers are decreased with the increase in temperature from 30ºC to 120ºC. PUOHMMA1 has the highest G` values at all temperatures. On the other hand, PUOHMMA3 has the lowest G` and G`` values. This difference might be attributed to the nature of diisocyanate used. Thus, TDI may affect the rheological properties of the final polymer in a better way when compared with that of MDI. It is interesting to observe that the decreasing trend of G` and G`` for PUOMMA1 and PUNCOHEMA1 polymers follow each other and have a similar character. The FTIR-ATR results confirmed this behavior that the hydrogen bonding between NH…O groups leads to a phase mixing in these polymers. These kinds of interactions made the polymers much stiffer. On the other hand, PUNCOMMA1 has a relatively low storage modulus value among the TDI based polymers. The FTIR-ATR data revealed that the carbonyl frequency band of PUNCOMMA1 was on the free vibrational side that in order terms the hydrogen bonding is very low compared

to the others. Therefore, we could expect a decrease in the relative stiffness. Similar trend was observed in loss modulus values.

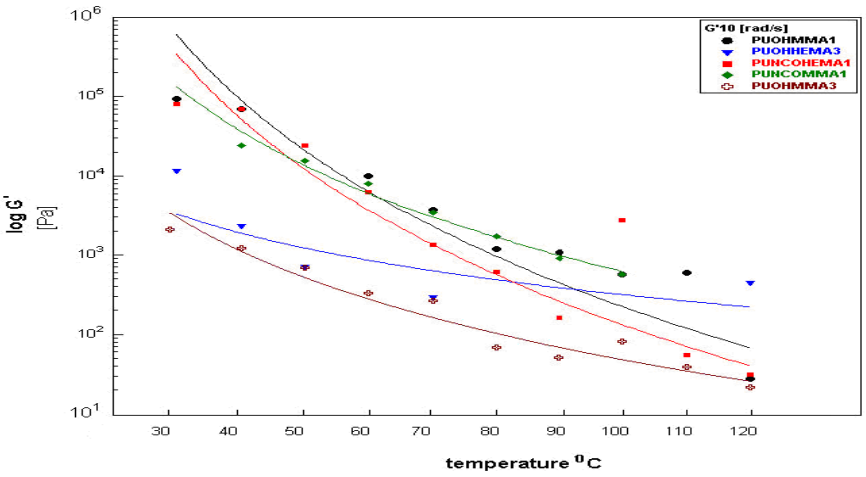

Figure 83 Temperature dependence of the storage modulus (G`) at 10 rad/s

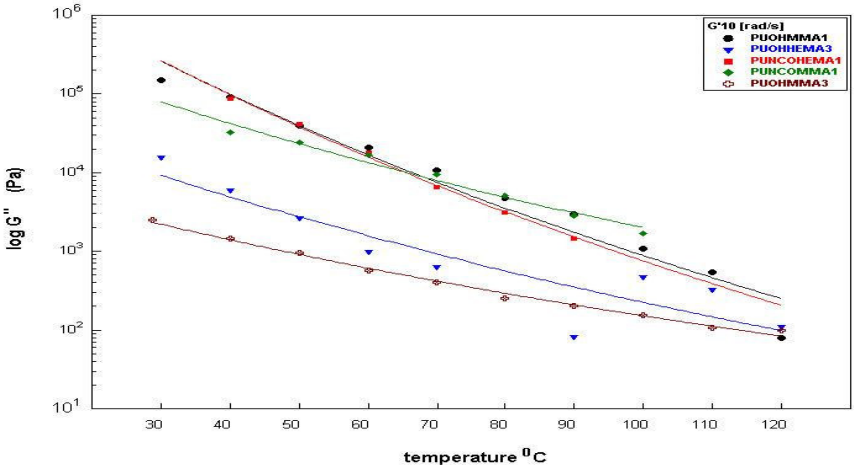

Figure 84 Temperature dependence of the loss modulus (G``) at 10 rad/s

At low shear rates polymer melts has a Newtonian viscosity (Figure 7). However, as the shear rate increases the viscosity decrease nearly linearly with shear rate. In this linear range, the so-called power law equation holds in which $y= C_1 x ^{C_2,}$ where y is viscosity, x is shear rate. The power law index (PLI) is defined by the quantity: $PLI= 1 +C_2$. $0 < PLI < 1$ indicates a shear thinning (pseudoplastic), whereas PLI>1 indicates shear thickening (dilatant) material. For the materials that are considered as Newtonian has PLI=1.

The shear rate dependence of complex viscosity (η) for some urethane acrylate copolymers are compared at four different temperatures in Figures 85-88. At 30ºC, all the samples gave regular changes in viscosity with shear rate. The slopes are almost the same and they are almost linear. Thus, the η_0 for different samples are different from each other but η values are much similar, giving almost straight line with slope very close to zero. Obtained data were fitted to power law viscosity model. The power law index was calculated and is given in Table 19. PUOHMMA3 and PUNCOMMA1 exhibit shear-thinning behavior ($0<PLI<1$) within the temperature range of 30-120ºC. Shear-thinning property of PUOHHEMA3 is only present at 30ºC. Power law model is useful mathematical model because of its simplicity, but only approximately describes the behavior of real non-Newtonian fluids. Therefore, the negative values shown in Table 19 could be explained with this kind of deviation from the model.

Table 19 Power law index values of urethane acrylate polymers

	30ºC	60ºC	90ºC	120ºC
PUOHMMA1	0.53	0.82	0.41	-1.19
PUOHMMA3	0.52	0.68	0.43	0.42
PUOHHEMA3	0.65	-0.55	-1.21	-0.75
PUNCOHEMA1	0.45	0.88	-0.32	-1.07
PUNCOMMA1	0.56	0.79	0.79	0.72

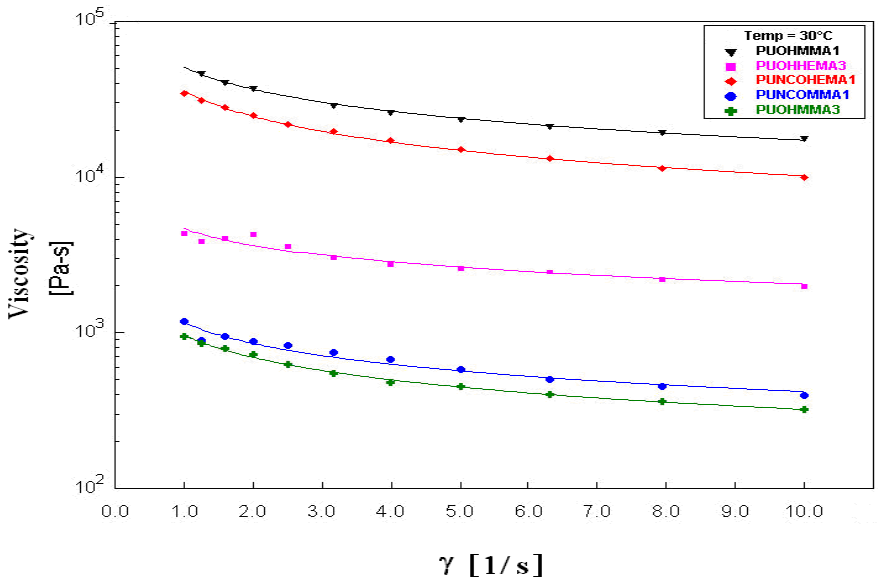

Figure 85 Complex viscosity as a function of shear rate at 30ºC

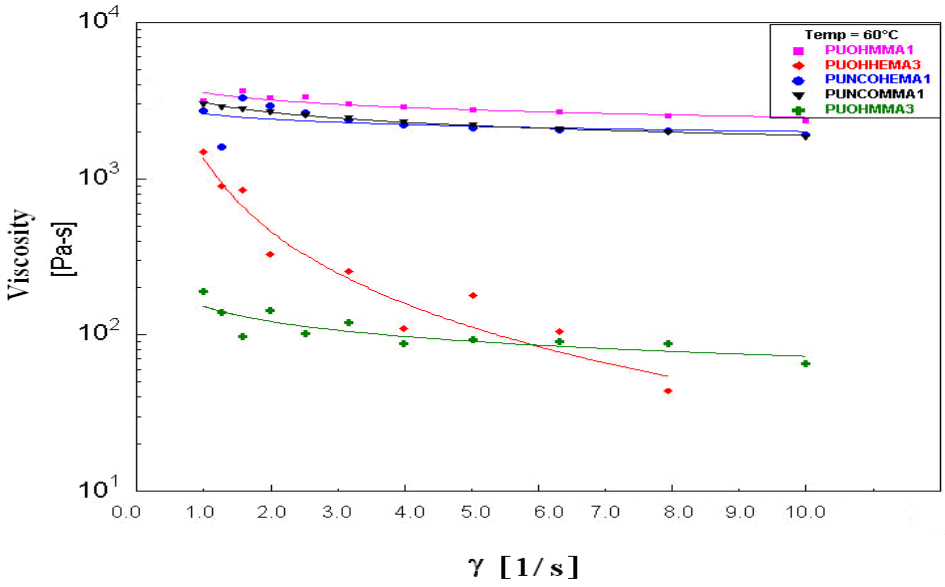

Figure 86 Complex viscosity as a function of shear rate at 60ºC

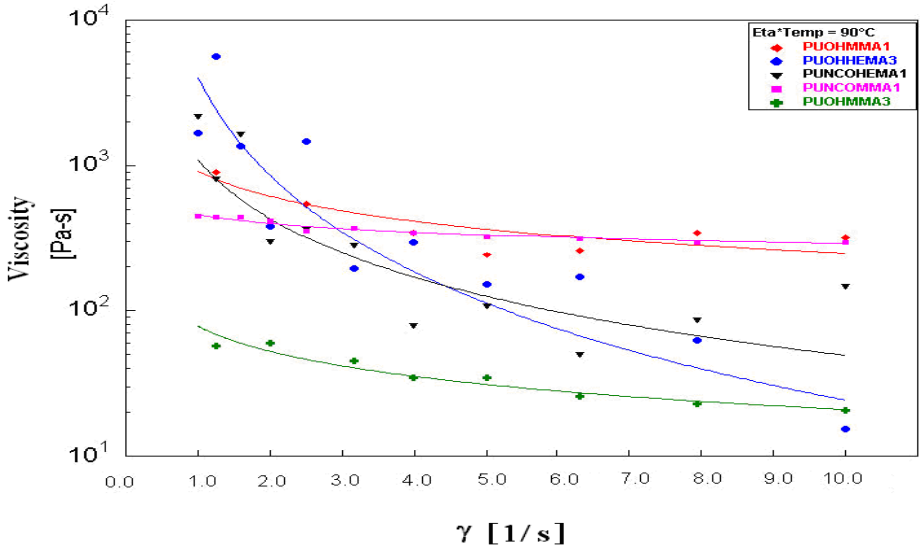

Figure 87 Complex viscosity as a function of shear rate at 90ºC

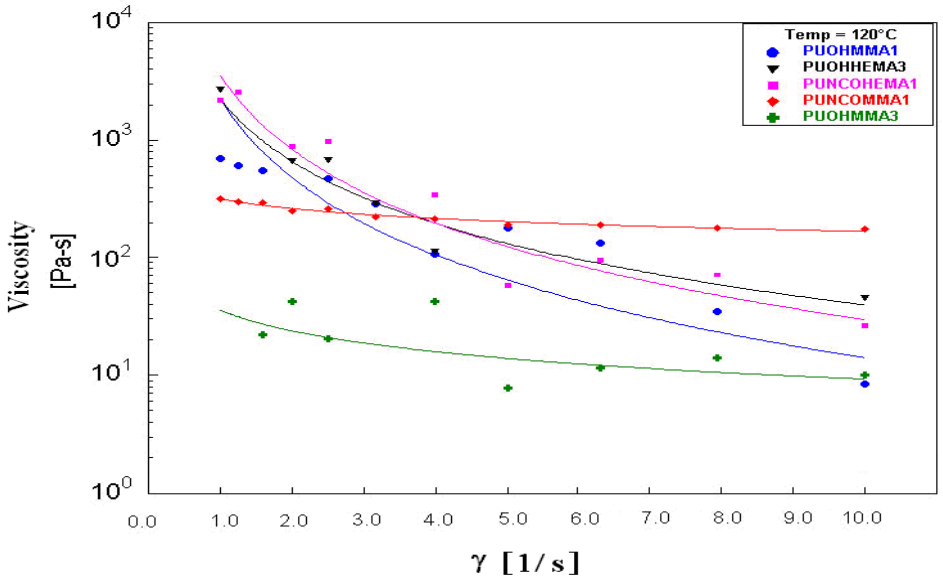

Figure 88 Complex viscosity as a function of shear rate at 120ºC

Log shear stress versus log shear rate graphs are given in Figures 89-92. As the structure of the polymer changes, certain changes are expected in the stress strain curves. The slope of the curve increases with the increase in crystallinity, crosslinking density and amount of orientation. At 30ºC, a regular trend is observed with a straight line of almost all the same slope for different samples. On the other hand, log shear stress values for different polymers exhibit different values. This regular trend was deviated with the increase of temperature from 30ºC to 120ºC. For PUOH, the trend of the line is almost the same at all temperatures in this range. It is not as close to a straight line as the others, but deviation is also similar for different temperatures. PUOH has a low stress value at a definite shear rate at all temperatures. Therefore, the acrylate end capping was end up with a much stiffer polymer.

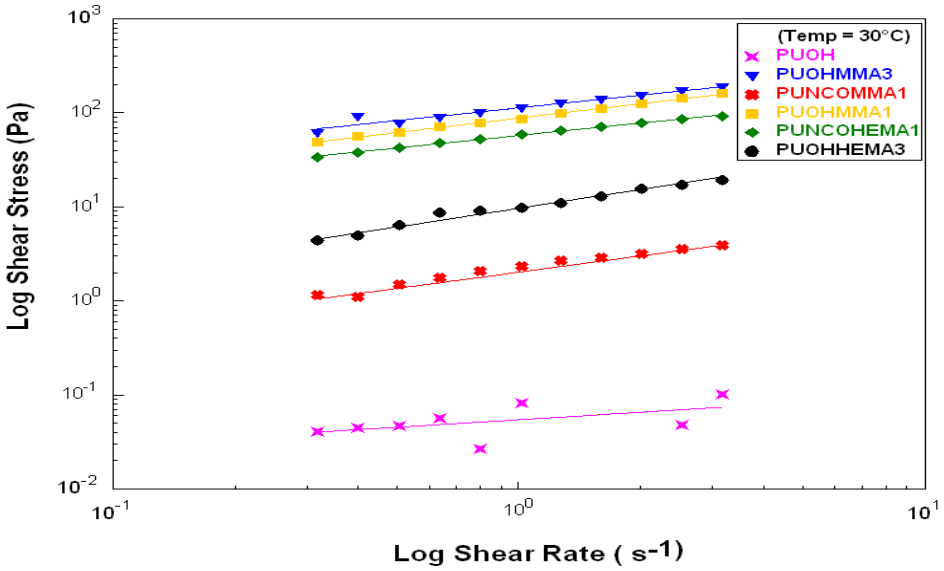

Figure 89 Shear stress as a function of shear rate at 30ºC

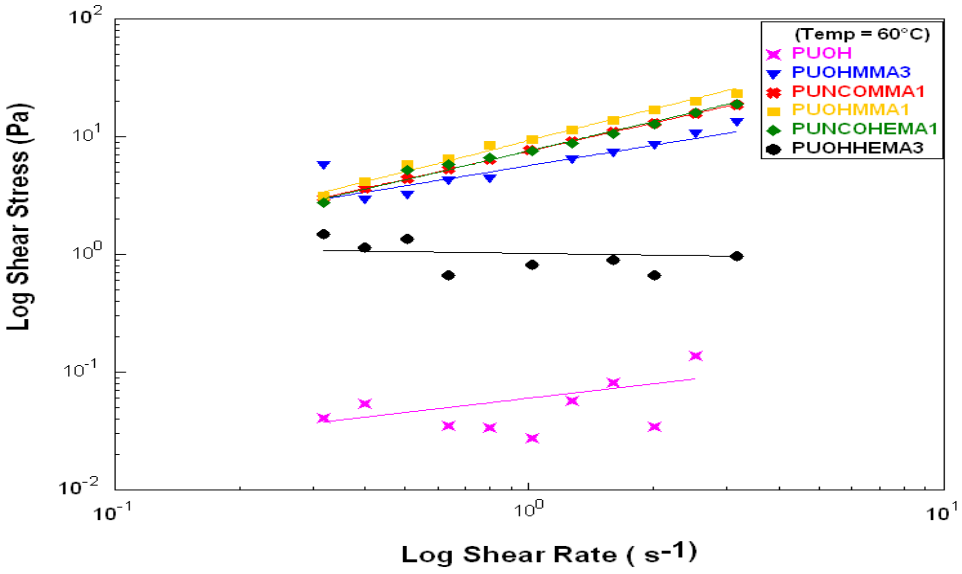

Figure 90 Shear stress as a function of shear rate at 60ºC

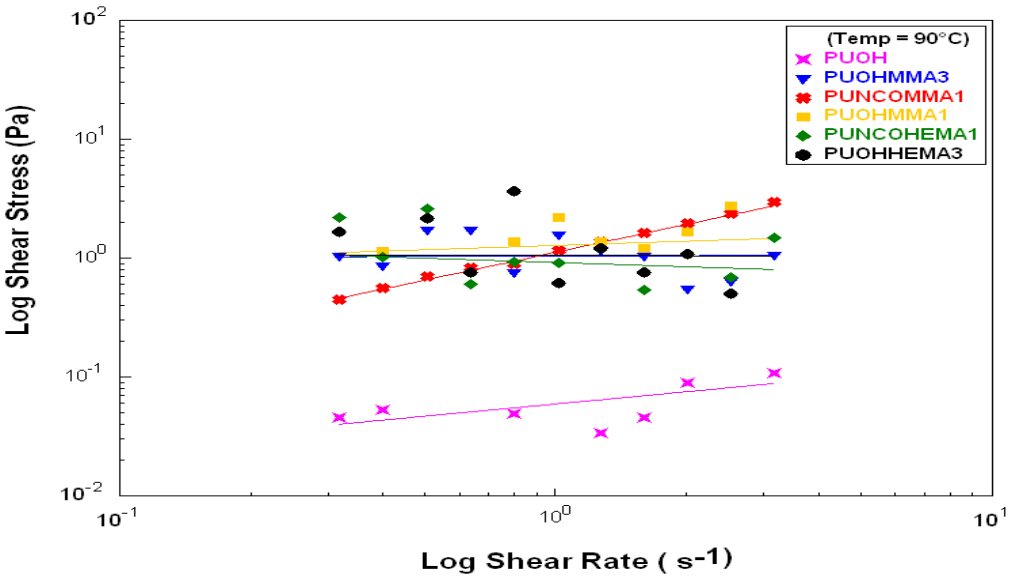

Figure 91 Shear stress as a function of shear rate at 90ºC

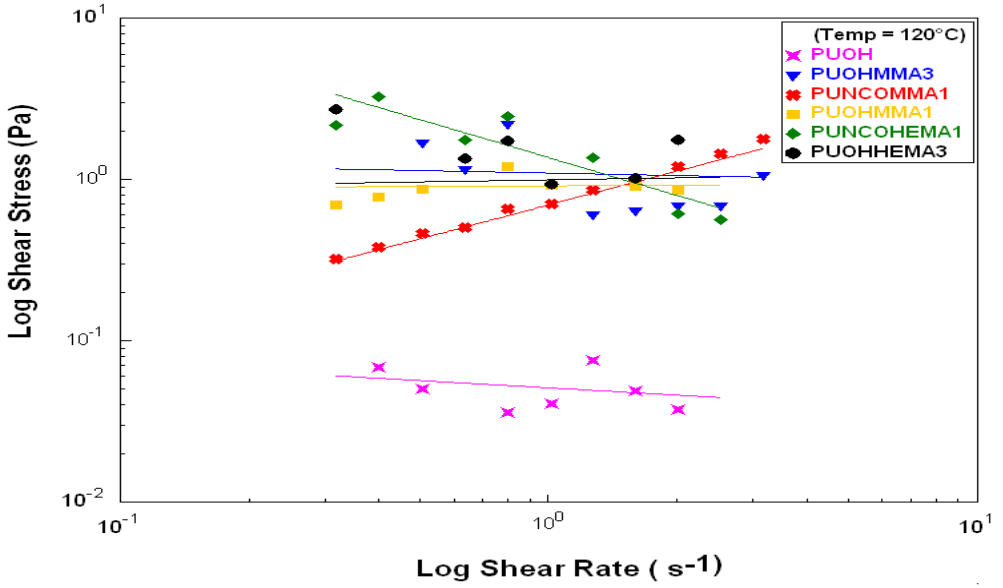

Figure 92 Shear stress as a function of shear rate at 120ºC

The Arrhenius behavior was tried at two frequency values; 1 rad/s and 10 rad/s, but the normal behavior of viscoelastic properties were obtained with a frequency of 10 rad/s. At this frequency Ln viscosity as a function of 1/T graph is given in Figure 93. The slopes are different for all samples and this behavior can be attributed to difference in chain entanglements due to the change in temperature values. Best lines were obtained from the data for each polymer and slopes of these lines are equal to –Ea/R. The calculated activation energies, Ea, are given in Table 20. Lowest activation energy observed in PUNCOMMA1 (0.6 kj/mol) whereas PUOHMMA3 has the highest activation energy (2.89 kj/mol). These results are in agreement with the data obtained from FTIR, NMR for the extend of hydrogen bonding.

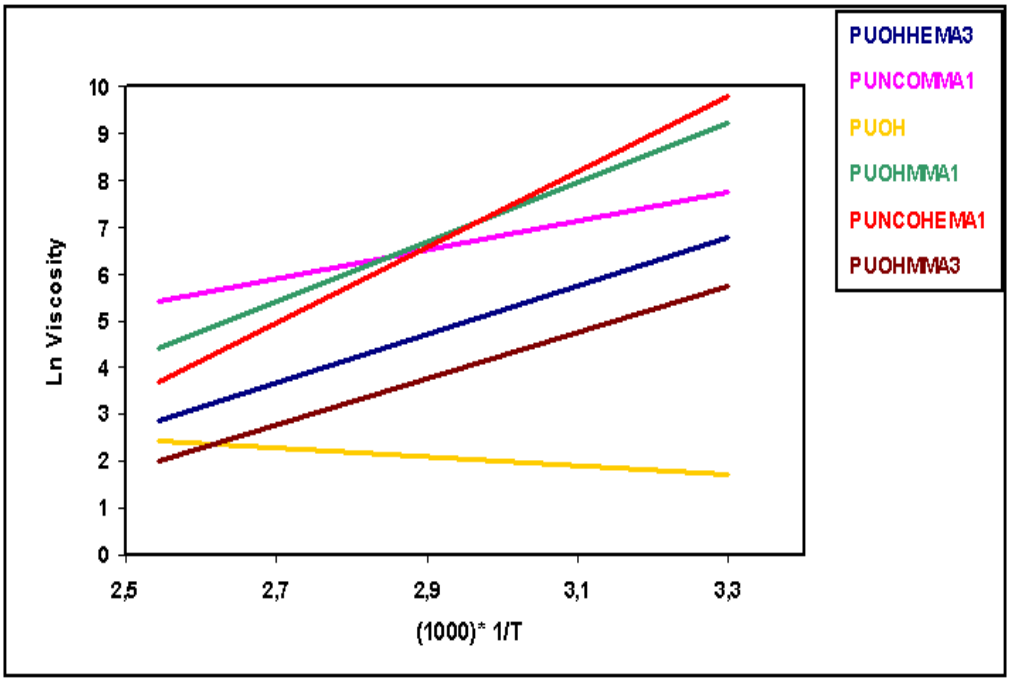

Figure 93 Ln viscosity versus 1/T at a frequency of 10 rad/sn

Table 20 Arrhenius equation fit results and the activation energy

	Ln A	SLOPE	Ea
PUOHMMA1	0,60	0,15	1,26
PUNCOMMA1	0,36	0,072	0,60
PUOHMMA3	1,29	0,35	2,89
PUNCOHEMA1	0,85	0,24	1,95
PUOHHEMA3	0,87	0,22	1,82

SEM Analysis Results

The SEM micrographs of PUNCOMMA1 are given in Figures 94a and 94b at a x150 and x10000 magnifications, respectively. Limited number of phase separation domains is observed in the micrographs. The dark areas represent the hard segments, whereas white spots/areas represent the soft segments. For PUNCOMMA sample, hard domains are much more than the soft domains.

The SEM micrographs of PUOHA sample is given in Figure 95a and 95b at x150 and x10000 magnifications, respectively. The white domains appeared to be more that indicates the number of soft segment domains. On the other hand, the number of hard segment domains is quiet limited. This is supported further in Figure 95b.

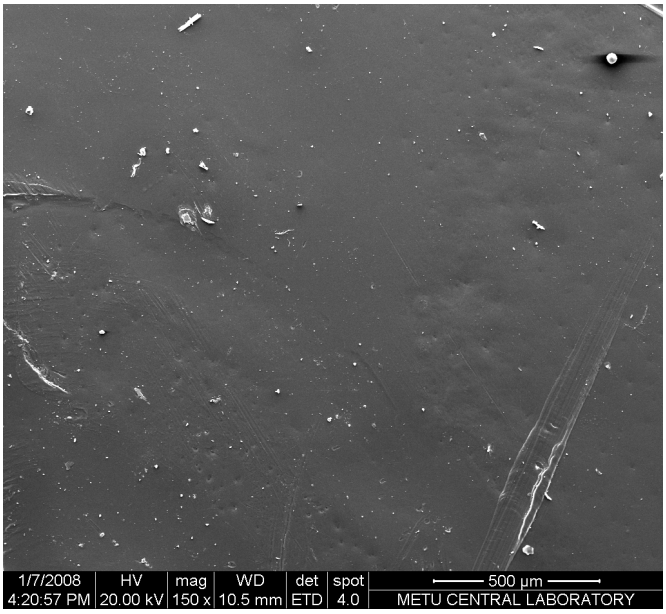

Figure 94a SEM micrograph of PUNCOMMA at x150 magnification

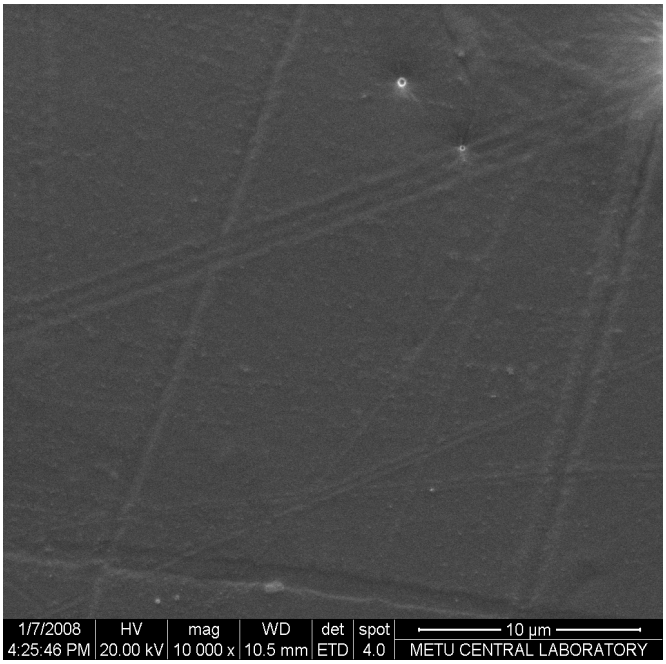

Figure 94b SEM micrograph of PUNCOMMA at x10000 magnification

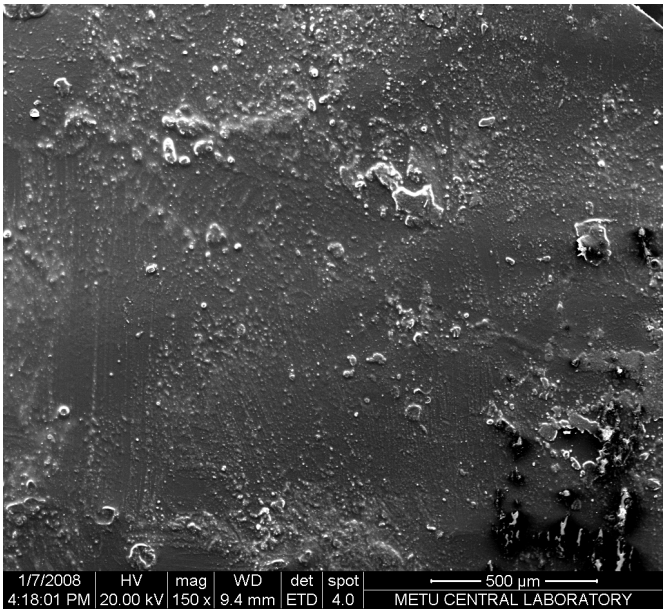

Figure 95a SEM micrograph of PUOHMMA at x150 magnification

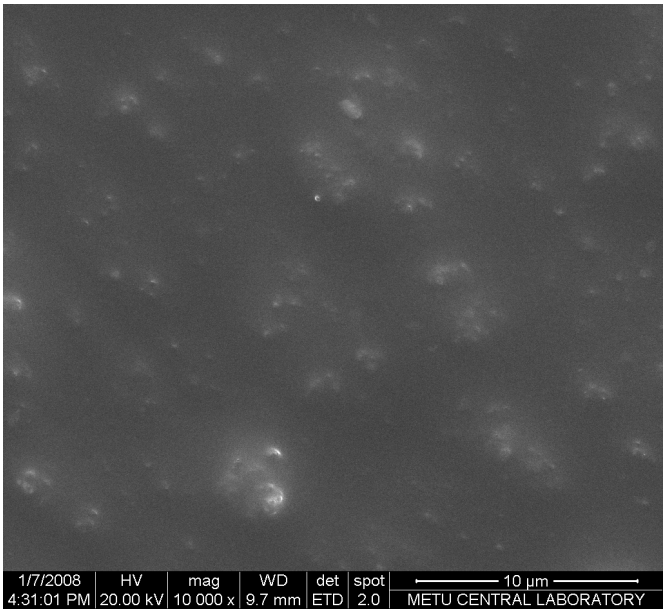

Figure 95 b SEM micrograph of PUOHMMA at x10000 magnification

Cytotoxicity Analysis

Size distribution graph of the Ag nano particles is given in Figure 96. Particle diameter of 40-50 nm is the maximum value obtained from the graph. In addition to small particles, there exist relatively large particles which might be due to the formation of the agglomerates in the solution. Intensity of agglomerates is low when compared with the intensity of the nano particles. These particles were also visualized by the SEM technique. Diameters of the nano particles on a carbon tape substrate are shown in Figure 97 and the particle size results are in good agreement with that of particle size analyzer. Particle size diameter varies between 47.9-55.2 nm.

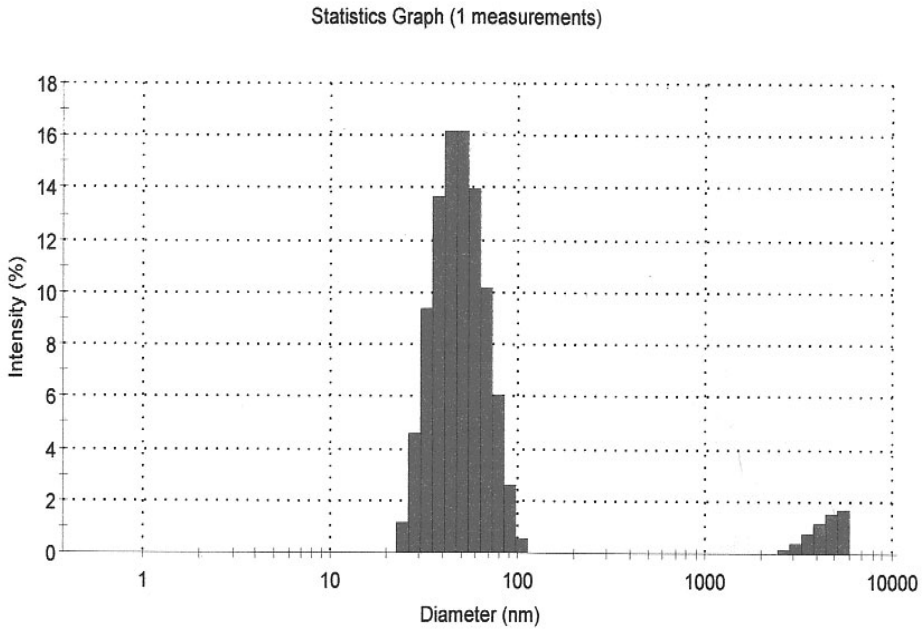

Figure 96 Particle size analysis of silver nano particle

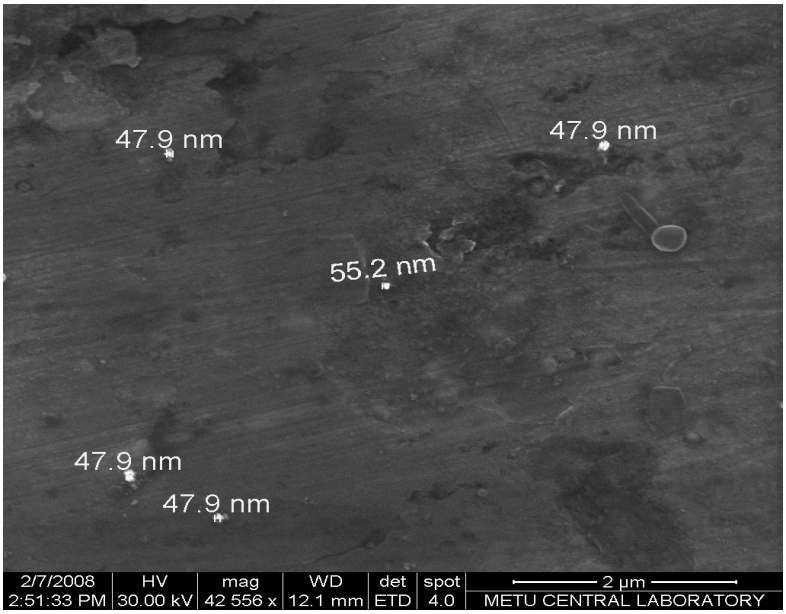

Figure 97 SEM micrograph of silver nano particles

SEM micrograph of silver nano particle added PUOHMMA sample is given in Figure 98. Silver nano particles were homogeneously distributed within the polymer. The morphology of sample itself with hard and soft segment separation is also observed in the SEM image. However, the separation is not very distinct.

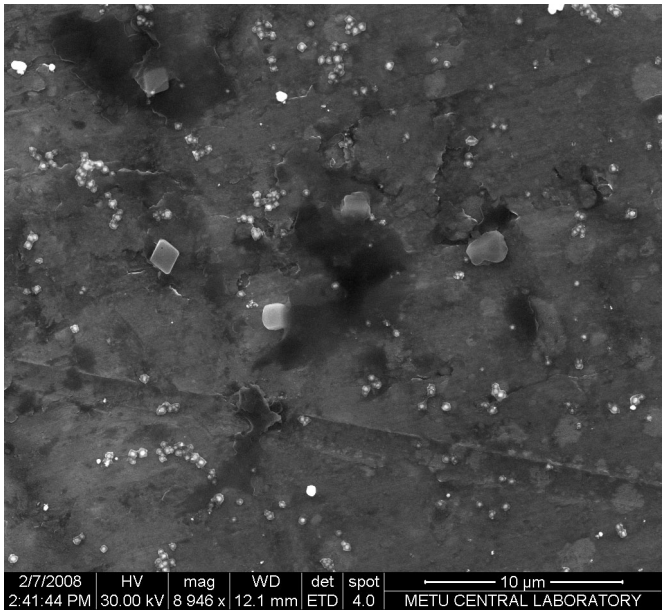

Figure 98 SEM micrograph of silver nano particle added PUOHMMA sample

Cytotoxicity analysis results of nano silver added PUOHMMA polymers after 24 h and 1 week are given in Figures 99 and 100, respectively. Group 1 represents the PUOHMMA1, group 2 is PUOHMMA2, and group 3 is PUOHMMA3.

Cytotoxicity was rated based on cell viability and obtained relative to control group. Absorbance value of >90 % is regarded as non-cytotoxicity, 60-90 % is slightly cytotoxic, 30-59 % is moderately cytotoxic and <30% is severely cytotoxic. In this respect, after 24 hours slight changes are observed and almost all the samples are in the range of moderately toxic. Nano particle addition decreased the toxicity only in group 2. It is also observed from the graph that the control of group1 was slightly toxic, whereas nano particle addition caused it to be moderately toxic.

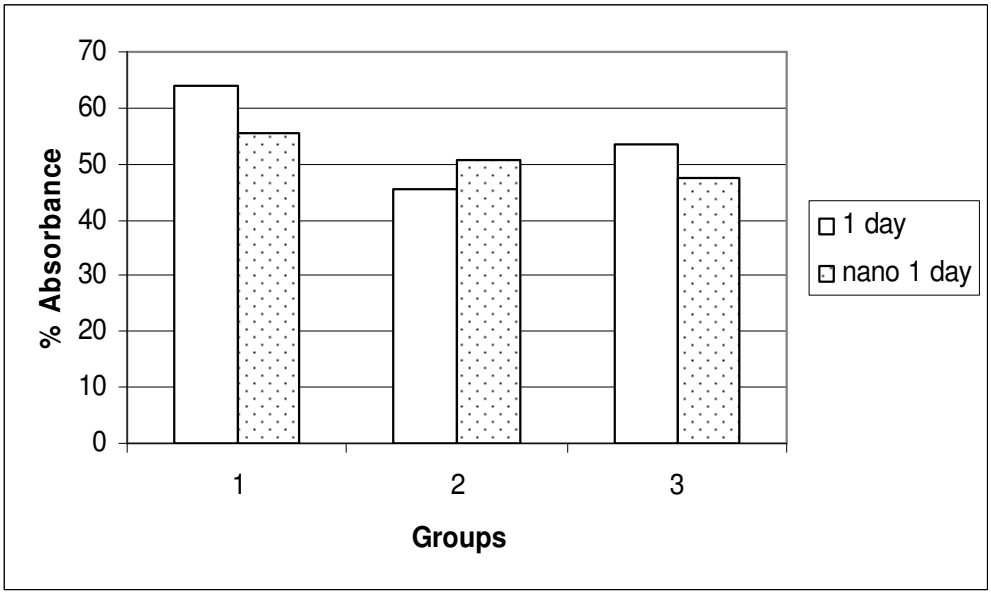

Figure 99 Cytotoxicity results of nano particle added polymers after 24hr

After a week, almost all the control and nano added samples cytotoxicity is increased and they are in the moderately cytotoxic range. The cytotoxicity of control group of group 2 remained unchanged and it reached to a limiting value. In other groups, cytotoxicity was changing with time and did not reached to a limiting value after a week.

The enhanced cytotoxicity in some groups with the addition of silver particles could be explained in two ways. Since the cytotoxicity was evaluated on the 100 ppm added silver nanoparticles, the reason for toxicity might be the concentration of the particles in the polymers. On the other hand it is also possible that the remained oligomers or homopolymers might cause a considerable amount of cytotoxicity.

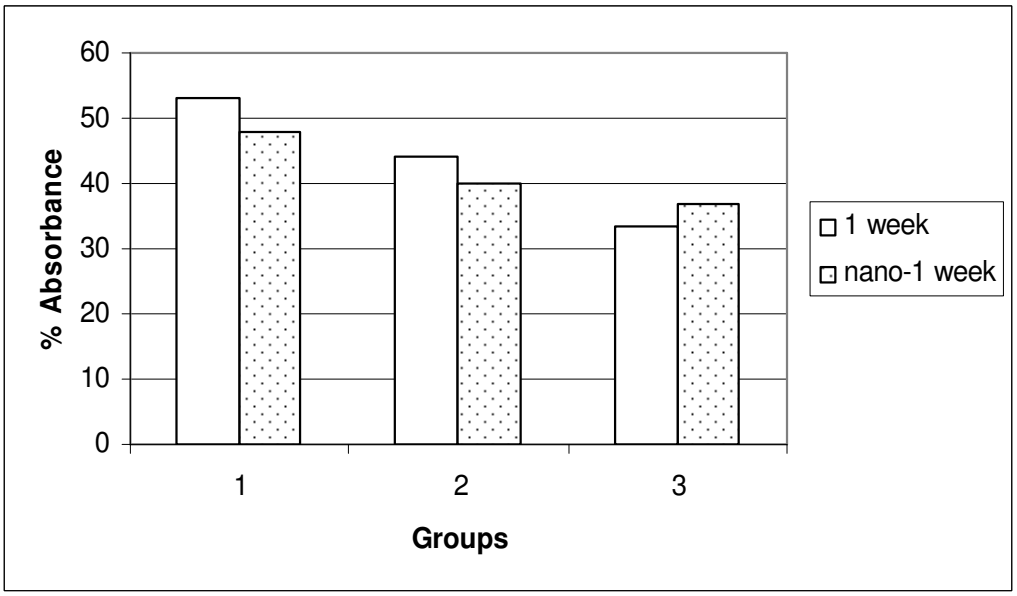

Figure 100 Cytotoxicity results of nano particle added polymers after 1 week

CHAPTER 4

CONCLUSION

Polyurethanes are one of the most important commercial polymers. Their commercial synthesis got much attention from the very beginning. The low cost synthesis is popular in many industries. However, there are sample applications that require very special type of urethanes and require elaborate method of synthesis. One of the applications is the biomedical application to obtain materials such as soft liners that can be used for relining of removable prosthesis. For this purpose, a low molecular prepolymer has to be synthesized. It is then end capped with acrylate to get macromonomer, which can be cured to give a macromolecule of final thermosetting polymer or relatively more viscoelastic material of soft liner. PUNCOA polymers have a Mn value in between 3500-5417 g/mol. Similarly, PUOHA polymers have Mn values of 2590-6234 g/mol. In this synthesis, the types of diisocyanate and diol (PEG) are very important. The additions of acrylate to urethane prepolymer require specific conditions; the rate of addition reaction by inter-esterification, the temperature control and preventing vinyl addition reactions. Inter esterification reaction is highly exothermic and the local temperature increase causes gelation. This can be controlled by adjusting rate esterification reaction and dissipating the exothermic heat of reaction. Therefore, the reaction temperature was maintained at 40-60°C.

The DSC results showed the liquid nature of some of the samples. The corresponding polymorphs for PUNCOMMA2 were observed at 26.85 °C and 41.31 °C. On the other hand, these polymorphs for PUOHMMA2 were observed at 22.94 °C and 33.47 °C.

The FTIR-ATR investigation clarified the phase mixing and/or phase separation of some samples. The samples that show phase mixing have more hydrogen bonding and parallel linear chains, which show liquid crystal properties. In the case of phase separation, the hard and soft samples showed different morphological domains in SEM micrographs and two Tg values. Even though acrylates are usually added to reaction medium slowly, due to the mobility of reaction medium some acrylates give low molecular homopolymer of polyacrylates. The formation of homopolymer could be predicted from DSC thermogram, which could also be used to estimate the molecular weight of homopolymer of acrylate. PUOHMMA3 with a Pd value of 7.19 contains a polymethylmethacrylate with Mn of 3049 g/mol.

The viscosity-temperature relation gives information for the optimum temperature of synthesis. Therefore, the rheological properties gave important information about the way of applications of samples. All the polymers showed expected regular trend of decreasing viscosity with increase in shear rate at 30 °C and also they obeyed the power law at this temperature and showed a shear thinning behavior.

The samples showed considerable toxicity and all have an absorbance value lower than 70 %. The Ag nano particle addition increased/ decreased the cytotoxicity 2-5 %. Therefore, the toxicity should be lowered. This is most probably due to residual monomer and solvent in the synthesized materials. Further works are needed to decrease the toxicity and to observe the effects of addition of silver nanoparticles on antibacterial properties of the final product.

REFERENCES

[1] Wolinska-Grabczyk, A, Muszynski, J., Jankowski, A., Chem Papers-Chemicke Zvesti, **54** (6A), p. 389-392 (2000).

[2] Ray, A.R., Bhowmick, J Biomed Mater Res, **25** (10), p. 1249-1257 (1991).

[3] Boretos, J. W., Detmer, D. E., Donachy, J.H., Mirkovitch, V., J Biomed Mater Res, **5**, p. 373 (1971).

[4] Estes, G. M., Seymour, R. W., Cooper, S. L., Macromol, **4**, p. 452 (1972).

[5] Brauman, S., Fritzinger, B., J Appl Polym Sci, **16**, p.2439 (1972).

[6] Tang, R.Y.W., Gonzalez, J.B., Roberts, G.D., J Dent Res, **54** (5), p. 1039-1045 (1975).

[7] Wong, E.W.C., Abstracts of Papers of the Amer Chem Soc, **180**, p. 38 (1980).

[8] Szycher, M., Poirier, V.L., Dempsey, D. J., J Elastomers and Plastics, **15** (2), p.81-95 (1983).

[9] DeGroot, J.H., deVrijer, R., Wildeboer, B.S., Polym Bulletin, **38** (2), p. 211-218 (1997).

[10] Anderson, J.M., Hiltner, A., Wiggins, M.J., et al., Polym International, **46** (3), p. 163-171 (1998).

[11] Spaans, C.J., De Groot, J.H., Belgraver, V.W., et al. J Mater Sci-Mater in Medicine, **9** (12), p.: 675-678 (1998).

[12] Phaneuf, M.D., Bide, M.J., Szycher, M., et al. Asaio J, **47**(6), p. 634-640 (2001).

[13] Matheson, L.A., Santerre, J.P., Labow, R.S., J Cellular Phys, **199** (1), p.8-19 (2004).

[14] Heijkants, R.G..JC., Van Calck, R.V., De Groot, J.H., J Mater Sci-Mater in Medicine, **15**(4), p. 423-427 (2004).

[15] O. Bayer, Angew. Chem **A59**, p.257 (1947).

[16] Bayer, O., Muller, E., Petersen, S., Piepenbrink, H. F., Windemuth, E., Rubber Chem Tech, **23**, 812 (1950).

[17] Bayer, O., Rinke, H., Siefken, W., Orthner, L., Schild, H., Ger. Pat. 728, (to I. G.Farbenindustrie), **12**, p. 981 (1942).

[17] Farbenfabrien Bayer, *DE-PS 913.474*, (1941).

[19] T. Lieser, *U.S. Patent 2266*, 777, (1941).

[20] C. S. Schollenberger, (to B.F.Goodrich), *U.S. Patent 2871218*, (1955).

[21] K. A. Pigott , *Kirk-Othmer Encyclopedia of Chemical Technology,* vol.24, John Willey & Sons Inc., (1998).

[22] Boretos, J.W., Pierce, W.S., J. Biomed. Mat. Res., **2**, 121 (1968).

[23] Boretos, J.W., *Concise Guide to Biomedical Polymers, Their Design Fabrication and Molding, Charles C. Thomas-Publisher, Springfield*, IL, pp. 10 (1973).

[24] Szycher, M., Poirier, V.L., *Polyurethanes in Implantable Devices. Plastic Technology*, pp.45 (1984).

[25] Wilkes, G.L., Samuels, S.L., J. Biomed. Mater. Res. 7, 541 (1973); C.A. 80,121583c (1974).

[26] Lyman, D. J., Loo, B. H., J Biomed Mater Res, **1**, p.17 (1967).

[27] C. Hepburn, *Polyurethane elastomers*, 2 nd edition, (1992).

[28] P. Wright, A.P.C. Cumming, *Solid Polyurethane Elastomers*, NewYork, Gordon & Breach Sci Pub., (1969).

[29] J. M. Buist, H. Gudgeon, *Advances in Polyurethane Technology*, Wiley (Interscience), New York, (1968).

[30] Bruins, P.F., *Polyurethane Technology*, NewYork, Interscience, (1969).

[31] Oertel, G. *Polyurethane Handbook*, Hanser Publisher, NewYork, (1985).

[32] Saunders, J.H., Frisch, K.C., *Polyurethanes Chemistry and Technology, Part I*, John Wiley and Sons, USA, (1962).

[33] S. Petersen, Justus Liebigs Ann. Chem., **562**, p. 205 (1949).

[34] K. B. Wagner, M. A. Murla,Polym. Prep. Am. Chem. Soc. Div. Polym. Chem., **30**, 287 (1989).

[35] US-PS 2437867, DuPont (1946); US-PS 2476779, (1947).

[36] J. W. Baker, J. B. Holdsworth, J. Chem. Soc., **148**, p. 713 (1947).

[37] A. Wurtz, Justus Liebigs Ann. Chem., **71**, p.326 (1849).

[38] H. Kleimann, Angew. Makromol. Chem., **98**, p. 185 (1981).

[39] A. W. Hofmann, Ber. Dtsch. Chem. Ges., **18**, p. 764 (1885).

[40] A. W. Hofmann, Ber. Dtsch. Chem. Ges., **4**, p. 246 (1871).

[41] L. C. Raiford, H. B. Freyermuth, J. Org. Chem., **8**, p. 230 (1943).

[42] Thi, ATD., Camberlin, Y., Lam, TM., Angew Makrom Chemie, **111**, p. 29-51 (1983).

[43] T. W. Campbell, K. C. Smeltz, J. Org. Chem., **28**, p. 2069 (1963).

[44] E. Dyer, R. E. Read, J. Org. Chem., **26**, p.4677 (1961).

[45] W. Neumann, P. Fischer, Angew. Chem., **74**, p. 801 (1962).

[46] H. G. Khorana, Chem. Rev., **53**, p. 145 (1953).

[47] DE-PS 1092007, Bayer AG (1959).

[48] C. S. Schollenberger, H. Scott, G. R. Moore, Rubber World, **137**, p. 549 (1958).

[49] R. Adams, J. L. Anderson, J. Am. Chem. Soc., **72**, p.5154 (1950).

[50] O. G. Takakanov, L. V. Nevskji, V. K. Beljakov, J. Polym. Sci. Part C, **23**, p. 193 (1968).

[51] EP 0453914, Mobay Corp., (1990).

[52] J.W Baker, J.B Holdsworth, J.Chem Soc., **7**, p.13 (1947).

[53] Britain, J.W., Gemeinhardt, P.G., J. Appl. Polymer Sci., **4**, p. 207 (1960).

[54] Smith, H.A., J. Appl. Polymer Sci., **7**, p. 85 (1963).

[55] Carreher, C.H., *Polymer Chemistry An Introduction*, 4 th ed, Marcel Dekker, New York, (1996).

[56] Yokoyama, T., *Advances in Urethane Science and Technology*, (K. C. Frisch, J. H.Saunders, ed.), Technomic, Westport USA, 6, p.1-29 (1978).

[57] Seymour, R. W., Allegrezza, A. E., Cooper, S. L., Macromol, **6**(6), p. 896 (1973).

[58] Sung, P. C. S., Hu, C. B., Wu, C. S., Macromol, , **13**, p. 111 (1980).

[59] Seymour, R., W Cooper, S. L., Macromol, **6**, p.48 (1973).

[60] Srichatrapimuk, V. W., Cooper, S. L. J., Macromol. Sci. Phys., **B15**, p.267 (1978).

[61] Seymour, R. W., Estes, G. M., Cooper, S. L., Macromol, **3**(5),p. 579 (1970).

[62] Estes, G. M., Seymour, R. W., Cooper, S.L., Macromol, **4**, p.452 (1971).

[63] Paik, C. S., Schneider, N. S., Macromol, **8**(1), p. 68 (1975).

[64] Yamamoto, T., Shibayama, M., Nomura, S., Polym. J, **21**(11), p. 895 (1989).

[65] Nakayama, K., Ino, T., Matsubara, I. J., Macromol. Sci. Chem., **A3**(5), p. 1005 (1969).

[66] Eisenbach, C. D., Gronki, W., Makromol. Chem., Rapid Commun., **4**, p. 707 (1983).

[67] Luo, N., Wang, D. N., Ying, S. K., Polymer, **37**(14), p. 3045 (1996).

[68] Paik Sung, C. S., Schneider, N. S., Macromol, **10**(2), p.452 (1977).

[69] Brunette, C. M., Hsu, S. L., MacKnight, W. J., Macromol, **15**,p.71 (1982).

[70] Coleman, M. M., Lee, K. H., Skrovanek, D. J., Painter, P. C., Macromol, **19**, p.2149 (1986).

[71] Fried, J., *Polymer Science and Technology,* Prentice Hall, New Jersey, 2003.

[72] Thorn, M., Can. J. Chem., **45**, p. 2537 (1967).

[73] Dyer, E., Newborn, G. E. J., Am. Chem. Soc., **80**, p. 5495 (1958).

[74] Dyer, E., Reed, R. E., J. Org. Chem., **26**, p. 4388 (1961).

[75] Saunders, J. R., Rubber Chem. Technol., **32**, p.337 (1959).

[76] Grassie, N., Zulfiqar, M. J., Polym. Sci.: Polym. Chem. Ed., **16**, p.1563 (1978).

[77] Buist, J. M., Gudgeon, H., eds., *Advances in Polyurethane Technology*, Wiley (Interscience), New York, (1968).

[78] Schollenberger, C. S., Stewart, F. D., J. Elastoplastics, **4**, p.294 (1972).

[79] Takakanov, O.G., Nevskji, L.V., Beljakov, V.K.J., Polym. Sci. Part C, **23**, p.193 (1968).

[80] Schultze, H., Makromol. Chem., **172**, p.57 (1973).

[81] Mizuno, A., Takao, A., Jpn. Kokai Tokkyo Koho, **62**, 285, p. 959 (1987).

[82] Berner, G., European Patent Appl. **7**, 059 (1980).

[83] Sato, M., Kobayashi, J., Jpn. Kokai Tokkyo Koho, **79**, 58, p. 784 (1979).

[84] Kita, H., Hoshi, Y., Jpn. Kokai Tokkyo Koho, **61**, 198, p. 104 (1986).

[85] Matsui, A., Jpn. Kokai Tokkyo Koho, **79**, 97, p. 640 (1979).

[86] Berthet, J., Gaussens G., Nicaise, Fr. Demande 2, **429**, p. 838 (1980).

[87] Ishamuru, T., Tsukada, K., Hayashi, N., Koibuchi, S., Isobe, A., Fr. Demande 2, **490**, p. 838 (1982).

[88] Ortlepp, W., Ger. Offen., 3, **038**, p. 422 (1982).

[89] Ohta, T., Kanbara, H., Dobashi, A., Seki, Y., Radiat. Phys. Chem., **25**, p. 465 (1985).

[90] Lai, Y.C., Baccei, L.J., J. Appl. Sci., **42**, p. 3173 (1991).

[91] Plews, G., Phillips, R., Coating Technol., **51**, p. 648 (1979).

[92] Speckhard, T.A., Hwang, K.S., Lin, S.B., Tsay, S.Y., Koshiba, M., Ding, Y.S., Cooper, S.L., J. Appl. Sci., **30**, p. 647 (1985).

[93] Schmidle, C.J., J. Coated Fabr., **8**, p. 10 (1978).

[94] Holmes, M., Moran, J.P., European Patent Appl. **114**, 117 (1984).

[95] Suzuki, H., Miyake, H., Makimura, O., Goto, T., Jpn. Kokai 77, 155, p. 694 (1977).

[96] Chiao, W.B., U.S. Patent 4, 656, 229 (1987).

[97] Kanda, K., Urano, S., Aoki, K., Muramoto, H., European Patent Appl. 220, 862 (1987).

[98] Bryant, G.M., Carr, F.G., U.S. Patent 4, 153, 778 (1979).

[99] Fischer, W.F., Le Masters, D.P., Harbison, W.C., U.S. Patent 4, 594, 290 (1986).

[100] Saito, T., Jpn. Kokai Tokkyo Koho 61, 287, 976 (1987).

[101] Liu, C. J., Hsieh K. H., Ho, K. S., Hsieh T. T., J Biomed Mater Res, **34**, 2, p. 261-268 (1997).

[102] Daimatsu, K., Sugimoto, H., Nakanishi, E., Yasumura, T., Inomata, K., J Appl Polym Sci, **109**, 3, p. 1611-1617 (2008).

[103] Hsieh, K. H., Kuo, C. H., Dai, C. A., Chen, W. C., Peng, T. C., Ho, G. H., J Appl Polym Sci, **91**, 5, p. 3162-3166 (2004).

[104] Xiaobin, H., Tianbin, R., Xian, Z., Xiaozhen ,T., Polym Int, **52**, I 8, p. 1294-1299 (2003).

[105] Yildiz, E., Güngör, A., Yildirim, H., Baysal , B. M., Angewandte Makromolekulare Chemie, **233**, 1, p. 33-45 (1995).

[106] Akcelrud, L., Gomes, A. S., J Poly Sci Part A: Polym Chem, **24**, 11, p. 2831-2844 (1986).

[107] Ketley, A.D., Hein, P.R., Yang, W.C., U.S. Patent 4, 120, 721 (1978).

[108] Mariani, A., Fiori, S., Bidali, S., Alzari, V., Malucelli, G., J Polym Sci Part A: Polym Chem, **46**, 10, p. 3344-3352 (2008).

[109] Hu, T., Chen, S., Tian, Y., Pojman, J. A., Chen, L., J Polym Sci Part A: Polym Chem, 44, 9, p. 3018-3024 (2006).

[110] Džunuzović, E., Tasić, S., Božić, B., Jeremić, K., Dunjić B., React Func Polym, 66, p. 1097-1105 (2006).

[111] Lu, W.H., Xu, W.J., Wu, Y.M., Zhou, X., Lu, Y.B., Xiong, Y.Q., Progress Org Coat, **56**, 2-3, p. 252-255 (2006).

[112] Dzunuzovic, E., Tasic, S., Bozic, B., Babic, D., Dunjic, B., Progress Org Coat, **52**, 2, p. 136-143 (2005).

[113] Naruse, I., Hirose, S., Matsuyama, A., Jpn. Kokai Tokkyo Koho, 61, 50, p. 942 (1986).

[114] Kinoshita, H., Tanak, N., Arakai, T., Ooka, M., Macromol. Chem. Phys., **195**, pp. 413-425 (1994).

[115] Kinoshita, H., Tanak, N., Arakai, T., Macromol. Chem., **194**, pp. 829-839 (1993).

[116] Kinoshita, H., Tanak, N., Arakai, T., Ooka, M., Macromol. Chem., **194**, pp. 2335-2347 (1993).

[117] Cheikhalard, T., Massardier, V., Tighzert, L., Pascault, J.P., J Appl Polym Sci., **70**, p. 613-627 (1998).

[118] Oprea, S., Vlad, S., Stanciu, A., Polymer, 42, pp. 7257-7266 (2001).

[119] Barbeau, PH., Gerard, J.F., Magny, B., Pascault, J.P., J Polym Sci: Part B:Polym Phys, **38**, pp. 2750-2768 (2000).

[120] Kim, H.D., Kang, S.G., HA, S.C., J Appl Polym Sci., **46**, p.1339 (1992).

[121] Kimura, T., Yamakawa, S., J Polym Sci. Polym Ed., **24**, p.1161 (1986).

[122] Nocci, R., Attala, G., Cohen, R., EP99, **2**, p.271 (1984).

[123] Asha, S.K., Thirumal, M., Kavitha, A., Pillai, C.K.S., Europ Polym J, **41**, p. 23-33 (2005).

[124] Kim, B.K., Paik, S.H., J Polym Sci. Part A:Polym Chem., **37**, p. 2703-2709 (1999).

[125] Hsieh, K.H., Kuo, C.H., Dai, C.A., Chen, W.C., Peng, T.C., Ho, G.H., J Appl Polym Sci, **91**, p. 3162-3166 (2004).

[126] Yang, J., Wang, Z., Zeng, Z., Yuan, H., Chen, Y., Chinese J Polym Sci, **9**, p. 175-181 (2001).

[127] Finger, F.J., Fritz, U.B., Eur J Oral Sci, **105**(2), p.183-186 (1997).

[128] Asmussen, E., Peutzfeldt, A., Dent Mater, 14, p. 51-56 (1998).

[129] Krishnan, V.K., Lizymol, P.P., Nair, S.P., J Appl Polym Sci, 74, p. 735-746 (1999).

[130] Tanaka, J., Hashimoto, T., Stansbury, J.W., Antonucci, J.M., Suzuki, K., Dent Mater J, **20**(3), p. 206-215 (2001).

[131] Dickens, S.H., Stansbury, J.W., Choi, K.M., Floyd, C.J.E., Macromol, 36(16), p. 6043-6053 (2003).

[132] Atai, M., Ahmadi, M., Babanzadeh, S., Watts, D.C., Dent Mater, **23**, p. 1030-1041 (2007).

[133] Lytle RB. J Prosthet Dent., **7**, p. 27-42 (1957).

[134] Lytle RB.. J Prosthet Dent., **9**, p. 539-51 (1959).

[135] McCabe J.F., Walls A.W.G., *Applied Dental Materials*, 8th Ed., Blackwell Science (1988).

[136] Braden, M., *Polymeric Dental Materials*, Springer-Verlag, Berlin (1997).

[137] Ward, I.M., Hadley, D.W., *An introduction to the mechanical properties of solid polymers*, John Wiley & Sons, England, p 45- (1996).

[138] Nilsen, L.E., Landel, R.F., *Mechanical properties of polymers and composites*, Marcel Deker, 2nd edition, USA, (1994).

[139] Ferry, J.D., *Viscoelastic Properties of Polymers*, 2nd Ed., Wiley, New York, (1970).

[140] Nielesen, L.E., *Mechanical Properties of Polymers and Composites*, Vol. 1, Marcel Dekker, New York, (1974).

[141] Stratton, R.,J Colloid Interface Sci., **22**, p.517-530 (1966).

[142] Porter, R.S., Johnson, J.F., J. Polymer Sci., **C15**, p. 373 (1966).

[143] Bestul, A.B., Belcher, H.V., J. Appl. Phys., **24**, p.696 (1953).

[144] Williams, M.L., Landel, R.F., Ferry, J.D., J. Amer. Chem. Soc., **77**, p. 3701 (1955).

[145] Furstner, A., *Active metals*: Preparation *Characterization Applications*, John Wiley & Sons Canada, Ltd., 1996.

[146] Ayyappan, S., G.R. Srinivasa, G.N. Subbanna & C.N.R. Rao,. J. Mater. Res., **12**(2), p. 398–401 (1997).

[147] Longenberger, L., Mills, G., J. Phys. Chem., **99**(2), p. 475–480 (1995).

[148] Creighton, J.A., Blatchford, C.G., Albrecht, M.G., J. Chem. Soc., Faraday Trans. 2: Mol. Chem. Phys., **75**(5), p.790–798 (1979).

[149] Pomogailo, A.D., Kestelman, V.N., *Metallopolymer nanocomposites, Vol 81,* Springer Berlin Heidelberg, (2005).

[150] Lelah, M. D., Cooper, S. L., *Polyurethane in Medicine*, CRC press, Boca Raton, (1986).

[151] ASTM D-2572, Standard Test Method for Isocyanate Groups in Urethane Materials or Prepolymers, 1997.

[152] ISO 10993-5, Biological evaluation of medical devices: Part 5 Test for Cytotoxicity: in vitro methods, 1992.

[153] Lee, H.S., Hsu, S.L., Macromol, **22**, p. 1100 (1989).

[154] Brunette, C.M., Hsu, S.L., MacKnight, W.J., Macromol, **15, p.** 71-77 (1982).

[155] Kim, B.K., Lee, Y.M., Shin, J.H., Park, S.H., J. Macromol. Sci. Physics, **B40 6**, p. 1179-1191 (2001).

[156] Yilgor, E., Burgaz, E., Yurtsever, E., Yilgor, I., Polymer, **41**, p. 849-857 (2000).

[157] Yilgor, I., Yilgor, E., Guler, G.I., Ward, T.C., Wilkes, G.L., Polymer, **47**, p. 4105- 4114 (2006).

[158] Yilgor, I., Yilgor, E., Polymer Reviews, **47**, p. 487-510 (2007).

[159] Olabisi, O., *Handbook of thermoplastics*, Chapter 16 Thermoplastic polyurethanes, Marcel Dekker, p. 386-390, (1997).

[160] Coleman, M.M., Lee, K.H., Skrovanek, D.J., Painter, P.C., Macromol, **19**, p. 2149 (1986).

[161] Lee, H.S., Wang, Y.K., MacKnight, J.W., Hsu, S.L., Macromol, **21**, p. 270-273 (1988).

[162] MacKnight, W.J., Yang, J., J. Polym. Sci., Polym. Symp., **42**, p. 817 (1973).

[163] Coleman, M.M., Skrovanek, D.J., Hu, J., Painter, P.C., Macromol, **21**(1), p. 59-65 (1988).

[164] Varnel, D.F., Runt, J.P., Coleman, M., Macromol, **14**, p. 1350 (1981).

[165] Mack, P.J., Aust Dent J, **34**(6), p. 517-521 (1989).

APPENDIX A

VACUUM SYNTHESIS RESULTS

Table A1 Percent conversion results of prepolymer synthesized under vacuum.

Temperature °C	Time (day)	% Conversion
40	1	3.2
	7	13.6
	30	34
60	1	5.4
	7	11.2
	30	24.3
70	1	4.5
	7	28
	30	39
90	1	6.2
	7	29
	30	36

APPENDIX B

MOLECULAR WEIGHT DISTRIBUTION GRAPHS

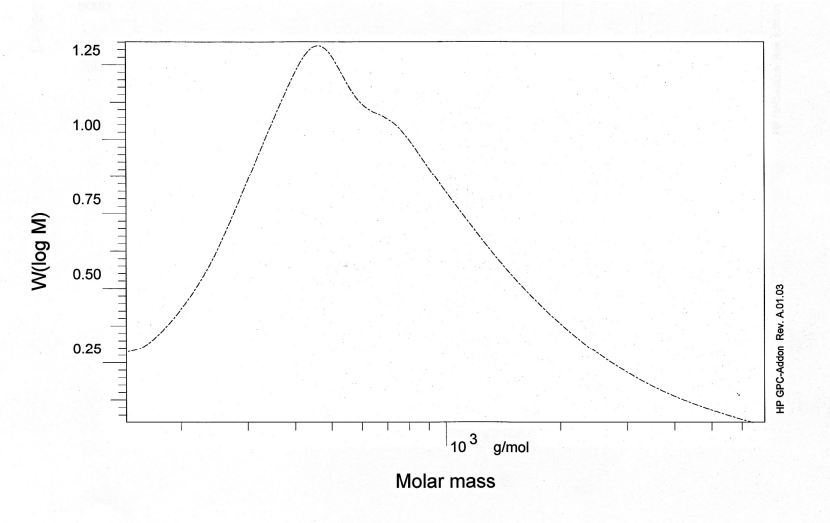

Figure B1 Molecular weight distribution of PU1v.

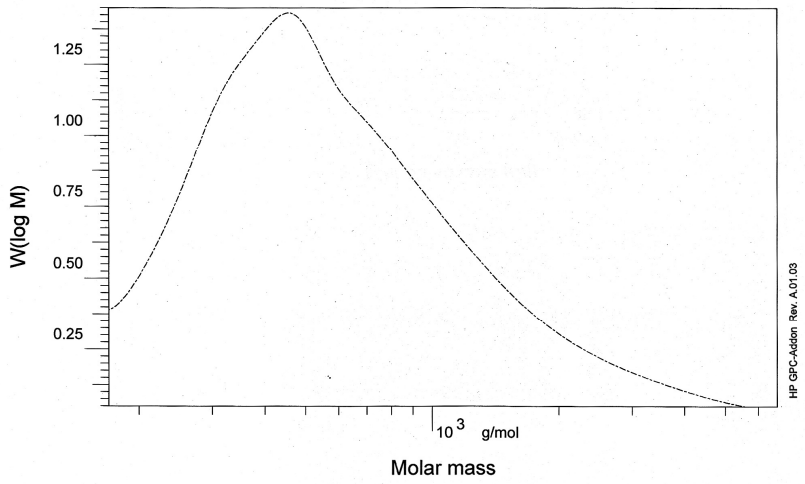

Figure B2 Molecular weight distribution of PU2v.

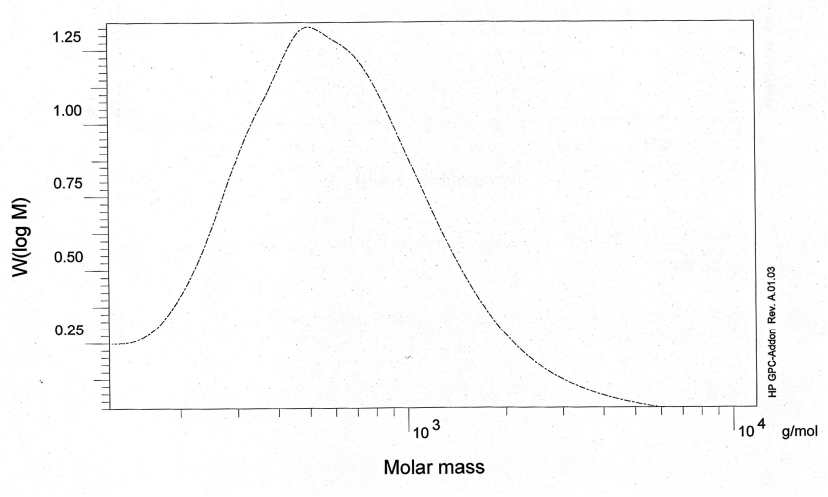

Figure B3 Molecular weight distribution of PU3v.

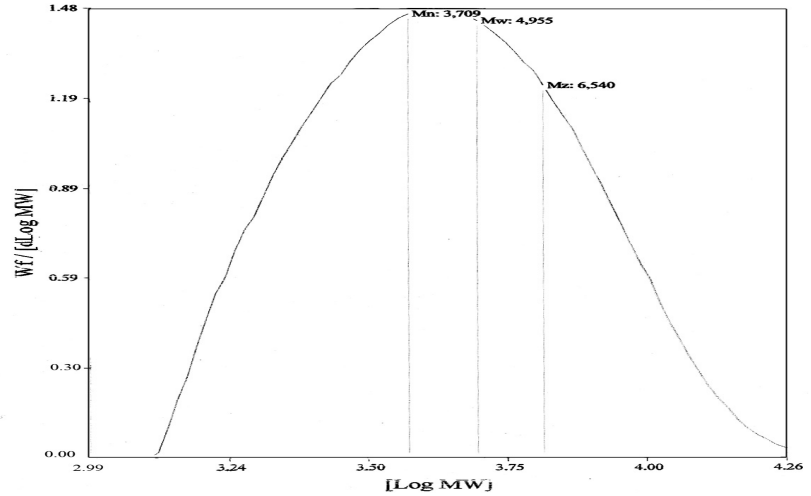

Figure B4 Molecular weight distribution of PU3.

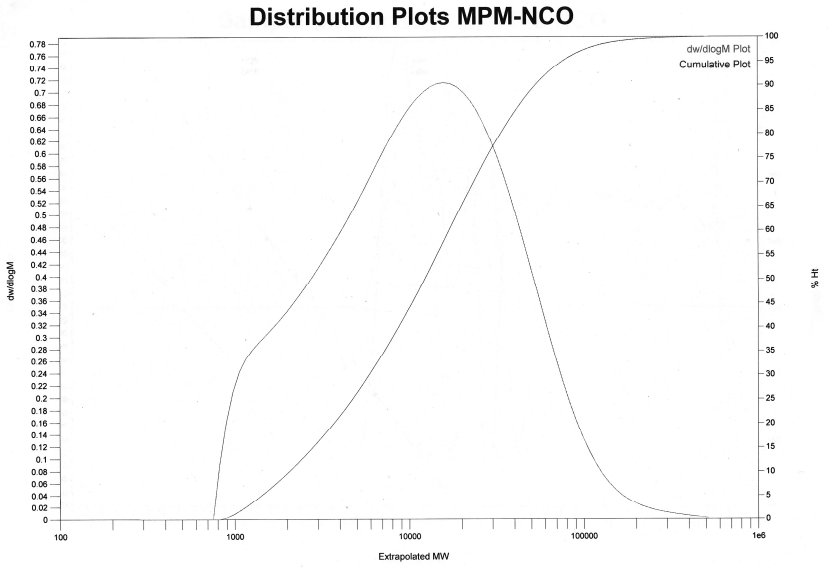

Figure B5 Molecular weight distribution of PUNCOMMA3.

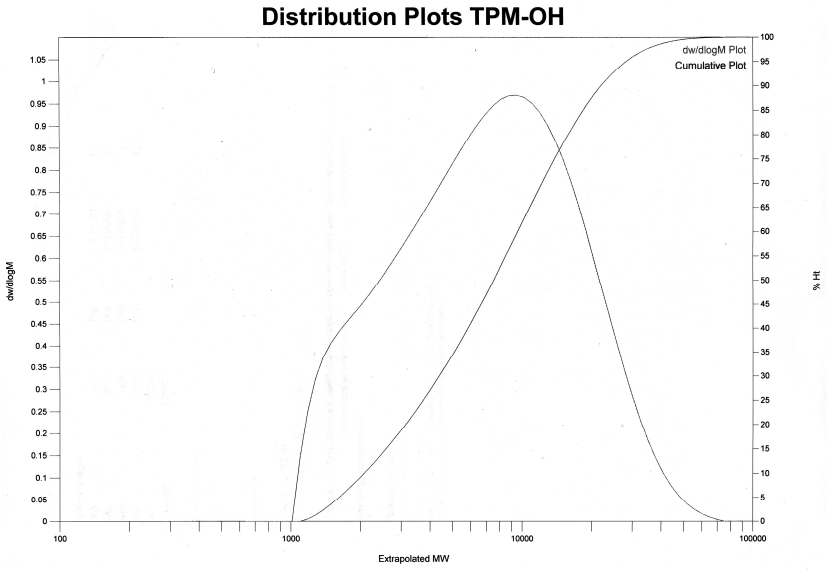

Figure B6 Molecular weight distribution of PUOHMMA1.

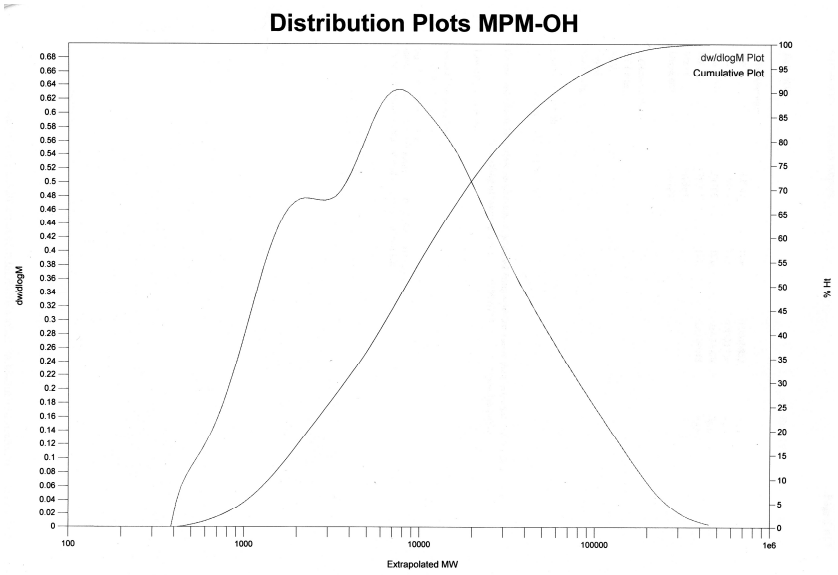

Figure B7 Molecular weight distribution of PUOHMMA3.

CURRICULUM VITAE

PERSONAL INFORMATION

Surname, Name: Keskin, Selda.

Nationality : Turkish (TC)

Date and Place of Birth : 10 June 1977 , Kayseri

Phone: +90 310 210 6423

Fax : +90 312 210 6425

Email : skeskin@metu.edu.tr

EDUCATION

Degree	Institution	Year of Graduation
MS	METU Chemistry	2002
BS	METU Chemistry	1999
High School	TED Ankara Collage, Ankara	1994

WORK EXPERIENCE

Year	Place	Enrollment
2001-present	METU Central Laboratory	Research Associate

PUBLICATIONS

1. Hubbezoğlu İ, Akoğlu B, Doğan A, **Keskin S**, Bolayır G, Özçelik S, Doğan OM. *Effect of bleaching on color change and refractive index of dental composite resins*. Dental Mater J. 27(1) :105-116, 2008.
2. Doğan OM, Bolayır G, **Keskin S**, Doğan A, Bek B. *The evaluation of some flexural properties of denture base resin reinforced with various aesthetic fibers*. J Mater Sci: Mater Med. 19(6): 2343-2349, 2008.

3. Turgut M, Bolayır G, Doğan OM, **Keskin S**, Doğan A, Boztuğ A. *Bond strength of a silicone soft lining material to pol(methyl methacrylate) resin treated with maleic anhydride and its terpolymers*. J Adhesion. 83(11):927-938,2007.
4. Vardereli TK, **Keskin S**, Usanmaz A. *Synthesis and characterization of Poly(allyl methacrylate) obtained by free radical initiator*. Journal of Macromolecular Science, Part A: Pure and Applied Chemistry.45:302-311, 2007.
5. Doğan OM, Bolayır G, **Keskin S**, Doğan A, Bek B, Boztuğ A. *The effect of esthetic fibers on impact resistance of a conventional heat-cured denture base resin*. Dent Mater J 26 (2): 232-239, 2007.
6. Doğan OM, **Keskin S,** Bolayır G, Usanmaz A, Bek B. *Flexural and bonding properties of a denture base polymer treated with nitric acid or ultraviolet radiation before relining with Molloplast-B.* J Adhesion, 83:129-137, 2007.
7. Bolayır G, Turgut M, Hubbezoğlu İ, Doğan OM, **Keskin S**, Doğan A, Bek B. *Evaluation of laser treatment on reline-base composites*. J Adhesion 83 (1): 117-127, 2007.
8. Vardereli TK, **Keskin S**, Usanmaz A. *Thermal degradation of poly(Allyl Methacrylate) by mass spectroscopy and TGA* . Journal of Macromolecular Science, Part A: Pure and Applied Chemistry. 43:1569-1581, 2006.
9. Doğan OM, Bolayır G, **Keskin S**, Boztuğ A, Doğan A, Bek B. *The effects of some methacrylate monomers used as liquid component on tensile and flexural strengths of a poly (methyl methacrylate) denture base resin*. Mater Res Innov. 10(4): 122-127, 2006.
10. Dogan OM, **Keskin S**, Dogan A, Ataman H, Usanmaz A. *Structure property of a soft liner material used in denture applications*. Dent Mater J 26(3): 329-337, (2007).
11. Bolayır G, **Keskin** S, Doğan OM, Bek B, Doğan A. *Astarlama öncesi akrilik yüzeyin ultraviyole ve nitrik asit uygulamasının kaide rezini ve*

yumuşak astarda oluşturduğu kimyasal değişikliklerin değerlendirilmesi. CÜ Diş Hek Fak Der 9:101-106, 2006.

CONGRESS REPORTS

1. **Keskin S**, Usanmaz A, Doğan A, Doğan OM. *The color change on denture base material caused by tea and coffee and effect of hypochloride and gluteraldehyde*. Turkish Dental Association, 13th International Dental Congress, Samsun, 19-24th June 2006.
2. **Keskin S**, Usanmaz A, Doğan A, Doğan OM. *Disinfection and discoloring of dental base material by hypochloride treatment*. Turkish Dental Association, 13th International Dental Congress, Samsun, 19-24th June 2006.
3. Doğan OM, **Keskin S**, Doğan A, Usanmaz A. *Structural properties of silicone type soft lining denture material used in dental applications*. Turkish Dental Association, 13th International Dental Congress, Samsun, 19-24th June 2006.
4. Doğan OM, Bolayır G, **Keskin S**, Doğan A, Bek B, Boztuğ A. *Reinforcement of a denture base resin with some aesthetic fibers*. 6th Aegean Region Chambers of Dentists International Scientific Congress and Exhibition, 1-3rd December, Antalya, 2006.
5. Hubbezoğlu İ, Bolayır G, **Keskin S**, Doğan OM, Özer A, Doğan A. *The effect of various types of light-curing on the microhardness of different composites*. 6th Aegean Region Chambers of Dentists International Scientific Congress and Exhibition, 1-3rd December , Antalya, 2006.
6. Bolayır G, Turgut M, Hubbezoğlu İ, Doğan OM, **Keskin S**, Doğan A, Bek B. *Evaluation of different laser treatment on reline-base*

composites. 6th Aegean Region Chambers of Dentists International Scientific Congress and Exhibition, 1-3rd December, Antalya, 2006.

7. Bolayır G, Doğan OM, **Keskin S**, Doğan A, Bek B. *The evaluation of some flexural properties of a denture base resin reinforced with various aesthetic fibers*. 6th Aegean Region Chambers of Dentists International Scientific Congress and Exhibition, 1-3 December, Antalya, 2006.

AWARDS

1. Reinforcement of a denture base resin with some aesthetic fibers (OM Doğan, G Bolayır, **S Keskin**, A Doğan, B Bek, A Boztuğ), 6th Aegean Region Chambers of Dentists International Scientific Congress and Exhibition. 1-3 December 2006, Antalya, Turkey.

2. Publications no. 1-10 were awarded by the TUBITAK UYT.

3. Publications no.2, 4, 6, 7, 8 were awarded by the METU Natural Science and Applied Science Institute.